PHY332

Atomic and Laser Physics

A.M. FOX

Autumn Semester 2011

Course synopsis

Outline syllabus

PART I: ATOMIC PHYSICS. Quantum mechanics of the hydrogen atom. Radiative emission by atoms and selection rules. Shell model and alkali spectra. Angular momentum coupling. Spin-orbit coupling and spectral fine structure. The Zeeman and Stark effects. Helium and the exchange energy.

Part II: LASER PHYSICS. Introduction to lasers and the properties of laser light. Einstein's A and B coefficients. Population inversion. Laser modes. Examples of lasers systems and their applications.

Lecture Notes

1. Introduction to atomic physics
2. The hydrogen atom
3. Radiative transitions
4. The shell model and alkali spectra
5. Angular momentum
6. Fine structure
7. External fields: the Zeeman and Stark effects
8. Helium and exchange symmetry
9. Introduction to lasers
10. Laser gain mechanisms
11. Laser cavities and modes
12. Different types of lasers

Other information

Course www page: http://www.mark-fox.staff.shef.ac.uk/PHY332/

Assessment: Homework 15%, Exam 85%

Recommended books

- Demtröder, W. *Atoms, Molecules and Photons*, (Springer-Verlag, 2006)
- Haken and Wolf, *The Physics of Atoms and Quanta*, (7th edn, Springer-Verlag, 2005)
- Wilson and Hawkes, *Optoelectronics, an introduction*, (3rd edn, Prentice Hall (1998): Chapters 5–6 on laser physics

Also useful

- Eisberg and Resnick, *Quantum Physics of Atoms, Molecules, Solids, Nuclei, and Particles* (Wiley, 1985)
- Hecht, *Optics* (3rd edn, Addison Wesley, 1998), Section 13.1
- Phillips, *Introduction to Quantum Mechanics* (Wiley, 2003)
- Smith and King, *Optics and Photonics* (Wiley 2000), chapters 15–17

More advanced texts

- Foot, *Atomic Physics* (Oxford, 2005)
- Hooker and Webb, *Laser Physics* (Oxford, 2010)
- Silfvast *Laser Fundamentals* (Cambridge, 2004)
- Svelto, *Principles of Lasers* (4th edn, Plenum, 1998)
- Woodgate, *Elementary Atomic Structure* (Oxford, 1980)
- Yariv, *Optical Electronics in Modern Communications* (Oxford, 1997)

Chapter 1

Introduction to atomic physics

1.1 The importance of atomic physics

Atomic Physics is the subject that studies the inner workings of the atom. It remains one of the most important testing grounds for quantum theory, and is therefore still an area of active research, both for its contribution to fundamental physics and to technology. Furthermore, many other branches of science rely heavily on atomic physics. The following list gives a few examples:

Physics Astrophysics, plasma physics, atmospheric physics, solid state physics, chemical physics and radiation physics.

Other science Chemistry (analysis, reaction rates), biology (molecular structure, physiology), materials science, energy research, fusion studies.

Applications Lasers, X-ray technology, NMR, pollution detection, medical applications of devices (lasers, NMR etc.).

In this chapter we shall give a brief overview of the main effects that will be considered in this course, and define a few important terms and concepts that underlie the whole subject. We shall also give a brief review of the Bohr theory, which was the basis of the "old" (i.e. pre-quantum mechanics) quantum theory of the atom.

1.2 Atomic spectroscopy

We gain most of our knowledge of atoms from studying the way light interacts with matter, and in particular from measuring atomic spectra. Optics has therefore played a key role in the development of atomic physics. The extreme precision with which optical spectral lines can be measured makes atomic physics the most precise branch of physics. For example, the frequencies of the spectral lines of hydrogen have been measured with extremely high accuracy, permitting the testing of small but important phenomena that are normally unobservable.

The basis for atomic spectroscopy is the measurement of the energy of the photon absorbed or emitted when an electron jumps between two quantum states, as shown in Fig. 1.1. These are called **radiative transitions**. The frequency (ν) of the photon (and hence its wavelength, λ) is determined by the difference in energy of the two levels according to:

$$h\nu = \frac{hc}{\lambda} = E_2 - E_1 \,, \tag{1.1}$$

where E_1 and E_2 are the energies of the lower and upper levels of the atom respectively.

Spectroscopists measure the wavelength of the photon, and hence deduce energy differences. The absolute energies are determined by fixing one of the levels (normally the ground state) by other methods, e.g. by measurement of the ionization potential.

1.3 Energy units

Atomic energies are frequently quoted in **electron volts** (eV). 1 eV is the energy acquired by an electron when it is accelerated by a voltage of 1 Volt. Thus 1 eV $= 1.6 \times 10^{-19}$ J. This is a convenient unit, because the energies of the electrons in atoms are typically a few eV.

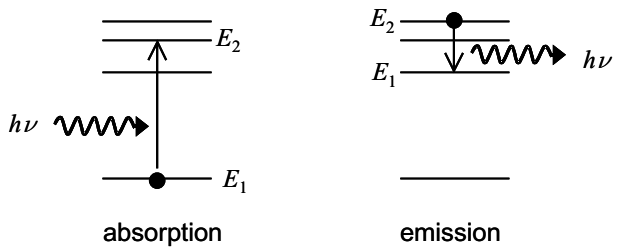

Figure 1.1: Absorption and emission transitions.

Energy scale	Energy (eV)	Energy (cm^{-1})	Contributing effects
Gross structure	1 – 10	10^4 – 10^5	electron–nuclear attraction electron-electron repulsion electron kinetic energy
Fine structure	0.001 – 0.01	10 – 100	spin-orbit interaction relativistic corrections
Hyperfine structure	10^{-6} – 10^{-5}	0.01 – 0.1	nuclear interactions

Table 1.1: Rough energy scales for the different interactions that occur within atoms.

Atomic energies are also often expressed in **wave number** units (cm^{-1}). The wave number $\overline{\nu}$ is the reciprocal of the wavelength of the photon with energy E. It is defined as follows:

$$\overline{\nu} = \frac{1}{\lambda\,(\text{in cm})} = \frac{\nu}{c} = \frac{E}{hc}\,. \tag{1.2}$$

Note that the wavelength should be worked out in cm. Thus $1\,\mathrm{eV} = (e/hc)\,\mathrm{cm}^{-1} = 8066\,\mathrm{cm}^{-1}$.

Wave number units are particularly convenient for atomic spectroscopy. This is because they dispense with the need to introduce fundamental constants in our calculation of the wavelength. Thus the wavelength of the radiation emitted in a transition between two levels is simply given by:

$$\frac{1}{\lambda} = \overline{\nu}_2 - \overline{\nu}_1\,, \tag{1.3}$$

where $\overline{\nu}_1$ and $\overline{\nu}_2$ are the energies of levels 1 and 2 in cm^{-1} units, and λ is measured in cm.

1.4 Energy scales in atoms

In atomic physics it is traditional to order the interactions that occur inside the atom into a three-level hierarchy according to the scheme summarized in Table 1.1. The effect of this hierarchy on the observed atomic spectra is illustrated schematically in Fig. 1.2.

1.4.1 Gross structure

The first level of the hierarchy is called the **gross structure**, and covers the largest interactions within the atom, namely:

- the kinetic energy of the electrons in their orbits around the nucleus;
- the attractive electrostatic potential between the positive nucleus and the negative electrons;
- the repulsive electrostatic interaction between the different electrons in a multi-electron atom.

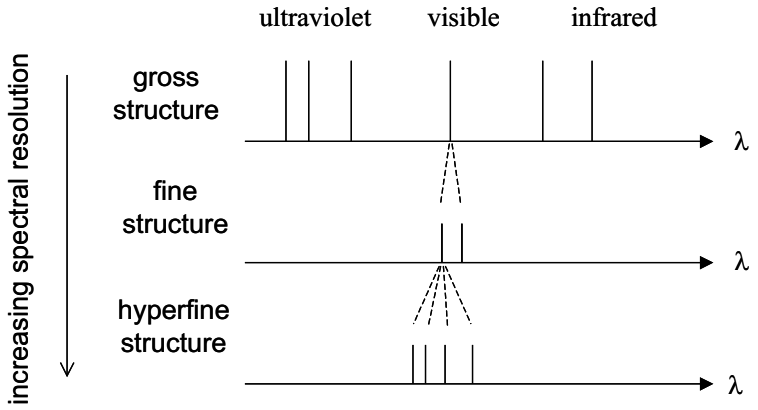

Figure 1.2: Hierarchy of spectral lines observed with increasing spectral resolution.

The size of these interactions gives rise to energies in the 1–10 eV range and upwards. They thus determine whether the photon that is emitted is in the infrared, visible, ultraviolet or X-ray spectral regions, and more specifically, whether it is violet, blue, green, yellow, orange or red for the case of a visible transition.

1.4.2 Fine structure

Close inspection of the spectral lines of atoms reveals that they often come as multiplets. For example, the strong yellow line of sodium that is used in street lamps is actually a doublet: there are two lines with wavelengths of 589.0 nm and 589.6 nm. This tells us that there are smaller interactions going on inside the atom in addition to the gross structure effects. The gross structure interactions determine that the emission line is yellow, but fine structure effects cause the splitting into the doublet. In the case of the sodium yellow line, the fine structure energy splitting is 2.1×10^{-3} eV or 17 cm^{-1}.

Fine structure arises from the **spin-orbit** interaction. Electrons in orbit around the nucleus are equivalent to current loops, which give rise to atomic magnetism. The magnitude of the magnetic dipole moment of the electron is typically of the order of the **Bohr magneton** μ_B:

$$\mu_\mathrm{B} = \frac{e\hbar}{2m_\mathrm{e}} = 9.27 \times 10^{-24}\ \mathrm{J\,T^{-1}}\,. \tag{1.4}$$

The atomic dipoles generate strong magnetic fields within the atom, and the spin of the electron can then interact with the internal field. This produces small shifts in the energies, which can be worked out by measuring the fine structure in the spectra. In this way we can learn about the way the spin and the orbital motion of the atom couple together. In more advanced theories of the atom (e.g. the Dirac theory), it becomes apparent that the spin-orbit interaction is actually a relativistic effect.

1.4.3 Hyperfine structure

Even closer inspection of the spectral lines with a very high resolution spectrometer reveals that the fine-structure lines are themselves split into more multiplets. The interactions that cause these splitting are called **hyperfine** interactions.

The hyperfine interactions are caused by the interactions between the electrons and the nucleus. The nucleus has a small magnetic moment of magnitude $\sim \mu_\mathrm{B}/2000$ due to the nuclear spin. This can interact with the magnetic field due to the orbital motion of the electron just as in spin-orbit coupling. This gives rise to shifts in the atomic energies that are about 2000 times smaller than the fine structure shifts. The well-known 21 cm line of radio astronomy is caused by transitions between the hyperfine levels of atomic hydrogen. The photon energy in this case is 6×10^{-6} eV, or 0.05 cm^{-1}.

1.5 External fields

Further information about the inner workings of atoms can be obtained by studying the effects of external magnetic and electric fields. (See Table 1.2.) These effects will be considered in detail in Chapter 7.

The splitting of atomic spectral lines when a weak external magnetic field is applied is called the **Zeeman effect**. When the field strength is very large, a different type of effect is observed called the

Applied field	Field strength	Effect
Magnetic	weak strong	Zeeman Paschen-Back
Electric	all	Stark

Table 1.2: Names of the effects of external fields in atomic physics.

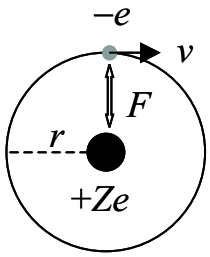

Figure 1.3: The Bohr model of the atom considers the electrons to be in orbit around the nucleus. The central force is provided by the Coulomb attraction. The angular momentum of the electron is quantized in integer units of $\hbar$.

Paschen-Back effect. However, for most atoms, the size of the field required to observe the transition from the Zeeman effect to the Paschen-Back effect is beyond the range of laboratory magnets, and so only the Zeeman effect is commonly observed.

In the case of electric fields, the weak and strong field limits are not normally distinguished, and all the phenomena are collectively called the **Stark effect**. These effects are named after J. Stark, who was the first person to study the effect of electric fields on atomic spectral lines, when he measured the splitting of the hydrogen Balmer lines in an electric field in 1913.

1.6 The Bohr model

In 1911 Rutherford discovered the nucleus. This then led to the idea of atoms consisting of electrons in classical orbits in which the central forces are provided by the Coulomb attraction to the positive nucleus, as shown in Fig. 1.3. The problem with this idea is that the electron in the orbit is constantly accelerating. Accelerating charges emit radiation called **bremsstrahlung**, and so the electrons should be radiating all the time. This would reduce the energy of the electron, and so it would gradually spiral into the nucleus, like an old satellite crashing to the earth.

In 1913 Bohr produced his model for the atom. The key new elements of the model are:

- The angular momentum L of the electron is quantized in units of $\hbar$ ($\hbar = h/2\pi$):

$$L = n\hbar\,, \tag{1.5}$$

  where n is an integer.

- The atomic orbits are stable, and light is only emitted or absorbed when the electron jumps from one orbit to another.

When Bohr made these hypotheses in 1913, there was no justification for them other than they were spectacularly successful in predicting the energy spectrum of hydrogen. With the hindsight of quantum mechanics, we now know why they work. The first assumption is equivalent to stating that the orbit must correspond to a fixed number of de Broglie wavelengths. For a circular orbit, this can be written:

$$2\pi r = \text{integer} \times \lambda_{\text{deB}} = n \times \frac{h}{p} = n \times \frac{h}{mv}\,, \tag{1.6}$$

which can be rearranged to give

$$L \equiv mvr = n \times \frac{h}{2\pi}\,. \tag{1.7}$$

The second assumption is a consequence of the fact that the Schrödinger equation leads to time-independent solutions (**eigenstates**).

The derivation of the quantized energy levels proceeds as follows. Consider an electron orbiting a nucleus of mass $m_{\rm N}$ and charge $+Ze$. The central force is provided by the Coulomb force:

$$F = \frac{mv^2}{r} = \frac{Ze^2}{4\pi\epsilon_0 r^2}\,. \tag{1.8}$$

As with all two-body orbit systems, the mass m that enters here is the **reduced mass**:

$$\frac{1}{m} = \frac{1}{m_{\rm e}} + \frac{1}{m_{\rm N}}\,. \tag{1.9}$$

The energy is given by:[1]

$$\begin{aligned} E_n &= \text{kinetic energy} + \text{potential energy} \\ &= \tfrac{1}{2}mv^2 - \frac{Ze^2}{4\pi\epsilon_0 r} \\ &= -\frac{mZ^2e^4}{8\epsilon_0^2 h^2 n^2}\,, \end{aligned} \tag{1.10}$$

where we made use of eqns 1.7 and 1.8 in the last line. This can be written in the form:

$$E_n = -\frac{R'}{n^2} \tag{1.11}$$

where R' is given by:

$$R' = \left(\frac{m}{m_{\rm e}}Z^2\right) R_\infty hc\,, \tag{1.12}$$

and $R_\infty hc$ is the **Rydberg energy**:[2]

$$R_\infty hc = \frac{m_{\rm e}e^4}{8\epsilon_0^2 h^2}\,. \tag{1.13}$$

The Rydberg energy is a fundamental constant and has a value of 2.17987×10^{-18} J, which is equivalent to 13.606 eV. This tells us that the gross energy of the atomic states in hydrogen is of order 1 – 10 eV, or $10^4 - 10^5\,{\rm cm}^{-1}$ in wave number units.

R' is the effective Rydberg energy for the system in question. In the hydrogen atom we have an electron orbiting around a proton of mass $m_{\rm p}$. The reduced mass is therefore given by

$$m = m_{\rm e} \times \frac{m_{\rm p}}{m_{\rm e} + m_{\rm p}} = 0.9995\, m_{\rm e}$$

and the effective Rydberg energy for hydrogen is:

$$R_{\rm H} = 0.9995\, R_\infty hc\,. \tag{1.14}$$

Atomic spectroscopy is very precise, and 0.05% factors such as this are easily measurable. Furthermore, in other systems such as positronium (an electron orbiting around a positron), the reduced mass effect is much larger, because $m = m_{\rm e}/2$.

By following through the mathematics, we also find that the orbital radius and velocity are quantized. The relevant results are:

$$r_n = \frac{n^2}{Z}\,\frac{m_{\rm e}}{m} a_0\,, \tag{1.15}$$

[1] In atoms the electron moves in free space, where the relative dielectric constant ϵ_r is equal to unity. However, in solid state physics we frequently encounter hydrogenic systems inside crystals where ϵ_r is not equal to 1. In this case, we must replace ϵ_0 by $\epsilon_r\epsilon_0$ throughout.

[2] Note the difference between the Rydberg *energy* $R_\infty hc$ (13.606 eV) and the Rydberg *constant* R_∞ ($109{,}737\,{\rm cm}^{-1}$). The former has the dimensions of energy, while the latter has the dimensions of inverse length. They differ by a factor of hc. (See Table 1.3.) When high precision is not required, it is convenient just to use the symbol $R_{\rm H}$ for the Rydberg energy, although, strictly speaking, $R_{\rm H}$ differs from the true Rydberg energy by 0.05%. (See eqn 1.14.)

Quantity	Symbol	Formula	Numerical Value
Rydberg energy	$R_\infty hc$	$m_e e^4/8\epsilon_0^2 h^2$	2.17987×10^{-18} J 13.6057 eV
Rydberg constant	R_∞	$m_e e^4/8\epsilon_0^2 h^3 c$	109,737 cm^{-1}
Bohr radius	a_0	$\epsilon_0 h^2/\pi e^2 m_e$	5.29177×10^{-11} m
Fine structure constant	α	$e^2/2\epsilon_0 hc$	1/137.04

Table 1.3: Fundamental constants that arise from the Bohr model of the atom.

and

$$v_n = \alpha \frac{Z}{n} c\,. \tag{1.16}$$

The two fundamental constants that appear here are the **Bohr radius** a_0:

$$a_0 = \frac{h^2 \epsilon_0}{\pi m_e e^2}\,, \tag{1.17}$$

and the **fine structure constant** α:

$$\alpha = \frac{e^2}{2\epsilon_0 hc}\,. \tag{1.18}$$

The fundamental constants arising from the Bohr model are related to each other according to:

$$a_0 = \frac{\hbar}{m_e c}\frac{1}{\alpha}\,, \tag{1.19}$$

and

$$R_\infty hc = \frac{\hbar^2}{2m_e}\frac{1}{a_0^2}\,. \tag{1.20}$$

The definitions and values of these quantities are given in Table 1.3.

The energies of the photons emitted in transition between the quantized levels of hydrogen can be deduced from eqn 1.11:

$$h\nu = R_H \left(\frac{1}{n_1^2} - \frac{1}{n_2^2}\right)\,, \tag{1.21}$$

where n_1 and n_2 are the quantum numbers of the two states involved. Since $\nu = c/\lambda$, this can also be written in form:

$$\frac{1}{\lambda} = \frac{m}{m_e} R_\infty \left(\frac{1}{n_1^2} - \frac{1}{n_2^2}\right)\,. \tag{1.22}$$

In absorption we start from the ground state, so we put $n_1 = 1$. In emission, we can have any combination where $n_1 < n_2$. Some of the series of spectral lines have been given special names. The emission lines with $n_1 = 1$ are called the **Lyman series**, those with $n_1 = 2$ are called the **Balmer series**, etc. The Lyman and Balmer lines occur in the ultraviolet and visible spectral regions respectively.

1.7 The need for quantum mechanics

A simple back-of-the-envelope calculation can easily show us that the Bohr model is not fully consistent with quantum mechanics. In the Bohr model, the linear momentum of the electron is given by:

$$p = mv = \left(\frac{\alpha Z}{n}\right) mc = \frac{n\hbar}{r_n}\,. \tag{1.23}$$

However, we know from the Heisenberg uncertainty principle that the precise value of the momentum must be uncertain. If we say that the uncertainty in the position of the electron is about equal to the radius of the orbit r_n, we find:

$$\Delta p \sim \frac{\hbar}{\Delta x} \approx \frac{\hbar}{r_n}\,. \tag{1.24}$$

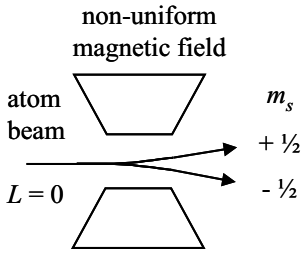

Figure 1.4: The Stern–Gerlach experiment. A beam of monovalent atoms with $L = 0$ (i.e. zero orbital angular momentum and hence zero orbital magnetic dipole moment) is deflected in two discrete ways by a non-uniform magnetic field. The force on the atoms arises from the interaction between the field and the magnetic moment due to the electron spin.

On comparing Eqs. 1.23 and 1.24 we see that

$$|p| \approx n\Delta p\,. \tag{1.25}$$

This shows us that the magnitude of p is undefined except when n is large. This is hardly surprising, because the Bohr model is a mixture of classical and quantum models, and we can only expect the arguments to be fully self-consistent when we approach the classical limit at large n. For small values of n, the Bohr model fails when we take the full quantum nature of the electron into account.

1.8 Spin

We shall discuss the spin of the electron and its consequences in detail from Chapter 6 onwards. At this stage we just need to know the basic facts. Spin is a completely quantum mechanical property with no classical equivalent. The Stern-Gerlach experiment (Fig. 1.4) showed that atoms with no orbital angular momentum still possess angular momentum.[3] For want of a better name, this angular momentum was called "spin". Paul Dirac at Cambridge successfully accounted for electron spin when he produced the relativistic wave equation that bears his name in 1928.

The fact that there were two deflections in the Stern–Gerlach experiment led to the conclusion that the z-component of the spin can take two possible values. We therefore assign two spin quantum numbers to the electron, namely s and m_s, where $s = 1/2$ and $m_s = \pm 1/2$. The magnitude of the spin angular momentum is given by

$$S = \sqrt{s(s+1)}\hbar\,, \tag{1.26}$$

and the component along the z axis is given by

$$S_z = m_s\hbar\,. \tag{1.27}$$

The fact that the electron has a half-integer spin makes it a **fermion**. Fermions obey the **Pauli exclusion principle**. Particles with integer values of the spin (eg α-particles) do not obey the Pauli exclusion principle. The Pauli exclusion principle states that only one electron can occupy a particular quantum state. This is very important for the explanation of the periodic table of elements, as we shall see in Chapter 4.

Reading

Demtröder, W., *Atoms, Molecules and Photons*, §3.4
Haken, H. and Wolf, H.C., *The Physics of Atoms and Quanta*, chapter 8.
Beisser, A., *Concepts of Modern Physics*, chapter 4.
Eisberg, R. and Resnick, R., *Quantum Physics*, chapter 4.

[3] In the Bohr model, the orbital angular momentum L is equal to $n\hbar$, and since $n \geq 1$, L cannot be zero. However, we shall see in the next chapter that L is actually equal to $\sqrt{l(l+1)}\hbar$, where l is the orbital quantum number. Since l can take values from 0 to $n-1$, some atoms *can* have $L = 0$. Moreover, we shall see in Chapter 6 that the magnetic dipole moment of an atom is directly proportional to its angular momentum. Hence an atom with $L = 0$ should *not* be deflected by a non-uniform magnetic field if we do not include the effects of spin.

Chapter 2

The Hydrogen atom

In the previous chapter we gave a quick overview of the Bohr model, which is only really valid in the semiclassical limit. (cf. section 1.7.) We now begin our task in earnest by applying quantum mechanics to the simplest atom we know, namely the hydrogen atom.

It is well known from classical physics that planetary orbits are characterized by their energy and angular momentum. In this chapter we apply the Schrödinger equation to the hydrogen atom to find the allowed energies and angular momenta of the nucleus-electron system. In classical systems we are also able to calculate the precise trajectory of the orbit. This is not possible in quantum systems. The best we shall be able to do is to find the wave functions. These will then give us the probability amplitudes that allow us to calculate all the measurable properties of the system.

2.1 The Schrödinger Equation

The time-independent Schrödinger equation for hydrogen is given by:

$$\left(-\frac{\hbar^2}{2m}\nabla^2 - \frac{Ze^2}{4\pi\epsilon_0 r}\right)\,\Psi(r,\theta,\phi) = E\,\Psi(r,\theta,\phi)\,. \tag{2.1}$$

This is written in terms of the spherical polar co-ordinates (r,θ,ϕ) because atoms are spheres, and the use of spherical polar co-ordinates simplifies the solutions. Note that we are considering the motion of the electron relative to a stationary nucleus here. As with all two-body problems, this means that the mass that enters into the equation is the **reduced mass** defined previously in eqn 1.9:

$$\frac{1}{m} = \frac{1}{m_{\rm e}} + \frac{1}{m_{\rm N}}\,. \tag{2.2}$$

For hydrogen where $m_{\rm N} = m_{\rm p}$, the reduced mass is very close to m_e, and has a value of $0.9995m_e$.

Written out explicitly, we have

$$-\frac{\hbar^2}{2m}\left[\frac{1}{r^2}\frac{\partial}{\partial r}\left(r^2\frac{\partial\Psi}{\partial r}\right) + \frac{1}{r^2\sin\theta}\frac{\partial}{\partial\theta}\left(\sin\theta\frac{\partial\Psi}{\partial\theta}\right) + \frac{1}{r^2\sin^2\theta}\frac{\partial^2\Psi}{\partial\phi^2}\right] - \frac{Ze^2}{4\pi\epsilon_0 r}\,\Psi = E\,\Psi \tag{2.3}$$

Our task is to find the wave functions $\Psi(r,\theta,\phi)$ that satisfy this equation, and hence to find the allowed quantized energies E.

2.2 Angular momentum

In classical mechanics, the rate of change of the angular momentum is given by:

$$\frac{{\rm d}\boldsymbol{L}}{{\rm d}t} = \boldsymbol{\Gamma}\,, \tag{2.4}$$

where $\boldsymbol{\Gamma}$ is the torque defined by:

$$\boldsymbol{\Gamma} = \boldsymbol{r}\times\boldsymbol{F}\,. \tag{2.5}$$

In the hydrogen atom, the electron is bound to the nucleus by the Coulomb force, which is parallel to $\boldsymbol{r}$. The torque is therefore zero, and so the angular momentum of the electron does not change. This

means that the angular momentum is a **constant of the motion**, and is therefore very important in the specification of the quantum states of the atom.[1]

The classical definition of angular momentum is:

$$\boldsymbol{L} = \boldsymbol{r} \times \boldsymbol{p} \,. \tag{2.6}$$

For circular orbits this simplifies to $L = mvr$, and in Bohr's model, L was quantized in integer units of $\hbar$. (See eqn 1.7.) However, the full quantum treatment is more complicated, and requires the introduction of two other quantum numbers l and m_l, as we shall now see.

The components of $\boldsymbol{L}$ are given by

$$\begin{pmatrix} L_x \\ L_y \\ L_z \end{pmatrix} = \begin{pmatrix} x \\ y \\ z \end{pmatrix} \times \begin{pmatrix} p_x \\ p_y \\ p_z \end{pmatrix} = \begin{pmatrix} yp_z - zp_y \\ zp_x - xp_z \\ xp_y - yp_x \end{pmatrix} \,. \tag{2.7}$$

In quantum mechanics we represent the linear momentum by differential operators of the type

$$\hat{p}_x = -i\hbar \frac{\partial}{\partial x} \,. \tag{2.8}$$

Therefore, the quantum mechanical operators for the angular momentum are given by:

$$\hat{L}_x = \frac{\hbar}{i}\left(y\frac{\partial}{\partial z} - z\frac{\partial}{\partial y}\right) \tag{2.9}$$

$$\hat{L}_y = \frac{\hbar}{i}\left(z\frac{\partial}{\partial x} - x\frac{\partial}{\partial z}\right) \tag{2.10}$$

$$\hat{L}_z = \frac{\hbar}{i}\left(x\frac{\partial}{\partial y} - y\frac{\partial}{\partial x}\right) \,. \tag{2.11}$$

Note that the "hat" symbol indicates that we are representing an operator and not just a number.

The magnitude of the angular momentum is given by:

$$L^2 = L_x^2 + L_y^2 + L_z^2 \,.$$

We therefore define the quantum mechanical operator $\hat{\boldsymbol{L}}^2$ by

$$\hat{\boldsymbol{L}}^2 = \hat{L}_x^2 + \hat{L}_y^2 + \hat{L}_z^2 \,. \tag{2.12}$$

Note that operators like $\hat{L}_x^2$ should be understood in terms of repeated operations:

$$\begin{aligned} \hat{L}_x^2\psi &= -\hbar^2\left(y\frac{\partial}{\partial z} - z\frac{\partial}{\partial y}\right)\left(y\frac{\partial\psi}{\partial z} - z\frac{\partial\psi}{\partial y}\right) \\ &= -\hbar^2\left(y^2\frac{\partial^2\psi}{\partial z^2} - y\frac{\partial\psi}{\partial y} - z\frac{\partial\psi}{\partial z} - 2yz\frac{\partial^2\psi}{\partial y\partial z} + z^2\frac{\partial^2\psi}{\partial y^2}\right) \,. \end{aligned}$$

It can be shown that the components of the angular momentum operator do not commute, that is

$$\hat{L}_x\hat{L}_y \neq \hat{L}_y\hat{L}_x \,.$$

In fact we can show that:

$$[\hat{L}_x, \hat{L}_y] = i\hbar\hat{L}_z \,, \tag{2.13}$$

where the "commutator bracket" $[\hat{L}_x, \hat{L}_y]$ is defined by

$$[\hat{L}_x, \hat{L}_y] = \hat{L}_x\hat{L}_y - \hat{L}_y\hat{L}_x \,. \tag{2.14}$$

The other commutators of the angular momentum operators, namely $[\hat{L}_y, \hat{L}_z]$ and $[\hat{L}_z, \hat{L}_x]$ are obtained by cyclic permutation of the indices in Eq. 2.13: $x \to y$, $y \to z$, $z \to x$.

[1] The starting approximation for the treatment of multi-electron atoms is the **central field approximation** in which we assume that the dominant force is radial (i.e. pointing centrally towards the nucleus), so that the potential only depends on r. (See Section 4.1.) In this case the torque is also zero, so that again the angular momentum is constant.

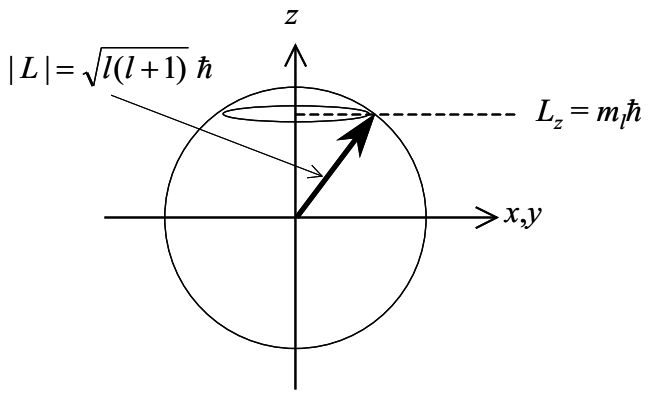

Figure 2.1: Vector model of the angular momentum in an atom. The angular momentum is represented by a vector of length $\sqrt{l(l+1)}\hbar$ precessing around the z-axis so that the z-component is equal to $m_l\hbar$.

This rather esoteric point has deep significance. If two quantum mechanical operators do not commute, then it is not possible to know their values simultaneously. Consider, for example, the operators for position and momentum in a one-dimensional system:

$$[\hat{x},\hat{p}]\psi = (\hat{x}\hat{p} - \hat{p}\hat{x})\psi = -i\hbar\, x\left(\frac{\mathrm{d}\psi}{\mathrm{d}x}\right) + i\hbar\frac{\mathrm{d}(x\psi)}{\mathrm{d}x} = i\hbar\psi\,.$$

Thus we have:

$$[\hat{x},\hat{p}] = i\hbar \;\neq\; 0\,. \tag{2.15}$$

The fact that $[\hat{x},\hat{p}] \neq 0$ means that the operators do not commute. This is intrinsically linked to the fact that we cannot measure precise values for the position and momentum simultaneously, which we know from the Heisenberg uncertainty principle. The argument based on commutators is thus a more formal way of understanding uncertainty products.

In the case of the angular momentum operators, the fact that $\hat{L}_x$, $\hat{L}_y$ and $\hat{L}_z$ do not commute means that we can only know *one* of the components of $\hat{\boldsymbol{L}}$ at any time. If we know the value of L_z, we cannot know L_x and L_y as well. However, we *can* know the length of the angular momentum vector, because we can show that $\hat{L}^2$ and $\hat{L}_z$ commute. In summary:

- We can know the length of the angular momentum vector L and one of its components.
- For mathematical convenience, we usually take the component we know to be the z component, ie L_z.
- We cannot know the values of all three components of the angular momentum simultaneously.

This is represented pictorially in the **vector model** of the atom shown in figure 2.1. In this model the angular momentum is represented as a vector of length $\sqrt{l(l+1)}\hbar$ precessing around the z axis so that the component along that axis is equal to $m_l\hbar$. The x and y components of the angular momentum are not known.

In spherical polar co-ordinates, the two key angular momentum operators are given by:

$$\hat{L}_z = \frac{\hbar}{i}\frac{\partial}{\partial\phi} \tag{2.16}$$

and

$$\hat{\boldsymbol{L}}^2 = -\hbar^2\left[\frac{1}{\sin\theta}\frac{\partial}{\partial\theta}\left(\sin\theta\frac{\partial}{\partial\theta}\right) + \frac{1}{\sin^2\theta}\frac{\partial^2}{\partial\phi^2}\right]. \tag{2.17}$$

It is easy to see that the Schrödinger equation given in Eq. 2.3 can be re-written as follows:

$$-\frac{\hbar^2}{2m}\frac{1}{r^2}\frac{\partial}{\partial r}\left(r^2\frac{\partial\Psi}{\partial r}\right) + \frac{\hat{\boldsymbol{L}}^2}{2mr^2}\Psi - \frac{Ze^2}{4\pi\epsilon_0 r}\Psi = E\;\Psi\,. \tag{2.18}$$

The eigenfunctions of the angular momentum operator are found by solving the equation:

$$\hat{\boldsymbol{L}}^2 F(\theta,\phi) \equiv -\hbar^2\left[\frac{1}{\sin\theta}\frac{\partial}{\partial\theta}\left(\sin\theta\frac{\partial}{\partial\theta}\right) + \frac{1}{\sin^2\theta}\frac{\partial^2}{\partial\phi^2}\right]F(\theta,\phi) = CF(\theta,\phi)\,. \tag{2.19}$$

For reasons that will become clearer later, the constant C is usually written in the form:

$$C = l(l+1)\hbar^2 \,. \tag{2.20}$$

At this stage, l can take any value, real or complex. We can separate the variables by writing:

$$F(\theta, \phi) = \Theta(\theta)\Phi(\phi) \,. \tag{2.21}$$

On substitution into eqn 2.19 and cancelling the common factor of $\hbar^2$, we find:

$$-\frac{1}{\sin\theta}\frac{\mathrm{d}}{\mathrm{d}\theta}\left(\sin\theta\frac{\mathrm{d}\Theta}{\mathrm{d}\theta}\right)\Phi - \frac{1}{\sin^2\theta}\Theta\frac{\mathrm{d}^2\Phi}{\mathrm{d}\phi^2} = l(l+1)\Theta\Phi \,. \tag{2.22}$$

Multiply by $-\sin^2\theta/\Theta\Phi$ and re-arrange to obtain:

$$\frac{\sin\theta}{\Theta}\frac{\mathrm{d}}{\mathrm{d}\theta}\left(\sin\theta\frac{\mathrm{d}\Theta}{\mathrm{d}\theta}\right) + \sin^2\theta\, l(l+1) = -\frac{1}{\Phi}\frac{\mathrm{d}^2\Phi}{\mathrm{d}\phi^2} \,. \tag{2.23}$$

The left hand side is a function of θ only, while the right hand side is a function of ϕ only. The equation must hold for all values of the θ and ϕ and hence both sides must be equal to a constant. On writing this arbitrary separation constant m^2, we then find:[2]

$$\sin\theta\frac{\mathrm{d}}{\mathrm{d}\theta}\left(\sin\theta\frac{\mathrm{d}\Theta}{\mathrm{d}\theta}\right) + l(l+1)\sin^2\theta\,\Theta = m^2\Theta \,, \tag{2.24}$$

and

$$\frac{\mathrm{d}^2\Phi}{\mathrm{d}\phi^2} = -m^2\Phi \,. \tag{2.25}$$

The equation in ϕ is easily solved to obtain:

$$\Phi(\phi) = A\mathrm{e}^{\mathrm{i}m\phi} \,. \tag{2.26}$$

The wave function must have a single value for each value of ϕ, and hence we require:

$$\Phi(\phi + 2\pi) = \Phi(\phi) \,, \tag{2.27}$$

which requires that the separation constant m must be an integer. Using this fact in eqn 2.24, we then have to solve

$$\sin\theta\frac{\mathrm{d}}{\mathrm{d}\theta}\left(\sin\theta\frac{\mathrm{d}\Theta}{\mathrm{d}\theta}\right) + [l(l+1)\sin^2\theta - m^2]\,\Theta = 0 \,, \tag{2.28}$$

with the constraint that m must be an integer. On making the substitution $u = \cos\theta$ and writing $\Theta(\theta) = P(u)$, eqn 2.28 becomes:

$$\frac{\mathrm{d}}{\mathrm{d}u}\left((1-u^2)\frac{\mathrm{d}P}{\mathrm{d}u}\right) + \left[l(l+1) - \frac{m^2}{1-u^2}\right]P = 0 \,. \tag{2.29}$$

Equation 2.29 is known as either the Legendre equation or the associated Legendre equation, depending on whether m is zero or not. Solutions only exist if l is an integer $\geq |m|$ and $P(u)$ is a polynomial function of u. This means that the solutions to eqn 2.28 are of the form:

$$\Theta(\theta) = P_l^m(\cos\theta) \,, \tag{2.30}$$

where $P_l^m(\cos\theta)$ is a polynomial function in $\cos\theta$ called the (associated) **Legendre polynomial** function.

Putting this all together, we then find:

$$F(\theta, \phi) = \text{normalization constant} \times P_l^m(\cos\theta)\,\mathrm{e}^{\mathrm{i}m\phi} \,, \tag{2.31}$$

where m and l are integers, and m can have values from $-l$ to $+l$. The correctly normalized functions are called the **spherical harmonic** functions $Y_{l,m}(\theta, \phi)$.

[2]Be careful not to confuse the magnetic quantum number m with the reduced mass that has the same symbol! Note also that a subscript l is often added (i.e. m_l) to distinguish it from the quantum number for the z-component of the spin (m_s).

l	m	$Y_{l,m}(\theta,\phi)$
0	0	$\sqrt{\frac{1}{4\pi}}$
1	0	$\sqrt{\frac{3}{4\pi}}\cos\theta$
1	±1	$\mp\sqrt{\frac{3}{8\pi}}\sin\theta e^{\pm i\phi}$
2	0	$\sqrt{\frac{5}{16\pi}}(3\cos^2\theta-1)$
2	±1	$\mp\sqrt{\frac{15}{8\pi}}\sin\theta\cos\theta e^{\pm i\phi}$
2	±2	$\sqrt{\frac{15}{32\pi}}\sin^2\theta e^{\pm 2i\phi}$

Table 2.1: Spherical harmonic functions.

It is apparent from eqns 2.19 and 2.20 that the spherical harmonics satisfy:

$$\hat{\boldsymbol{L}}^2 Y_{l,m}(\theta,\phi) = l(l+1)\hbar^2 Y_{l,m}(\theta,\phi)\,. \tag{2.32}$$

Furthermore, on substituting from eqn 2.16, it is also apparent that

$$\hat{L}_z Y_{l,m}(\theta,\phi) = m\hbar Y_{l,m}(\theta,\phi)\,. \tag{2.33}$$

The integers l and m that appear here are called the orbital and magnetic quantum numbers respectively. Some of the spherical harmonic functions are listed in Table 2.1. Equations 2.32–2.33 show that the magnitude of the angular momentum and its z-component are equal to $\sqrt{l(l+1)}\hbar$ and $m\hbar$ respectively, as consistent with Fig. 2.1.

The spherical harmonics have the property that:

$$\int_{\theta=0}^{\pi}\int_{\phi=0}^{2\pi} Y^*_{l,m}(\theta,\phi)Y_{l',m'}(\theta,\phi)\,\sin\theta\,\mathrm{d}\theta\mathrm{d}\phi = \delta_{l,l'}\delta_{m,m'}\,. \tag{2.34}$$

The symbol $\delta_{k,k'}$ is called the **Kronecker delta function**. It has the value of 1 if $k = k'$ and 0 if $k \neq k'$. The $\sin\theta$ factor in Eq. 2.34 comes from the volume increment in spherical polar co-ordinates: see Eq. 2.49 below.

2.3 Separation of variables in the Schrödinger equation

The Coulomb potential is an example of a **central field**. This means that the force only lies along the radial direction. This allows us separate the motion into the radial and angular parts. Hence we write:

$$\Psi(r,\theta,\phi) = R(r)\,Y(\theta,\phi)\,. \tag{2.35}$$

On substituting this into Eq. 2.18, we find

$$-\frac{\hbar^2}{2m}\frac{1}{r^2}\frac{\mathrm{d}}{\mathrm{d}r}\left(r^2\frac{\mathrm{d}R}{\mathrm{d}r}\right)Y + R\frac{\hat{\boldsymbol{L}}^2 Y}{2mr^2} - \frac{Ze^2}{4\pi\epsilon_0 r}RY = E\,RY\,. \tag{2.36}$$

Multiply by r^2/RY and re-arrange to obtain:

$$-\frac{\hbar^2}{2m}\frac{1}{R}\frac{\mathrm{d}}{\mathrm{d}r}\left(r^2\frac{\mathrm{d}R}{\mathrm{d}r}\right) - \frac{Ze^2 r}{4\pi\epsilon_0} - Er^2 = -\frac{1}{Y}\frac{\hat{\boldsymbol{L}}^2 Y}{2m}\,. \tag{2.37}$$

The left hand side is a function of r only, while the right hand side is only a function of the angular co-ordinates θ and ϕ. The only way this can be true is if both sides are equal to a constant. Let's call

this constant $-\hbar^2\ell(\ell+1)/2m$, where ℓ is an arbitrary number at this stage. This gives us, after a bit of re-arrangement:

$$-\frac{\hbar^2}{2m}\frac{1}{r^2}\frac{\mathrm{d}}{\mathrm{d}r}\left(r^2\frac{\mathrm{d}R(r)}{\mathrm{d}r}\right)+\frac{\hbar^2\ell(\ell+1)}{2mr^2}R(r)-\frac{Ze^2}{4\pi\epsilon_0 r}R(r)=ER(r)\,, \tag{2.38}$$

and

$$\hat{\boldsymbol{L}}^2Y(\theta,\phi)=\hbar^2\ell(\ell+1)Y(\theta,\phi)\,. \tag{2.39}$$

On comparing Eqs. 2.32 and 2.39 we can now identify the arbitrary separation constant ℓ with the angular momentum quantum number l, and we can see that the function $Y(\theta,\phi)$ that enters Eq. 2.39 must be one of the spherical harmonics.

We can tidy up the radial equation Eq. 2.38 by writing:

$$R(r)=\frac{P(r)}{r}\,.$$

This gives:

$$\left[-\frac{\hbar^2}{2m}\frac{\mathrm{d}^2}{\mathrm{d}r^2}+\frac{\hbar^2 l(l+1)}{2mr^2}-\frac{Ze^2}{4\pi\epsilon_0 r}\right]P(r)=EP(r)\,. \tag{2.40}$$

This now makes physical sense. It is a Schrödinger equation of the form:

$$\hat{H}P(r)=EP(r)\,, \tag{2.41}$$

where the energy operator $\hat{H}$ (i.e. the Hamiltonian) is given by:

$$\hat{H}=-\frac{\hbar^2}{2m}\frac{\mathrm{d}^2}{\mathrm{d}r^2}+V_{\text{effective}}(r)\,. \tag{2.42}$$

The first term in eqn 2.42 is the **radial kinetic energy** given by

$$\text{K.E.}_{\text{radial}}=\frac{p_r^2}{2m}=-\frac{\hbar^2}{2m}\frac{\mathrm{d}^2}{\mathrm{d}r^2}\,.$$

The second term is the **effective potential energy**:

$$V_{\text{effective}}(r)=\frac{\hbar^2 l(l+1)}{2mr^2}-\frac{Ze^2}{4\pi\epsilon_0 r}\,, \tag{2.43}$$

which has two components. The first of these is the orbital kinetic energy given by:

$$\text{K.E.}_{\text{orbital}}=\frac{L^2}{2I}=\frac{\hbar^2 l(l+1)}{2mr^2}\,,$$

where $I\equiv mr^2$ is the moment of inertia. The second is the usual potential energy due to the Coulomb energy.

This analysis shows that the quantized orbital motion adds quantized kinetic energy to the radial motion. For $l>0$ the orbital kinetic energy will always be larger than the Coulomb energy at small r, and so the effective potential energy will be positive. This has the effect of keeping the electron away from the nucleus, and explains why states with $l>0$ have nodes at the origin (see below).

2.4 The wave functions and energies

The wave function we require is given by Eq. 2.35. We have seen above that the $Y(\theta,\phi)$ function that appears in Eq. 2.35 must be one of the spherical harmonics, some of which are listed in Table 2.1. The radial wave function $R(r)$ can be found by solving the radial differential equation given in Eq. 2.38. The mathematics is somewhat complicated and is considered in Section 2.5. Here we just quote the main results.

Solutions are only found if we introduce an integer quantum number n. The energy depends only on n, but the functional form of $R(r)$ depends on both n and l, and so we must write the radial wave function as $R_{nl}(r)$. A list of some of the radial functions is given in Table 2.2. Representative wave functions are plotted in Fig. 2.2.

We can now write the full wave function as:

$$\Psi_{nlm}(r,\theta,\phi)=R_{nl}(r)Y_{lm}(\theta,\phi)\,. \tag{2.44}$$

The quantum numbers must obey the following rules:

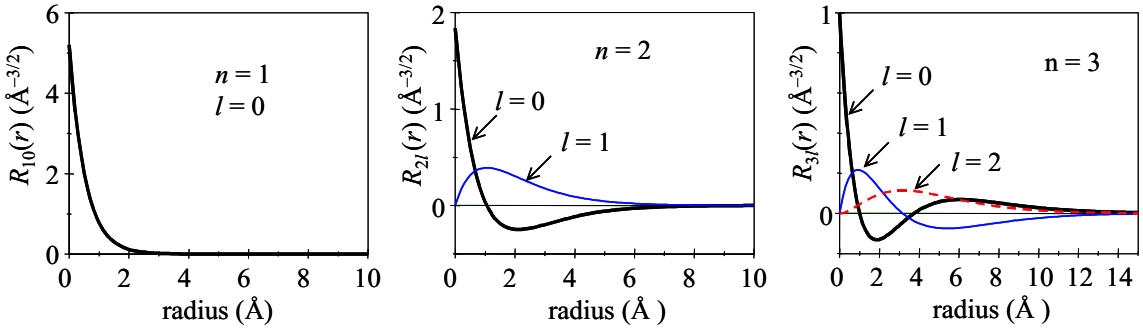

Figure 2.2: The radial wave functions $R_{nl}(r)$ for the hydrogen atom with $Z = 1$. Note that the axes for the three graphs are not the same.

n	l	$R_{nl}(r)$
1	0	$(Z/a_0)^{\frac{3}{2}} 2 \exp(-Zr/a_0)$
2	0	$(Z/2a_0)^{\frac{3}{2}} 2 \left(1 - \frac{Zr}{2a_0}\right) \exp(-Zr/2a_0)$
2	1	$(Z/2a_0)^{\frac{3}{2}} \frac{2}{\sqrt{3}} \left(\frac{Zr}{2a_0}\right) \exp(-Zr/2a_0)$
3	0	$(Z/3a_0)^{\frac{3}{2}} 2 \left[1 - (2Zr/3a_0) + \frac{2}{3}\left(\frac{Zr}{3a_0}\right)^2\right] \exp(-Zr/3a_0)$
3	1	$(Z/3a_0)^{\frac{3}{2}} (4\sqrt{2}/3) \left(\frac{Zr}{3a_0}\right) \left(1 - \frac{1}{2}\frac{Zr}{3a_0}\right) \exp(-Zr/3a_0)$
3	2	$(Z/3a_0)^{\frac{3}{2}} (2\sqrt{2}/3\sqrt{5}) \left(\frac{Zr}{3a_0}\right)^2 \exp(-Zr/3a_0)$

Table 2.2: Radial wave functions of the hydrogen atom. a_0 is the Bohr radius (5.29×10^{-11} m). The wave functions are normalized so that $\int_{r=0}^{\infty} R_{nl}^* R_{nl} r^2 dr = 1$.

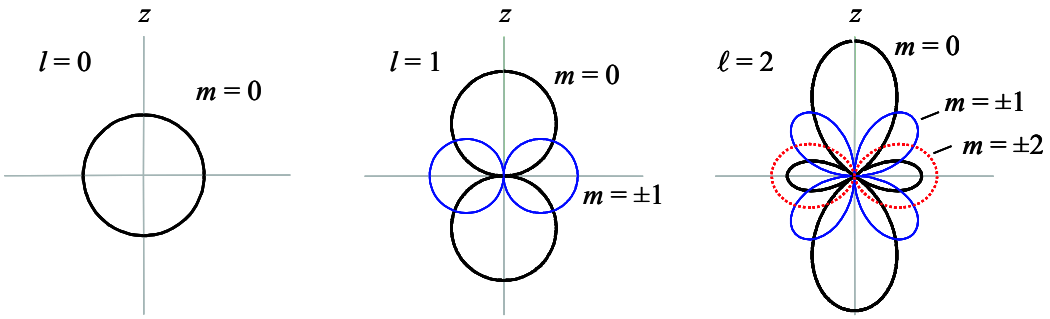

Figure 2.3: Polar plots of the spherical harmonics with $l \leq 2$. The plots are to be imagined with spherical symmetry about the z axis. In these polar plots, the value of the function for a given angle θ is plotted as the distance from the origin. Prettier pictures may be found, for example, at: `http://mathworld.wolfram.com/SphericalHarmonic.html`.

- n can have any integer value ≥ 1.
- l can have integer values up to $(n-1)$.
- m can have integer values from $-l$ to $+l$.

These rules drop out of the mathematical solutions. Functions that do not obey these rules will not satisfy the Schrödinger equation for the hydrogen atom.

The radial wave functions listed in Table 2.2 are of the form:

$$R_{nl}(r) = C_{nl} \cdot (\text{polynomial in } r) \cdot \mathrm{e}^{-r/a}\,, \tag{2.45}$$

where $a = na_{\mathrm{H}}/Z$, a_{H} being the Bohr radius of Hydrogen, namely 5.29×10^{-11} m. C_{nl} is a normalization constant. The polynomial functions that drop out of the equations are polynomials of order $n-1$, and have $n-1$ nodes. If $l = 0$, all the nodes occur at finite r, but if $l > 0$, one of the nodes is at $r = 0$.

The angular part of the wave function is of the form (see eqn 2.31 and Table 2.1):

$$Y_{l,m}(\theta,\phi) = C'_{lm} \cdot P_l^m(\cos\theta) \cdot e^{im\phi}\,, \tag{2.46}$$

where $P_l^m(\cos\theta)$ is a Legendre polynomial, e.g. $P_1^1(\cos\theta) = \text{constant}$, $P_1^0(\cos\theta) = \cos\theta$, etc. C'_{lm} is another normalization constant. Representative polar wave functions are shown in figure 2.3.

The energy of the system is found to be:

$$E_n = -\frac{mZ^2e^4}{8\epsilon_0^2h^2}\frac{1}{n^2}\,, \tag{2.47}$$

which is the same as the Bohr formula given in Eq. 1.10. Note that this depends only on the principal quantum number n: all the l states for a given value of n are **degenerate** (i.e. have the same energy), even though the radial wave functions depend on both n and l. This degeneracy with respect to l is called "accidental", and is a consequence of the fact that the electrostatic energy has a precise $1/r$ dependence in hydrogen. In more complex atoms, the electrostatic energy will depart from a pure $1/r$ dependence due to the shielding effect of inner electrons. In this case, the gross energy depends on l as well as n, even before we start thinking of higher order fine structure effects. We shall see how this works in more detail when we consider the alkali atoms later.

The wave functions are nomalized so that

$$\int_{r=0}^{\infty}\int_{\theta=0}^{\pi}\int_{\phi=0}^{2\pi} \Psi^*_{n,l,m}\Psi_{n',l'm'}\,\mathrm{d}V = \delta_{n,n'}\delta_{l,l'}\delta_{m,m'} \tag{2.48}$$

where $\mathrm{d}V$ is the incremental volume element in spherical polar co-ordinates:

$$\mathrm{d}V = r^2\sin\theta\,\mathrm{d}r\mathrm{d}\theta\mathrm{d}\phi\,. \tag{2.49}$$

The radial probability function $P_{nl}(r)$ is the probability that the electron is found between r and $r+\mathrm{d}r$:

$$\begin{aligned} P_{nl}(r)\,\mathrm{d}r &= \int_{\theta=0}^{\pi}\int_{\phi=0}^{2\pi} \Psi^*\Psi\; r^2\sin\theta\mathrm{d}r\mathrm{d}\theta\mathrm{d}\phi \\ &= |R_{nl}(r)|^2\, r^2\,\mathrm{d}r\,. \end{aligned} \tag{2.50}$$

The factor of r^2 that appears here is just related to the surface area of the radial shell of radius r (i.e. $4\pi r^2$.) Some representative radial probability functions are sketched in Fig. 2.4. 3-D plots of the shapes of the atomic orbitals are available at: `http://www.shef.ac.uk/chemistry/orbitron/`.

Expectation values of measurable quantities are calculated as follows:

$$\langle A \rangle = \int\int\int \Psi^* A \Psi \, \mathrm{d}V \; . \tag{2.51}$$

Thus, for example, the expectation value of the radius is given by:

$$\begin{aligned} \langle r \rangle &= \int\int\int \Psi^* r \Psi \mathrm{d}V \\ &= \int_{r=0}^{\infty} R_{nl}^* r R_{nl} r^2 \mathrm{d}r \int_{\theta=0}^{\pi} \sin\theta \mathrm{d}\theta \int_{\phi=0}^{2\pi} \mathrm{d}\phi \\ &= \int_{r=0}^{\infty} R_{nl}^* r R_{nl} r^2 \mathrm{d}r \, . \end{aligned} \tag{2.52}$$

This gives:

$$\langle r \rangle = \frac{n^2 a_{\mathrm{H}}}{Z} \left(\frac{3}{2} - \frac{l(l+1)}{2n^2} \right) \; . \tag{2.53}$$

Note that this only approaches the Bohr value, namely $n^2 a_{\mathrm{H}}/Z$ (see eqn 1.15), for the states with $l = n-1$ at large n.

Reading

Demtröder, W., *Atoms, Molecules and Photons*, §4.3 – §5.1.
Haken, H. and Wolf, H.C., *The Physics of Atoms and Quanta*, chapter 10.
Phillips, A.C., *Introduction to Quantum Mechanics*, chapters 8 & 9.
Beisser, A., *Concepts of Modern Physics*, chapter 6.
Eisberg, R. and Resnick, R., *Quantum Physics*, chapter 7.

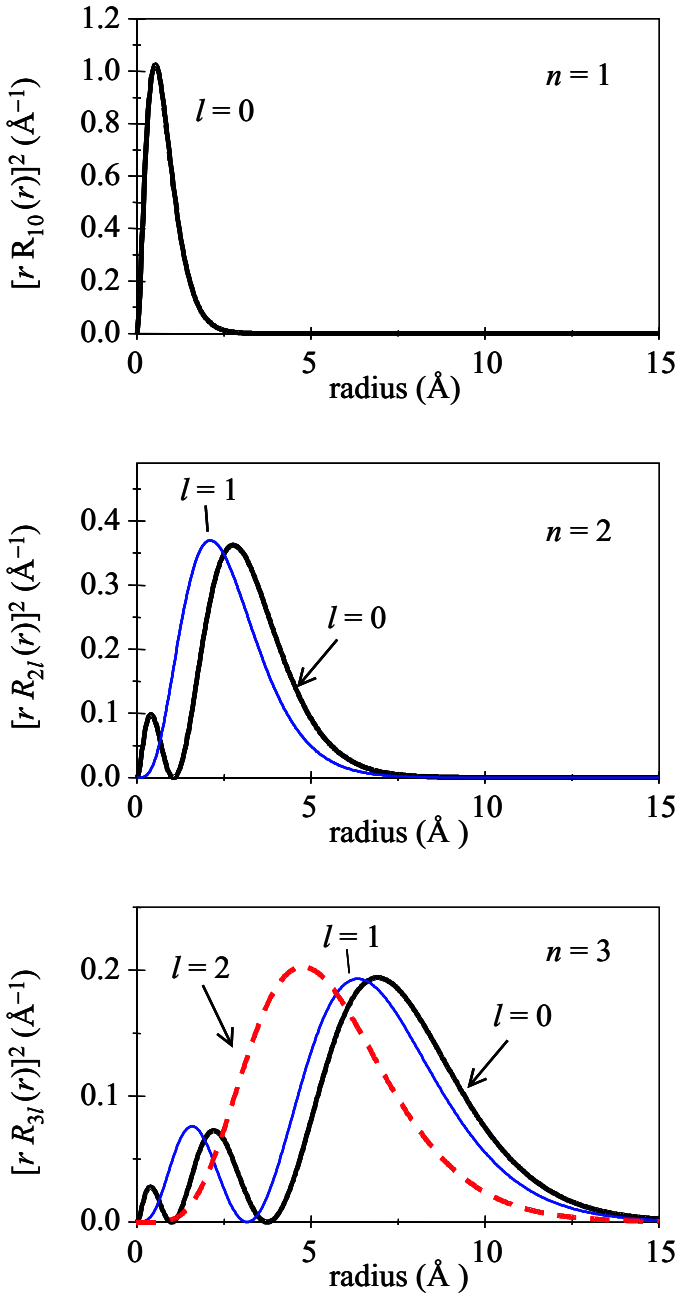

Figure 2.4: Radial probability functions for the first three n states of the hydrogen atom with $Z = 1$. Note that the radial probability is equal to $r^2|R_{nl}(r)|^2$, not just to $|R_{nl}(r)|^2$. Note also that the horizontal axes are the same for all three graphs, but not the vertical axes.

2.5 Appendix: Mathematical solution of the radial equation

The radial wave equation for hydrogen is given from eqn 2.38 as:

$$-\frac{\hbar^2}{2m}\frac{1}{r^2}\frac{\mathrm{d}}{\mathrm{d}r}\left(r^2\frac{\mathrm{d}R(r)}{\mathrm{d}r}\right)+\frac{\hbar^2 l(l+1)}{2mr^2}R(r)-\frac{Ze^2}{4\pi\epsilon_0 r}R(r)=ER(r)\,, \tag{2.54}$$

where l is an integer ≥ 0. We first put this in a more user-friendly form by introducing the dimensionless radius ρ according to:

$$\rho=\left(\frac{8m|E|}{\hbar^2}\right)^{1/2}r\,. \tag{2.55}$$

The modulus sign around E is important here because we are seeking bound solutions where E is negative. The radial equation now becomes:

$$\frac{\mathrm{d}^2R}{\mathrm{d}\rho^2}+\frac{2}{\rho}\frac{\mathrm{d}R}{\mathrm{d}\rho}-\left(\frac{l(l+1)}{\rho^2}+\frac{\lambda}{\rho}-\frac{1}{4}\right)R=0\,, \tag{2.56}$$

where

$$\lambda=\frac{1}{4\pi\epsilon_0}\frac{Ze^2}{\hbar}\left(\frac{m}{2|E|}\right)^{1/2}. \tag{2.57}$$

We first consider the behaviour at $\rho\to\infty$, where eqn 2.56 reduces to:

$$\frac{\mathrm{d}^2R}{\mathrm{d}\rho^2}-\frac{1}{4}R=0\,. \tag{2.58}$$

This has solutions of $\mathrm{e}^{\pm\rho/2}$. The $\mathrm{e}^{+\rho/2}$ solution cannot be normalized and is thus excluded, which implies that $R(\rho)\sim\mathrm{e}^{-\rho/2}$.

Now consider the bahaviour for $\rho\to 0$, where the dominant terms in eqn 2.56 are:

$$\frac{\mathrm{d}^2R}{\mathrm{d}\rho^2}+\frac{2}{\rho}\frac{\mathrm{d}R}{\mathrm{d}\rho}-\frac{l(l+1)}{\rho^2}R=0\,, \tag{2.59}$$

with solutions $R(\rho)=\rho^l$ or $R(\rho)=\rho^{-(l+1)}$. The latter diverges at the origin and is thus unacceptable.

The consideration of the asymptotic behaviours suggests that we should look for general solutions of the radial equation with $R(\rho)$ in the form:

$$R(\rho)=L(\rho)\,\rho^l\,\mathrm{e}^{-\rho/2}\,. \tag{2.60}$$

On substituting into eqn 2.56 we find:

$$\frac{\mathrm{d}^2L}{\mathrm{d}\rho^2}+\left(\frac{2l+2}{\rho}-1\right)\frac{\mathrm{d}L}{\mathrm{d}\rho}+\frac{\lambda-l-1}{\rho}L=0\,. \tag{2.61}$$

We now look for a series solution of the form:

$$L(\rho)=\sum_{k=0}^{\infty}a_k\rho^k\,. \tag{2.62}$$

Substitution into eqn 2.61 yields:

$$\sum_{k=0}^{\infty}\left[k(k-1)a_k\rho^{k-2}+\left(\frac{2l+2}{\rho}-1\right)ka_k\rho^{k-1}+\frac{\lambda-l-1}{\rho}a_k\rho^k\right]=0\,, \tag{2.63}$$

which can be re-written:

$$\sum_{k=0}^{\infty}\left[(k(k-1)+2k(l+1))a_k\rho^{k-2}+(\lambda-l-1-k)a_k\rho^{k-1}\right]=0\,, \tag{2.64}$$

or alternatively:

$$\sum_{k=0}^{\infty}\left[((k+1)k+2(k+1)(l+1))a_{k+1}\rho^{k-1}+(\lambda-l-1-k)a_k\rho^{k-1}\right]=0\,. \tag{2.65}$$

This will be satisfied if

$$((k+1)k + 2(k+1)(l+1))a_{k+1} + (\lambda - l - 1 - k)a_k = 0\,, \tag{2.66}$$

which implies:

$$\frac{a_{k+1}}{a_k} = \frac{-\lambda + l + 1 + k}{(k+1)(k+2l+2)}\,. \tag{2.67}$$

At large k we have:

$$\frac{a_{k+1}}{a_k} \sim \frac{1}{k}\,. \tag{2.68}$$

Now the series expansion of e^{ρ} is

$$\mathrm{e}^{\rho} = 1 + \rho + \frac{\rho^2}{2!} + \cdots \frac{\rho^k}{k!} + \cdots\,, \tag{2.69}$$

which has the same limit for a_{k+1}/a_k. With $R(\rho)$ given by eqn 2.60, we would then have a dependence of $\mathrm{e}^{+\rho} \cdot \mathrm{e}^{-\rho/2} = \mathrm{e}^{+\rho/2}$, which is unacceptable. We therefore conclude that the series expansion must terminate for some value of k. Let n_{r} be the value of k for which the series terminates. It then follows that $a_{n_{\mathrm{r}}+1} = 0$, which implies:

$$-\lambda + l + 1 + n_{\mathrm{r}} = 0\,, \qquad n_{\mathrm{r}} \geq 0\,, \tag{2.70}$$

or

$$\lambda = l + 1 + n_{\mathrm{r}}\,. \tag{2.71}$$

We now introduce the **principal quantum number** n according to:

$$n = n_{\mathrm{r}} + l + 1\,. \tag{2.72}$$

It follows that:

1. n is an integer,
2. $n \geq l + 1$,
3. $\lambda = n$.

The first two points establish the general rules for the quantum numbers n and l. The third one fixes the energy. On inserting $\lambda = n$ into eqn 2.57 and remembering that E is negative, we find:

$$E_n = -\frac{me^4}{(4\pi\epsilon_0)^2 2\hbar^2}\,\frac{Z^2}{n^2}\,. \tag{2.73}$$

This is the usual Bohr result. The wave functions are of the form given in eqn 2.60:

$$R(\rho) = \rho^l\, L(\rho)\, \mathrm{e}^{-\rho/2}\,. \tag{2.74}$$

The polynomial series $L(\rho)$ that satisfies eqn 2.61 is known as an **associated Laguerre function**. On substituting for ρ from eqn 2.55 with $|E|$ given by eqn 2.73, we then obtain:

$$R(r) = \text{normalization constant} \times \text{Laguerre polynomial in } r \times r^l \mathrm{e}^{-r/a} \tag{2.75}$$

as before (cf. eqn 2.45), with

$$a = \left(\frac{\hbar^2}{2m|E|}\right)^{1/2} = \frac{4\pi\epsilon_0\hbar^2}{me^2}\,\frac{n}{Z} \equiv \frac{n}{Z}a_{\mathrm{H}}\,, \tag{2.76}$$

where a_{H} is the Bohr radius of hydrogen.

Chapter 3

Radiative transitions

In this chapter we shall look at the classical and quantum theories of radiative emission and absorption. This will enable us to derive certain selection rules which determine whether a particular transition is allowed or not. We shall also investigate the physical mechanisms that affect the shape of the spectral lines that are observed in atomic spectra.

3.1 Classical theories of radiating dipoles

The classical theories of radiation by atoms were developed at the end of the 19^{th} century before the discoveries of the electron and the nucleus. With the benefit of hindsight, we can understand more clearly how the classical theory works. We model the atom as a heavy nucleus with electrons attached to it by springs with different spring constants, as shown in Fig. 3.1(a). The spring represents the binding force between the nucleus and the electrons, and the values of the spring constants determine the resonant frequencies of each of the electrons in the atom. Every atom therefore has several different natural frequencies.

The nucleus is heavy, and so it does not move very easily. However, the electrons can readily vibrate about their mean position, as illustrated in Fig. 3.1(b). The vibrations of the electron create a fluctuating **electric dipole**. In general, electric dipoles consist of two opposite charges of $\pm q$ separated by a distance d. The dipole moment $\boldsymbol{p}$ is defined by:

$$\boldsymbol{p} = q\boldsymbol{d} \,, \tag{3.1}$$

where $\boldsymbol{d}$ is a vector of length d pointing from $-q$ to $+q$. In the case of atomic dipoles, the positive charged is fixed, and so the time dependence of $\boldsymbol{p}$ is just determined by the movement of the electron:

$$p(t) = -ex(t) \,, \tag{3.2}$$

where $x(t)$ is the time dependence of the electron displacement.

It is well known that oscillating electric dipoles emit electromagnetic radiation at the oscillation frequency. This is how aerials work. Thus we expect an atom that has been excited into vibration to emit light waves at one of its natural resonant frequencies. This is the classical explanation of why atoms emit characteristic colours when excited electrically in a discharge tube. Furthermore, it is easy to see that an incoming light wave of frequency ω_0 can drive the natural vibrations of the atom through the oscillating force exerted on the electron by the electric field of the wave. This transfers energy from the light wave to the atom, which causes absorption at the resonant frequency. Hence the atom is also expected to absorb strongly at its natural frequency.

The classical theories actually have to assume that each electron has several natural frequencies of varying strengths in order to explain the observed spectra. If you do not do this, you end up predicting, for example, that hydrogen only has one emission frequency. There was no classical explanation of the origin of the atomic dipoles. It is therefore not surprising that we run into contradictions such as this when we try to patch up the model by applying our knowledge of electrons and nuclei gained by hindsight.

3.2 Quantum theory of radiative transitions

We have just seen that the classical model can explain why atoms emit and absorb light, but it does not offer any explanation for the frequency or the strength of the radiation. These can only be calculated

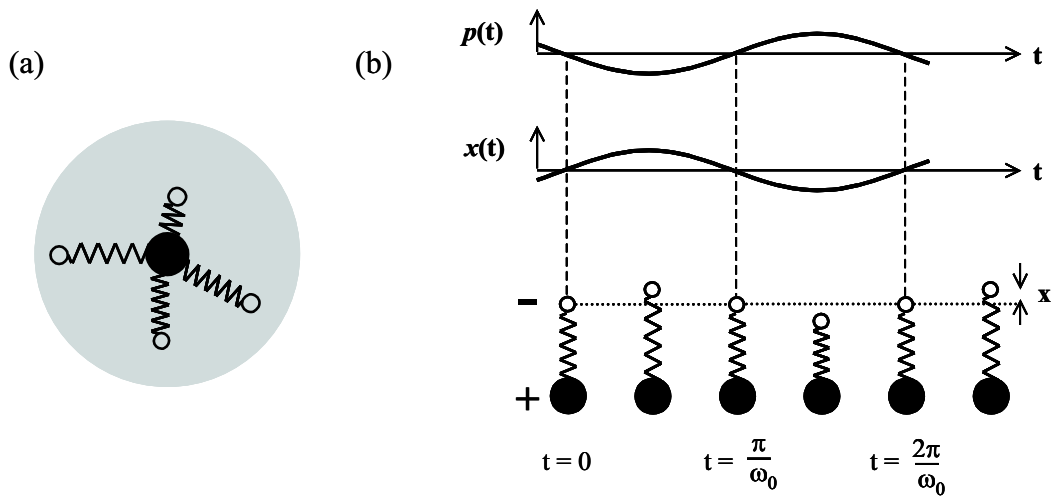

Figure 3.1: (a) Classical atoms consist of electrons bound to a heavy nucleus by springs with characteristic force constants. (b) The vibrations of an electron in an atom at its natural resonant frequency ω_0 creates an oscillating electric dipole. This acts like an aerial and emits electromagnetic waves at frequency ω_0. Alternatively, an incoming electromagnetic wave at frequency ω_0 can drive the oscillations at their resonant frequency. This transfers energy from the wave to the atom, which is equivalent to absorption.

by using quantum theory. Quantum theory tells us that atoms absorb or emit photons when they jump between quantized states, as shown in figure 3.2(a). The absorption or emission processes are called **radiative transitions**. The energy of the photon is equal to the difference in energy of the two levels:

$$h\nu = E_2 - E_1 \,. \tag{3.3}$$

Our task here is to calculate the *rate* at which these transitions occur.

The **transition rate** W_{12} can be calculated from the initial and final wave functions of the states involved by using **Fermi's golden rule**:

$$W_{12} = \frac{2\pi}{\hbar}|M_{12}|^2 g(h\nu)\,, \tag{3.4}$$

where M_{12} is the **matrix element** for the transition and $g(h\nu)$ is the **density of states**. The matrix element is equal to the overlap integral[1]:

$$M_{12} = \int \psi_2^*(\boldsymbol{r}) H'(\boldsymbol{r}) \psi_1(\boldsymbol{r})\, \mathrm{d}^3\boldsymbol{r}\,. \tag{3.5}$$

where H' is the **perturbation** that causes the transition. This represents the interaction between the atom and the light wave. There are a number of physical mechanisms that cause atoms to absorb or emit light. The strongest process is the electric dipole (E1) interaction. We therefore discuss E1 transitions first, leaving the discussion of higher order effects to Section 3.5.

The density of states factor is defined so that $g(h\nu)\mathrm{d}E$ is the number of *final* states per unit volume that fall within the energy range E to $E+\mathrm{d}E$, where $E = h\nu$. In the standard case of transitions between quantized levels in an atom, the initial and final electron states are *discrete*. In this case, the density of states factor that enters the golden rule is the density of *photon* states.[2] In free space, the photons can have any frequency and there is a continuum of states available, as illustrated in Fig. 3.2(b). The atom can therefore always emit a photon and it is the matrix element that determines the probability for this to occur. Hence we concentrate on the matrix element from now on.

3.3 Electric dipole (E1) transitions

Electric dipole transitions are the quantum mechanical equivalent of the classical dipole oscillator discussed in Section 3.1. We assume that the atom is irradiated with light, and makes a jump from level 1

[1] This is sometimes written in the shorthand **Dirac notation** as $M_{12} \equiv \langle 2|H'|1\rangle$.

[2] In solid-state physics, we consider transitions between electron *bands* rather than between discrete states. We then have to consider the density of electron states as well as the density of photon states when we calculate the transition rate. This point is covered in other courses, e.g. PHY475: Optical properties of solids.

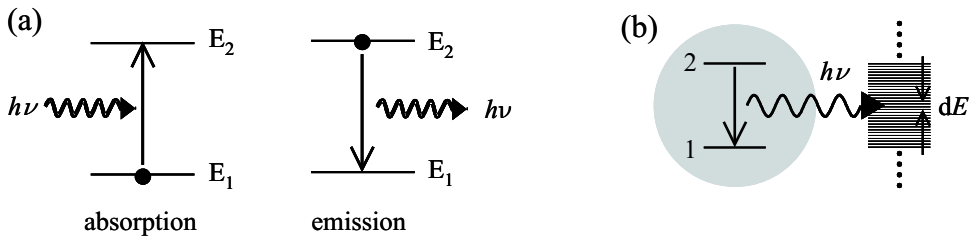

Figure 3.2: (a) Absorption and emission transitions in an atom. (b) Emission into a continuum of photon modes during a radiative transition between discrete atomic states.

to 2 by absorbing a photon. The interaction energy between an electric dipole $\boldsymbol{p}$ and an external electric field $\boldsymbol{\mathcal{E}}$ is given by

$$E = -\boldsymbol{p} \cdot \boldsymbol{\mathcal{E}} \,. \tag{3.6}$$

We presume that the nucleus is heavy, and so we only need to consider the effect on the electron. Hence the electric dipole perturbation is given by:

$$H' = +e\boldsymbol{r} \cdot \boldsymbol{\mathcal{E}} \,, \tag{3.7}$$

where $\boldsymbol{r}$ is the position vector of the electron and $\boldsymbol{\mathcal{E}}$ is the electric field of the light wave. This can be simplified to:

$$H' = e(x\mathcal{E}_x + y\mathcal{E}_y + z\mathcal{E}_z) \,, \tag{3.8}$$

where $\mathcal{E}_x$ is the component of the field amplitude along the x axis, etc. Now atoms are small compared to the wavelength of light, and so the amplitude of the electric field will not vary significantly over the dimensions of an atom. We can therefore take $\mathcal{E}_x$, $\mathcal{E}_y$, and $\mathcal{E}_z$ in Eq. 3.8 to be constants in the calculation, and just evaluate the following integrals:

$$\begin{aligned} M_{12} &\propto \int \psi_1 \, x \, \psi_2 \, \mathrm{d}^3\boldsymbol{r} \qquad x-\text{polarized light} \,, \\ M_{12} &\propto \int \psi_1 \, y \, \psi_2 \, \mathrm{d}^3\boldsymbol{r} \qquad y-\text{polarized light} \,, \\ M_{12} &\propto \int \psi_1 \, z \, \psi_2 \, \mathrm{d}^3\boldsymbol{r} \qquad z-\text{polarized light} \,. \end{aligned} \tag{3.9}$$

Integrals of this type are called **dipole moments**. The dipole moment is thus the key parameter that determines the transition rate for the electric dipole process.

At this stage it is helpful to give a hand-waving explanation for why electric dipole transitions lead to the emission of light. To do this we need to to consider the time-dependence of the quantum mechanical wave functions. This naturally drops out of the *time-dependent* Schrödinger equation:

$$\hat{H}(\boldsymbol{r})\Psi(\boldsymbol{r},t) = \mathrm{i}\hbar\frac{\partial}{\partial t}\Psi(\boldsymbol{r},t) \,, \tag{3.10}$$

where $\hat{H}(\boldsymbol{r})$ is the Hamiltonian of the system. The solutions of Eq. 3.10 are of the form:

$$\Psi(\boldsymbol{r},t) = \psi(\boldsymbol{r})\mathrm{e}^{-\mathrm{i}Et/\hbar} \,, \tag{3.11}$$

where $\psi(\boldsymbol{r})$ satisfies the *time-independent* Schrödinger equation:

$$\hat{H}(\boldsymbol{r})\psi(\boldsymbol{r}) = E\psi(\boldsymbol{r}) \,. \tag{3.12}$$

During a transition between two quantum states of energies E_1 and E_2, the electron will be in a superposition state with a mixed wave function given by

$$\begin{aligned} \Psi(\boldsymbol{r},t) &= c_1\Psi_1(\boldsymbol{r},t) + c_2\Psi_2(\boldsymbol{r},t) \\ &= c_1\psi_1(\boldsymbol{r})\mathrm{e}^{-\mathrm{i}E_1t/\hbar} + c_2\psi_2(\boldsymbol{r})\mathrm{e}^{-\mathrm{i}E_2t/\hbar} \,, \end{aligned} \tag{3.13}$$

where c_1 and c_2 are the mixing coefficients. The expectation value $\langle x \rangle$ of the position of the electron is given by:

$$\langle x \rangle = \int \Psi^* \, x \, \Psi \, \mathrm{d}^3\boldsymbol{r} \,. \tag{3.14}$$

Quantum number	Selection rule	
parity	changes	
l	$\Delta l = \pm 1$	
m	$\Delta m = 0, \pm 1$	unpolarized light
	$\Delta m = 0$	linear polarization $\parallel z$
	$\Delta m = \pm 1$	linear polarization in (x, y) plane
	$\Delta m = +1$	σ^+ circular polarization
	$\Delta m = -1$	σ^- circular polarization
s	$\Delta s = 0$	
m_s	$\Delta m_s = 0$	

Table 3.1: **Electric dipole selection rules** for the quantum numbers of the states involved in the transition.

With Ψ given by Eq. 3.13 we obtain:

$$\begin{aligned} \langle x \rangle &= c_1^* c_1 \int \psi_1^* \, x \, \psi_1 \, \mathrm{d}^3\boldsymbol{r} + c_2^* c_2 \int \psi_2^* \, x \, \psi_2 \, \mathrm{d}^3\boldsymbol{r} \\ &+ c_1^* c_2 \mathrm{e}^{-\mathrm{i}(E_2 - E_1)t/\hbar} \int \psi_1^* \, x \, \psi_2 \, \mathrm{d}^3\boldsymbol{r} \; + \; c_2^* c_1 \mathrm{e}^{-\mathrm{i}(E_1 - E_2)t/\hbar} \int \psi_2^* \, x \, \psi_1 \, \mathrm{d}^3\boldsymbol{r} \, . \end{aligned} \tag{3.15}$$

This shows that if the dipole moment defined in Eq. 3.9 is non-zero, then the electron wave-packet oscillates in space at angular frequency $(E_2 - E_1)/\hbar$. The oscillation of the electron wave packet creates an oscillating electric dipole, which then radiates light at angular frequency $(E_2 - E_1)/\hbar$. Hey presto!

3.4 Selection rules for E1 transitions

Electric dipole transitions can only occur if the **selection rules** summarized in Table 3.1 are satisfied. Transitions that obey these E1 selection rules are called **allowed** transitions. If the selection rules are not satisfied, the matrix element (i.e. the dipole moment) is zero, and we then see from Eq. 3.4 that the transition rate is zero. The origins of these rules are discussed below.

Parity

The parity of a function refers to the sign change under inversion about the origin. Thus if $f(-x) = f(x)$ we have even parity, whereas if $f(-x) = -f(x)$ we have odd parity. Now atoms are spherically symmetric, which implies that

$$|\psi(-\boldsymbol{r})|^2 = |\psi(+\boldsymbol{r})|^2 \, . \tag{3.16}$$

Hence we must have that

$$\psi(-\boldsymbol{r}) = \pm\psi(+\boldsymbol{r}) \, . \tag{3.17}$$

In other words, the wave functions have either even or odd parity. The dipole moment of the transition is given by Eq. 3.9. x, y and z are odd functions, and so the product $\psi_1\psi_2$ must be an odd function if M_{12} is to be non-zero. Hence ψ_1 and ψ_2 must have different parities.

The orbital quantum number l

The parity of the spherical harmonic functions is equal to $(-1)^l$. Hence the parity selection rule implies that Δl must be an odd number. Detailed evaluation of the overlap integrals tightens this rule to $\Delta l = \pm 1$. This can be seen as a consequence of the fact that the angular momentum of a photon is $\pm\hbar$, with the sign depending on whether we have a left or right circularly polarized photon. Conservation of angular momentum therefore requires that the angular momentum of the atom must change by one unit.

The magnetic quantum number m

The dipole moment for the transition can be written out explicitly:

$$M_{12} \propto \int_{r=0}^{\infty}\int_{\theta=0}^{\pi}\int_{\phi=0}^{2\pi} \Psi^*_{n',l',m'}\, \boldsymbol{r}\, \Psi_{n,l,m}\, r^2 \sin\theta \,\mathrm{d}r\mathrm{d}\theta\mathrm{d}\phi\,. \tag{3.18}$$

We consider here just the ϕ part of this integral:

$$M_{12} \propto \int_0^{2\pi} \mathrm{e}^{-\mathrm{i}m'\phi}\, \boldsymbol{r}\, \mathrm{e}^{\mathrm{i}m\phi}\,\mathrm{d}\phi\,, \tag{3.19}$$

where we have made use of the fact that (see Eq. 2.46 or Table 2.1):

$$\Psi_{n,l,m}(r,\theta,\phi) \propto \mathrm{e}^{\mathrm{i}m\phi}\,. \tag{3.20}$$

Now for z-polarized light we have from Eq. 3.9:

$$M_{12} \propto \int_0^{2\pi} \mathrm{e}^{-\mathrm{i}m'\phi}\, z\, \mathrm{e}^{\mathrm{i}m\phi}\,\mathrm{d}\phi \propto \int_0^{2\pi} \mathrm{e}^{-\mathrm{i}m'\phi}\cdot 1 \cdot \mathrm{e}^{\mathrm{i}m\phi}\,\mathrm{d}\phi\,, \tag{3.21}$$

because $z = r\cos\theta$. Hence we must have that $m' = m$ if M_{12} is to be non-zero. If the light is polarized in the (x, y) plane, we have integrals like

$$M_{12} \propto \int_0^{2\pi} \mathrm{e}^{-\mathrm{i}m'\phi}\, x\, \mathrm{e}^{\mathrm{i}m\phi}\,\mathrm{d}\phi \propto \int_0^{2\pi} \mathrm{e}^{-\mathrm{i}m'\phi}\cdot \mathrm{e}^{\pm\mathrm{i}\phi} \cdot \mathrm{e}^{\mathrm{i}m\phi}\,\mathrm{d}\phi\,. \tag{3.22}$$

This is because $x = r\sin\theta\cos\phi = r\sin\theta\frac{1}{2}(\mathrm{e}^{+\mathrm{i}\phi} + \mathrm{e}^{-\mathrm{i}\phi})$, and similarly for y. This give $m' - m = \pm 1$. This rule can be tightened up a bit by saying that $\Delta m = +1$ for σ^+ circularly polarized light and $\Delta m = -1$ for σ^- circularly polarized light. If the light is unpolarized, then all three linear polarizations are possible, and we can have $\Delta m = 0, \pm 1$.

Spin

The photon does not interact with the electron spin. Therefore, the spin state of the atom does not change during the transition. This implies that the spin quantum numbers s and m_s are unchanged.

3.5 Higher order transitions

How does an atom de-excite if E1 transitions are forbidden by the selection rules? In some cases it may be possible for the atom to de-excite by alternative methods. For example, the 3s → 1s transition is forbidden, but the atom can easily de-excite by two allowed E1 transitions, namely 3s → 2p, then 2p → 1s. However, this may not always be possible, and in these cases the atom must de-excite by making a **forbidden** transition. The use of the word "forbidden" is somewhat misleading here. It really means "electric-dipole forbidden". The transitions are perfectly possible, but they just occur at a slower rate.

After the electric-dipole interaction, the next two strongest interactions between the photon and the atom give rise to **magnetic dipole** (M1) and **electric quadrupole** (E2) transitions. There have different selection rules to E1 transitions (e.g. parity is conserved), and may therefore be allowed when when E1 transitions are forbidden. M1 and E2 transitions are second-order processes and have much smaller probabilities than E1 transitions.

In extreme cases it may happen that all types of radiative transitions are forbidden. In this case, the excited state is said to be **metastable**, and must de-excite by transferring its energy to other atoms in collisional processes or by multi-photon emission.

3.6 Radiative lifetimes

An atom in an excited state has a spontaneous tendency to de-excite by a radiative transition involving the emission of a photon. This follows from statistical physics: atoms with excess energy tend to want to get rid of it. This process is called **spontaneous emission**. Let us suppose that there are N_2 atoms

Transition	Einstein A coefficient	Radiative lifetime
E1 allowed	$10^8 - 10^9$ s^{-1}	1 – 10 ns
E1 forbidden (M1 or E2)	$10^3 - 10^6$ s^{-1}	1 μs – 1 ms

Table 3.2: Typical transition rates and radiative lifetimes for allowed and forbidden transitions at optical frequencies.

in level 2 at time t. We use quantum mechanics to calculate the transition rate from level 2 to level 1, and then write down a rate equation for N_2 as follows:

$$\frac{\mathrm{d}N_2}{\mathrm{d}t} = -AN_2\,. \tag{3.23}$$

This merely says that the total number of atoms making transitions is proportional to the number of atoms in the excited state and to the quantum mechanical probability. The parameter A that appears in eqn 3.23 is called the **Einstein A coefficient** of the transition.[3]

Equation 3.23 has the following solution:

$$\begin{aligned} N_2(t) &= N_2(0)\exp(-At) \\ &= N_2(0)\exp(-t/\tau)\,, \end{aligned} \tag{3.24}$$

where

$$\tau = \frac{1}{A}\,. \tag{3.25}$$

Equation 3.24 shows that if the atoms are excited into the upper level, the population will decay due to spontaneous emission with a time constant τ. τ is thus called the **natural radiative lifetime** of the excited state.

The values of the Einstein A coefficient and hence the radiative lifetime τ vary considerably from transition to transition. Allowed E1 transitions have A coefficients in the range $10^8 - 10^9\,\mathrm{s}^{-1}$ at optical frequencies, giving radiative lifetimes of $\sim 1 - 10\,\mathrm{ns}$. Forbidden transitions, on the other hand, are much slower because they are higher order processes. The radiative lifetimes for M1 and E2 transitions are typically in the millisecond or microsecond range. This point is summarized in Table 3.2.

3.7 The width and shape of spectral lines

The radiation emitted in atomic transitions is not perfectly monochromatic. The shape of the emission line is described by the **spectral line shape function** $g(\nu)$. This is a function that peaks at the line centre defined by

$$h\nu_0 = (E_2 - E_1)\,, \tag{3.26}$$

and is normalized so that:

$$\int_0^\infty g(\nu)\,\mathrm{d}\nu = 1\,. \tag{3.27}$$

The most important parameter of the line shape function is the **full width at half maximum** (FWHM) $\Delta\nu$, which quantifies the width of the spectral line. We shall see below how the different types of line broadening mechanisms give rise to two common line shape functions, namely the **Lorentzian** and **Gaussian** functions.

In a gas of atoms, spectral lines are broadened by three main processes:

- natural broadening,
- collision broadening,
- Doppler broadening.

[3]When we study laser physics in the second part of the course, we shall encounter the Einstein B coefficients that describe the processes of stimulated emission and absorption.

We shall look at each of these processes separately below. A useful general division can be made at this stage by classifying the broadening as either **homogeneous** or **inhomogeneous**.

- **Homogeneous** broadening affects all the individual atoms in the same way. Natural lifetime and collision broadening are examples of homogeneous processes. All the atoms are behaving in the same way, and each atom produces the same emission spectrum.
- **Inhomogeneous** broadening affects different individual atoms in different ways. Doppler broadening is the standard example of an inhomogeneous process. The individual atoms are presumed to behave identically, but they are moving at different velocities, and one can associate different parts of the spectrum with the subset of atoms with the appropriate velocity. Inhomogeneous broadening is also found in solids, where different atoms may experience different local environments due to the inhomogeneity of the medium.

3.8 Natural broadening

We have seen in Section 3.6 that the process of spontaneous emission causes the excited states of an atom to have a finite lifetime. Let us suppose that we somehow excite a number of atoms into level 2 at time $t = 0$. Equation 3.23 shows us that the rate of transitions is proportional to the instantaneous population of the upper level, and eqn 3.24 shows that this population decays exponentially. Thus the rate of atomic transitions decays exponentially with time constant τ. For every transition from level 2 to level 1, a photon of angular frequency $\omega_0 = (E_2 - E_1)/\hbar$ is emitted. Therefore a burst of light with an exponentially-decaying intensity will be emitted for $t > 0$:

$$I(t) = I(0) \exp(-t/\tau) \,. \tag{3.28}$$

This corresponds to a time dependent electric field of the form:

$$\begin{aligned} t < 0 : \qquad \mathcal{E}(t) &= 0 \,, \\ t \geq 0 : \qquad \mathcal{E}(t) &= \mathcal{E}_0 \, \mathrm{e}^{\mathrm{i}\omega_0 t} \, \mathrm{e}^{-t/2\tau} \,. \end{aligned} \tag{3.29}$$

The extra factor of 2 in the exponential in eqn 3.29 compared to eqn 3.28 arises because $I(t) \propto \mathcal{E}(t)^2$. We now take the Fourier transform of the electric field to derive the frequency spectrum of the burst:

$$\mathcal{E}(\omega) = \frac{1}{\sqrt{2\pi}} \int_{-\infty}^{+\infty} \mathcal{E}(t) \, \mathrm{e}^{\mathrm{i}\omega t} \, \mathrm{d}t \,. \tag{3.30}$$

The emission spectrum is then given by:

$$I(\omega) \propto \left| \mathcal{E}(\omega)^2 \right| \propto \frac{1}{(\omega - \omega_0)^2 + (1/2\tau)^2} \,. \tag{3.31}$$

Remembering that $\omega = 2\pi\nu$, we find the final result for the spectral line shape function:

$$g(\nu) = \frac{\Delta\nu}{2\pi} \, \frac{1}{(\nu - \nu_0)^2 + (\Delta\nu/2)^2} \,, \tag{3.32}$$

where the full width at half maximum is given by

$$\Delta\nu = \frac{1}{2\pi\tau} \,. \tag{3.33}$$

The spectrum described by eqn 3.32 is called a **Lorentzian** line shape. This function is plotted in Fig. 3.3. Note that we can re-write eqn 3.33 in the following form:

$$\Delta\nu \cdot \tau = \frac{1}{2\pi} \,. \tag{3.34}$$

By multiplying both sides by h, we can recast this as:

$$\Delta E \cdot \tau = h/2\pi \,. \tag{3.35}$$

If we realize that τ represents the average time the atom stays in the excited state (i.e the uncertainty in the time), we can interpret this as the **energy–time uncertainty principle**.

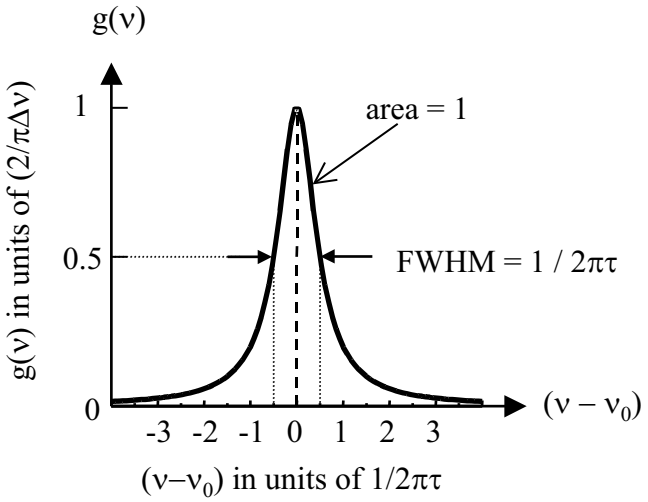

Figure 3.3: **The Lorentzian line shape**. The functional form is given in eqn 3.32. The function peaks at the line centre ν_0 and has an FWHM of $1/2\pi\tau$. The function is normalized so that the total area is unity.

3.9 Collision (Pressure) broadening

The atoms in a gas jostle around randomly and frequently collide into each other and the walls of the containing vessel. This interrupts the process of light emission and effectively shortens the lifetime of the excited state. This gives additional line broadening through the uncertainty principle, as determined by eqn 3.33 with τ replaced by τ_c, where τ_c is the mean time between collisions.

It can be shown from the kinetic theory of gases that the time between collisions in an ideal gas is given by:

$$\tau_c \sim \frac{1}{\sigma_s P}\left(\frac{\pi m k_B T}{8}\right)^{1/2}, \tag{3.36}$$

where σ_s is the collision cross-section, and P is the pressure. The collision cross-section is an effective area which determines whether two atoms will collide or not. It will be approximately equal to the size of the atom. For example, for sodium atoms we have:

$$\sigma_s \sim \pi r_{atom}^2 \sim \pi \times (0.2\,\mathrm{nm})^2 = 1.2 \times 10^{-19}\,\mathrm{m}^2\,.$$

Thus at S.T.P we find $\tau_c \sim 6 \times 10^{-10}\,\mathrm{s}$, which gives a line width of $\sim 1\,\mathrm{GHz}$. Note that τ_c is much shorter than typical radiative lifetimes. For example, the strong yellow D-lines in sodium have a radiative lifetime of 16 ns, which is nearly two orders of magnitude larger.

In conventional atomic discharge tubes, we reduce the effects of pressure broadening by working at low pressures. We see from eqn 3.36 that this increases τ_c, and hence reduces the linewidth. This is why we tend to use "low pressure" discharge lamps for spectroscopy.

3.10 Doppler broadening

The spectrum emitted by a typical gas of atoms in a low pressure discharge lamp is usually found to be much broader than the radiative lifetime would suggest, even when everything is done to avoid collisions. For example, the radiative lifetime for the 632.8 nm line in neon is 2.7×10^{-7} s. Equation 3.33 tells us that we should have a spectral width of 0.54 MHz. In fact, the line is about three orders of magnitude broader, and moreover, does not have the Lorentzian lineshape given by eqn 3.32.

The reason for this discrepancy is the thermal motion of the atoms. The atoms in a gas move about randomly with a root-mean-square thermal velocity given by:

$$\tfrac{1}{2} m v_x^2 = \tfrac{1}{2} k_B T\,, \tag{3.37}$$

where k_B is Boltzmann's constant. At room temperature the thermal velocities are quite large. For example, for sodium with a mass number of 23 we find $v_x \sim 330\,\mathrm{ms}^{-1}$ at 300 K. This random thermal

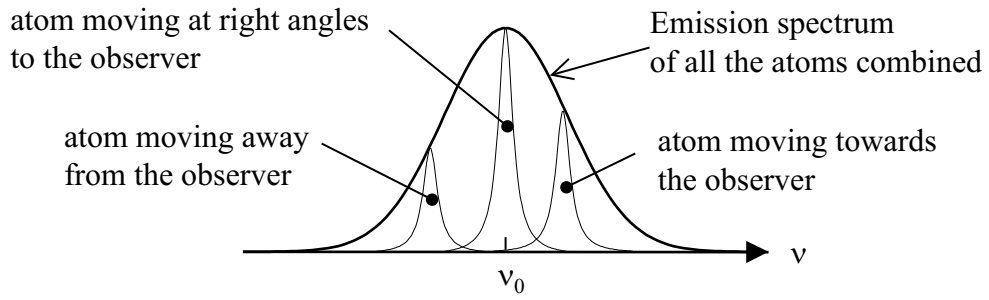

Figure 3.4: The Doppler broadening mechanism. The thermal motion of the atoms causes their frequency to be shifted by the Doppler effect.

motion of the atoms gives rise to Doppler shifts in the observed frequencies, which then cause line broadening, as illustrated in Fig. 3.4. This is Doppler line broadening mechanism.

Let us suppose that the atom is emitting light from a transition with centre frequency ν_0. An atom moving with velocity v_x will have its observed frequency shifted by the Doppler effect according to:

$$\nu = \nu_0 \left(1 \pm \frac{v_x}{c}\right) , \tag{3.38}$$

where the + and − sign apply to motion towards or away from the observer respectively. The number of atoms with a particular velocity $N(v_x)$ is given by the Maxwell-Boltzmann distribution:

$$N(v_x) = N_0 \left(\frac{2k_{\rm B}T}{\pi m}\right)^{1/2} \exp\left(-\frac{\frac{1}{2}mv_x^2}{k_{\rm B}T}\right) . \tag{3.39}$$

We can combine eqns 3.38 and 3.39, to find the number of atoms emitting at frequency ν:

$$N(\nu) = N_0 \left(\frac{2k_{\rm B}T}{\pi m}\right)^{1/2} \exp\left(-\frac{mc^2(\nu-\nu_0)^2}{2k_{\rm B}T\nu_0^2}\right) . \tag{3.40}$$

The frequency dependence of the light emitted is therefore given by:

$$I(\nu) \propto \exp\left(-\frac{mc^2(\nu-\nu_0)^2}{2k_{\rm B}T\nu_0^2}\right) . \tag{3.41}$$

This gives rise to a **Gaussian** line shape with $g(\nu)$ given by:

$$g(\nu) \propto \exp\left(-\frac{mc^2(\nu-\nu_0)^2}{2k_{\rm B}T\nu_0^2}\right) , \tag{3.42}$$

with a full width at half maximum equal to:

$$\Delta\nu_{\rm D} = 2\nu_0 \left(\frac{(2\ln 2)k_{\rm B}T}{mc^2}\right)^{1/2} = \frac{2}{\lambda}\left(\frac{(2\ln 2)k_{\rm B}T}{m}\right)^{1/2} . \tag{3.43}$$

The Doppler linewidth in a gas at S.T.P is usually several orders of magnitude larger than the natural linewidth. For example, the Doppler line width of the 632.8 nm line of neon at 300 K works out to be 1.3 GHz, i.e. three orders of magnitude larger than the broadening due to spontaneous emission. The dominant broadening mechanism in the emission spectrum of gases at room temperature is usually Doppler broadening, and the line shape is closer to Gaussian than Lorentzian. [4]

3.11 Atoms in solids

In laser physics we shall frequently be interested in the emission spectra of atoms in crystals. The spectra will be subject to lifetime broadening as in gases, since this is a fundamental property of radiative

[4]Since $\Delta\nu_{\rm D}$ is proportional to $\sqrt{T}$, we can reduce its value by cooling the gas. Cooling also reduces the collision broadening because $P \propto T$, and therefore $\tau_{\rm c} \propto T^{-1/2}$. (See eqn 3.36.) Laser cooling techniques can produce temperatures in the micro-Kelvin range, where we finally observe the natural line shape of the emission line.

emission. However, the atoms are locked in a lattice, and so collisional broadening is not relevant. Doppler broadening does not occur either, for the same reason. On the other hand, the emission lines can be broadened by other mechanisms.

In some cases it may be possible for the atoms to de-excite from the upper level to the lower level by making a **non-radiative transition**. One way this could happen is to drop to the lower level by emitting phonons (ie heat) instead of photons. To allow for this possibility, we must re-write eqn 3.23 in the following form:

$$\frac{\mathrm{d}N_2}{\mathrm{d}t} = -AN_2 - \frac{N_2}{\tau_{\mathrm{NR}}} = -\left(A + \frac{1}{\tau_{\mathrm{NR}}}\right) N_2 = -\frac{N_2}{\tau}\,, \tag{3.44}$$

where τ_{NR} is the non-radiative transition time. This shows that non-radiative transitions shorten the lifetime of the excited state according to:

$$\frac{1}{\tau} = A + \frac{1}{\tau_{\mathrm{NR}}}\,. \tag{3.45}$$

We thus expect additional lifetime broadening according to eqn 3.33. The phonon emission times in solids are often very fast, and can cause substantial broadening of the emission lines. This is the solid-state equivalent of collisional broadening.

Another factor that may cause line broadening is the inhomogeneity of the host medium, for example when the atoms are doped into a glass. If the environment in which the atoms find themselves is not entirely uniform, the emission spectrum will be affected through the interaction between the atom and the local environment. This is an example of an inhomogeneous broadening mechanism.

Reading

Demtröder, W., *Atoms, Molecules and Photons*, §7.1 – §7.4.
Haken, H. and Wolf, H.C., *The Physics of Atoms and Quanta*, chapter 16.
Smith, F.G. and King, T.A., *Optics and Photonics*, sections 13.1–4, 20.1–2
Beisser, A., *Concepts of Modern Physics*, sections 6.8–9
Eisberg, R. and Resnick, R., *Quantum Physics*, section 8.7.

Chapter 4

The shell model and alkali spectra

Everything we have been doing so far in this course applies to hydrogenic atoms. We have taken this approach because the hydrogen atom only contains two particles: the nucleus and the electron. This is a **two-body system** and can be solved exactly by separating the motion into the centre of mass and relative co-ordinates. This has allowed us to find the wave functions and understand the meaning of the quantum numbers n, l, m_l and m_s.

We are well aware, however, that hydrogen is only the first of about 100 elements. These are not two body problems: we have one nucleus and many electrons, which is a **many body problem**, with no exact solution. This chapter begins our consideration of the approximation techniques that are used to understand the behaviour of many-electron atoms.

4.1 The central field approximation

The Hamiltonian for an N-electron atom with nuclear charge $+Ze$ can be written in the form:

$$\hat{H} = \sum_{i=1}^{N} \left(-\frac{\hbar^2}{2m} \boldsymbol{\nabla}_i^2 - \frac{Ze^2}{4\pi\epsilon_0 r_i} \right) + \sum_{i>j}^{N} \frac{e^2}{4\pi\epsilon_0 r_{ij}} \,, \tag{4.1}$$

where $N = Z$ for a neutral atom. The subscripts i and j refer to individual electrons and $r_{ij} = |\boldsymbol{r}_i - \boldsymbol{r}_j|$. The first summation accounts for the kinetic energy of the electrons and their Coulomb interaction with the nucleus, while the second accounts for the electron-electron repulsion.

It is not possible to find an exact solution to the Schrödinger equation with a Hamiltonian of the form given by eqn 4.1, because the electron-electron repulsion term depends on the co-ordinates of two of the electrons, and so we cannot separate the wave function into a product of single-particle states. Furthermore, the electron-electron repulsion term is comparable in magnitude to the first summation, making it impossible to use perturbation theory either. The description of multi-electron atoms therefore usually starts with the **central field approximation** in which we re-write the Hamiltonian of eqn 4.1 in the form:[1]

$$\hat{H} = \sum_{i=1}^{N} \left(-\frac{\hbar^2}{2m} \boldsymbol{\nabla}_i^2 + V_{\text{central}}(r_i) \right) + V_{\text{residual}} \,, \tag{4.2}$$

where V_{central} is the **central field** and V_{residual} is the **residual electrostatic interaction**.

The central field approximation works in the limit where

$$\left| \sum_{i=1}^{N} V_{\text{central}}(r_i) \right| \gg |V_{\text{residual}}| \,. \tag{4.3}$$

In this case, we can treat V_{residual} as a perturbation, and worry about it later. We then have to solve a Schrödinger equation in the form:

$$\left[\sum_{i=1}^{N} \left(-\frac{\hbar^2}{2m} \boldsymbol{\nabla}_i^2 + V_{\text{central}}(r_i) \right) \right] \Psi = E\,\Psi \,. \tag{4.4}$$

[1] A field is described as "central" if the potential energy has spherical symmetry about the origin, so that $V(\boldsymbol{r})$ only depends on r. The fact that V does not depend on θ or ϕ means that the force is parallel to $\boldsymbol{r}$, i.e. it points *centrally* towards or away from the origin.

This is not as bad as it looks. By writing[2]

$$\Psi = \psi_1(\boldsymbol{r}_1)\,\psi_2(\boldsymbol{r}_2)\cdots\psi_N(\boldsymbol{r}_N)\,, \tag{4.5}$$

we end up with N separate Schrödinger equations of the form:

$$\left(-\frac{\hbar^2}{2m}\boldsymbol{\nabla}_i^2 + V_{\rm central}(r_i)\right)\psi_i(\boldsymbol{r}_i) = E_i\,\psi_i(\boldsymbol{r}_i)\,, \tag{4.6}$$

with

$$E = E_1 + E_2\cdots E_N\,. \tag{4.7}$$

This is much more tractable. We might need a computer to solve any one of the single particle wave Schrödinger equations of the type given in eqn 4.6, but at least it is possible in principle. Furthermore, the fact that the potentials that appear in eqn 4.6 only depend on the radial co-ordinate r_i (i.e. no dependence on the angles θ_i and ϕ_i) means that every electron is in a well-defined orbital angular momentum state,[3] and that the separation of variables discussed in Section 2.3 is valid. In analogy with eqn 2.35, we can then write:

$$\psi_i(\boldsymbol{r}_i) \equiv \psi(r_i,\theta_i,\phi_i) = R_i(r_i)\,Y_i(\theta_i,\phi_i)\,. \tag{4.8}$$

By proceeding exactly as in Section 2.3, we end up with two equations, namely:

$$\hat{\boldsymbol{L}}_i^{\,2} Y_{l_i m_i}(\theta_i,\phi_i) = \hbar^2 l_i(l_i+1) Y_{l_i m_i}(\theta_i,\phi_i)\,, \tag{4.9}$$

and

$$\left(-\frac{\hbar^2}{2m}\frac{1}{r_i^2}\frac{\mathrm{d}}{\mathrm{d}r_i}\left(r_i^2\frac{\mathrm{d}}{\mathrm{d}r_i}\right) + \frac{\hbar^2 l_i(l_i+1)}{2mr_i^2} + V_{\rm central}(r_i)\right)R_i(r_i) = E_i\,R_i(r_i)\,. \tag{4.10}$$

The first tells us that the angular part of the wave functions will be given by the spherical harmonic functions described in Section 2.2, while the second one allows us to work out the energy and radial wave function for a given form of $V_{\rm central}(r_i)$ and value of l_i. Each electron will therefore have four quantum numbers:

- l and m_l: these drop out of the angular equation for each electron, namely eqn 4.9.
- n: this arises from solving eqn 4.10 with the appropriate form of $V_{\rm central}(r)$ for a given value of l. n and l together determine the radial wave function $R_{nl}(r)$ (which cannot be expected to be the same as the hydrogenic ones given in Table 2.2) and the energy of the electron.
- m_s: spin has not entered the argument. Each electron can therefore either have spin up ($m_s = +1/2$) or down ($m_s = -1/2$), as usual. We do not need to specify the spin quantum number s because it is always equal to $1/2$.

The state of the many-electron atom is then found by working out the wave functions of the individual electrons and finding the total energy of the atom according to eqn 4.7. This provides a useful working model that will be explored in detail below.

In the following sections we shall consider the experimental evidence for the shell model which proves that the central approximation is a good one. The reason it works is based on the nature of the shells. An individual electron experiences an electrostatic potential due to the Coulomb repulsion from all the other electrons in the atom. Nearly all of the electrons in a many-electron atom are in closed sub-shells, which have spherically-symmetric charge clouds. The off-radial forces from electrons in these closed shells cancel because of the spherical symmetry. Furthermore, the off-radial forces from electrons in unfilled shells are usually relatively small compared to the radial ones. We therefore expect the approximation given in eqn 4.3 to be valid for most atoms.

4.2 The shell model and the periodic table

We summarize here what we know so far about atomic states.

[2]The fact that electrons are indistinguishable particles means that we cannot distinguish physically between the case with electron 1 in state 1, electron 2 in state 2, ..., and the case with electron 2 in state 1, electron 1 in state 2, ..., etc. We should therefore really write down a *linear combination* of all such possibilities. We shall reconsider this point when considering the helium atom in Chapter 8.

[3]As noted in Section 2.2, the torque on the electron is zero if the force points centrally towards the nucleus. This means that the orbital angular momentum is constant.

Quantum number	symbol	Value
principal	n	any integer > 0
orbital	l	integer up to $(n-1)$
magnetic	m_l	integer from $-l$ to $+l$
spin	m_s	$\pm 1/2$

Table 4.1: Quantum numbers for electrons in atoms.

1. The electronic states are specified by four quantum numbers: n, l, m_l and m_s. The values that these quantum numbers can take are summarized in Table 4.1. In spectroscopic notation, electrons with $l = 0, 1, 2, 3, \ldots$ are called s, p, d, f, $\ldots$ electrons.

2. The gross energy of the electron is determined by n and l, except in hydrogenic atoms, where the gross structure depends only on n.

3. In the absence of fine structure and external magnetic fields, all the states with the same values of n and l are degenerate. Each (n, l) term of the gross structure therefore contains $2(2l+1)$ degenerate levels.

In the shell model, we forget about fine structure and external magnetic fields, and just concentrate on the gross structure. This approximation is justified by the fact that the fine structure and magnetic field splittings are smaller than the gross structure energies by a factor of about $Z^2\alpha^2 = (Z^2/137)^2 \sim 10^{-4}\, Z^2$. If necessary, we will think about fine structure and field splittings after we have dealt with the gross structure of the multi-electron atoms, but note that the fine structure energy can get to be quite significant for large Z.

The **Pauli exclusion principle** tells us that we can only put one electron in each quantum state. This is a consequence of the fact that the electrons are indistinguishable fermions (ie spin 1/2 particles). We shall discuss some of the other consequences of the particle indistinguishability in Chapter 8. We concentrate here on how it leads to the notion of atomic shells.

The **shell model** assumes that we can order the energies of the gross structure terms of a multi-electron atom according to the quantum numbers n and l. We further assume that the energies of the terms increase in big jumps each time we move to the next set of quantum numbers. As we add electrons to the atom, the electrons therefore fill up the lowest available shell until it is full, and then go on to the next one. The filling up of the shells in order of increasing energy in multi-electron atoms is sometimes called the **Aufbau principle**,[4] and is the basis of the **periodic table** of elements. The shells are listed in order of increasing energy in Table 4.2.

Inspection of Table 4.2 shows us that the energy of the shells always increases with n and l. We build up multi-electron atoms by adding electrons one by one, putting each electron into the lowest energy shell that has unfilled states. In general, this will be the one with the lowest n, but there are exceptions to this rule. For example, the 19^{th} electron goes into 4s shell rather than the 3d shell. Similarly, the 37^{th} electron goes into 5s shell rather than the 4d shell. This happens because the energy of the shell with a large l value may be higher than that of another shell with a larger value of n but smaller value of l.

The periodic table of elements is built up by adding electrons into the shells as the atomic number increases. This allows us to determine the **electronic configuration** of the elements, that is, the quantum numbers of the electrons in the atom. The configurations of the first 11 elements are listed in Table 4.3. The superscript attached to the shell tells us how many electrons are in that shell. The process of filling the shells follows the pattern indicated in Table 4.2. The nl sub-shells are filled *diagonally* when laid out in rows determined by the principal quantum number n, as shown in Fig. 4.1.[5]

4.3 Justification of the shell model

The theoretical justification for the shell model relies on the concept of **screening**. The idea is that the electrons in the inner shells screen the outer electrons from the potential of the nucleus. To see how this works we take sodium as an example.

[4] The German word *Aufbau* means "building up".

[5] There are some exceptions to the general rules. For example, copper (Cu) with $Z = 29$ has a configuration of $\cdots 4s^1\ 3d^{10}$ instead of $\cdots 4s^2\ 3d^9$. This happens because filled shells are particularly stable. It is therefore energetically advantageous to promote the second 4s electron into the 3d shell to give the very stable $3d^{10}$ configuration. The energy difference between the two configurations is not particularly large, which explains why copper sometimes behaves as though it is monovalent, and sometimes divalent.

Shell	n	l	m_l	m_s	$\mathsf{N}_{\text{shell}}$	$\mathsf{N}_{\text{accum}}$
1s	1	0	0	$\pm 1/2$	2	2
2s	2	0	0	$\pm 1/2$	2	4
2p	2	1	$-1, 0, +1$	$\pm 1/2$	6	10
3s	3	0	0	$\pm 1/2$	2	12
3p	3	1	$-1, 0, +1$	$\pm 1/2$	6	18
4s	4	0	0	$\pm 1/2$	2	20
3d	3	2	$-2, -1, 0, +1, +2$	$\pm 1/2$	10	30
4p	4	1	$-1, 0, +1$	$\pm 1/2$	6	36
5s	5	0	0	$\pm 1/2$	2	38
4d	4	2	$-2, -1, 0, +1, +2$	$\pm 1/2$	10	48
5p	5	1	$-1, 0, +1$	$\pm 1/2$	6	54
6s	6	0	0	$\pm 1/2$	2	56
4f	4	3	$-3, -2, -1, 0, +1, +2, +3$	$\pm 1/2$	14	70
5d	5	2	$-2, -1, 0, +1, +2$	$\pm 1/2$	10	80
6p	6	1	$-1, 0, +1$	$\pm 1/2$	6	86
7s	7	0	0	$\pm 1/2$	2	88

Table 4.2: Atomic shells, listed in order of increasing energy. $\mathsf{N}_{\text{shell}}$ is equal to $2(2l+1)$ and is the number of electrons that can fit into the shell due to the degeneracy of the m_l and m_s levels. The last column gives the accumulated number of electrons that can be held by the atom once the particular shell and all the lower ones have been filled.

Element	Atomic number	Electronic configuration
H	1	$1s^1$
He	2	$1s^2$
Li	3	$1s^2\ 2s^1$
Be	4	$1s^2\ 2s^2$
B	5	$1s^2\ 2s^2\ 2p^1$
C	6	$1s^2\ 2s^2\ 2p^2$
N	7	$1s^2\ 2s^2\ 2p^3$
O	8	$1s^2\ 2s^2\ 2p^4$
F	9	$1s^2\ 2s^2\ 2p^5$
Ne	10	$1s^2\ 2s^2\ 2p^6$
Na	11	$1s^2\ 2s^2\ 2p^6\ 3s^1$

Table 4.3: The electronic configuration of the first 11 elements of the periodic table.

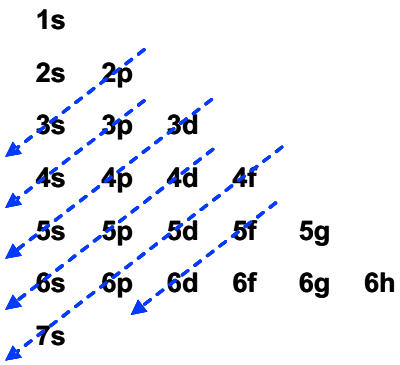

Figure 4.1: Atomic shells are filled in *diagonal* order when listed in rows according to the principal quantum number n.

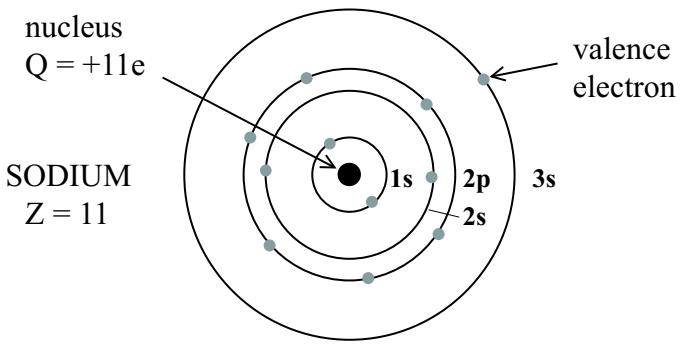

Figure 4.2: The electronic configuration of the sodium atom according to the shell model.

Shell	n	Z_{eff}	radius (Å)	Energy (eV)
1s	1	11	0.05	−1650
2s, 2p	2	9	0.24	−275
3s	3	1	4.8	−1.5

Table 4.4: Radii and energies of the principal atomic shells of sodium according to the Bohr model. The unit of 1 Ångstrom (Å) = 10^{-10} m.

Sodium has an atomic number of 11, and therefore has a nucleus with a charge of $+11e$ with 11 electrons orbiting around it. The picture of the atom based on the shell model is shown in Fig. 4.2. The radii and energies of the electrons in their shells are estimated using the Bohr formulæ:

$$r_n = \frac{n^2}{Z} a_{\text{H}} \,, \tag{4.11}$$

$$E_n = -\left(\frac{Z}{n}\right)^2 R_{\text{H}} \,, \tag{4.12}$$

where $a_{\text{H}} = 5.29 \times 10^{-11}$ m is the Bohr radius of hydrogen, $R_{\text{H}} = 13.6$ eV is the Rydberg constant and Z is the atomic number.

The first two electrons go into the $n = 1$ shell. These electrons see the full nuclear charge of $+11e$. With $n = 1$ and $Z = 11$, we find $r_1 = 1^2/11 \times a_{\text{H}} = 0.05$ Å and $E_1 = -11^2 R_{\text{H}} = -1650$ eV. The next eight electrons go into the $n = 2$ shell. These are presumed to orbit outside the $n = 1$ shell. The two inner electrons partly screen the nuclear charge, and the $n = 2$ electrons see an effective charge $Z_{\text{eff}} = +9e$. The radius is therefore $r_2 = (2^2/9) \times a_{\text{H}} = 0.24$ Å and the energy is $E_2 = -(9/2)^2 R_{\text{H}} = -275$ eV. Finally, the outermost electron in the $n = 3$ shell orbits outside the filled $n = 1$ and $n = 2$ shells, and therefore sees $Z_{\text{eff}} = 1$. With $Z = 1$ and $n = 3$ we find $r_3 = 4.8$ Å and $E_3 = -1.5$ eV. These values are summarized in Table 4.4. Note the large jump in energy and radius in moving from one shell to the next.

The treatment of the screening discussed in the previous paragraph is clearly over-simplified because it is based on Bohr-type orbits and does not treat the electron-electron repulsion properly. In Section 4.5 we shall see how we might improve on it. One point to realize, however, is that the model is reasonably self-consistent: by assuming that the inner shells screen the outer ones, we find that the orbital radius increases in each subsequent shell, which corroborates our original assumption. This is why the model works so well.

4.4 Experimental evidence for the shell model

There is a wealth of experimental evidence to confirm that the shell model is a good one. The main points are discussed briefly here.

Ionization potentials and atomic radii

The ionization potentials of the noble gas elements are the highest within a particular period of the atomic table, while those of the alkali metals are the lowest. This can be seen by looking at the data in Fig. 4.3. The ionization potential gradually increases as the atomic number increases until the shell is

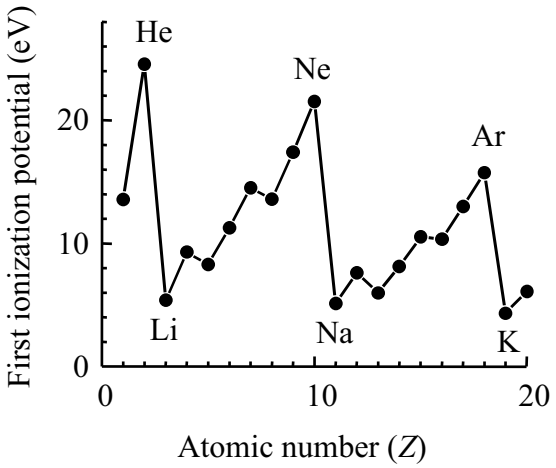

Figure 4.3: First ionization potentials of the elements up to calcium. The noble gas elements (He, Ne, Ar) have highly stable fully filled shells with large ionization potentials. The alkali metals (Li, Na, K) have one weakly-bound valence electron outside fully-filled shells.

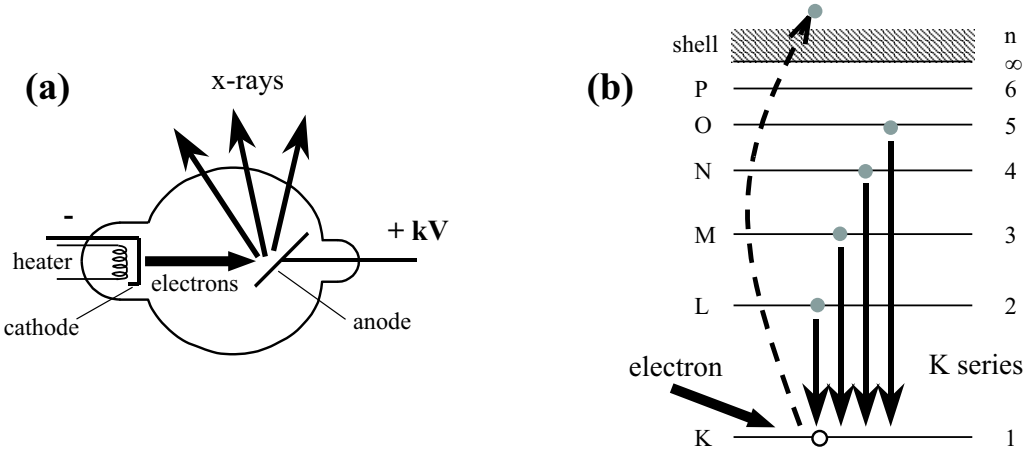

Figure 4.4: (a) A typical X-ray tube. Electrons are accelerated with a voltage of several kV and impact on a target, causing it to emit X-rays. (b) Transitions occurring in the K-series emission lines. An electron from the discharge tube ejects one of the K-shell electrons of the target, leaving an empty level in the K shell. X-ray photons are emitted as electrons from the higher shells drop down to fill the hole in the K-shell.

filled, and then it drops abruptly. This shows that the filled shells are very stable, and that the valence electrons go in larger, less tightly-bound orbits. The results correlate with the chemical activity of the elements. The noble gases require large amounts of energy to liberate their outermost electrons, and they are therefore chemically inert. The alkali metals, on the other hand, need much less energy, and are therefore highly reactive.

It is also found that the average atomic radius determined by X-ray crystallography on closely packed crystals is largest for the alkali metals. This is further evidence that we have weakly-bound valence electrons outside strongly-bound, small-radius, inner shells.

X-ray line spectra

Measurements of X-ray line spectra allow the energies of the inner shells to be determined directly. The experimental arrangement for observing an X-ray emission spectrum is shown in Fig. 4.4(a). Electrons are accelerated across a potential drop of several kV and then impact on a target. This ejects **core electrons** from the inner shells of the target, as shown in Fig. 4.4(b). X-ray photons are emitted as the higher energy electrons drop down to fill the empty level (or **hole**) in the lower shell.

Each target emits a series of characteristic lines. The series generated when a K-shell ($n = 1$) electron has been ejected is called the K-series. Similarly, the L- and M-series correspond to ejection of L-shell

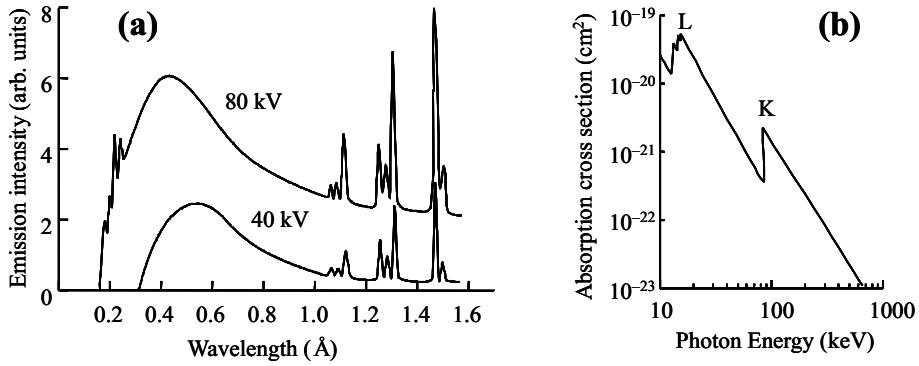

Figure 4.5: (a) X-ray emission spectra for tungsten at two different electron voltages. The sharp lines are caused by radiative transitions after the electron beam ejects an inner shell electron, as indicated in Fig. 4.4(b). The continuum is caused by bremsstrahlung, which has a short wavelength limit equal to hc/eV at voltage V. (b) X-ray absorption cross-section spectrum for lead.

($n = 2$) or M-shell ($n = 3$) core electrons respectively. This old spectroscopic notation dates back to the early work on X-ray spectra.

Figure 4.5(a) shows a typical X-ray emission spectrum. The spectrum consists of a series of sharp lines on top of a continuous spectrum. The groups of sharp lines are generated by radiative transitions following the ejection of an inner shell electron as indicated in Fig. 4.4(b). As the voltage is increased, new groups of lines appear, as the higher energy electron beam ejects ever deeper inner shell electrons. Several groups of lines are observed as the hole in the initial shell moves up through the higher shells. For example, L-shell lines follow K-shell lines after the electron in the L-shell drops to the hole in the K-shell, thus leaving a hole in the L-shell, and so on.

The continuous spectrum is caused by **bremsstrahlung**.[6] Bremsstrahlung occurs when the electron is scattered by the atoms without ejecting a core electron from the target. The acceleration of the electron associated with its change of direction causes it to radiate. Conservation of energy demands that the frequency of the radiation must cut off when $h\nu = eV$, V being the voltage across the tube. This means that the minimum wavelength is equal to hc/eV. The reduction of the short wavelength limit of the bremsstrahlung with increasing voltage is apparent in the data shown in Fig. 4.5(a).

The energy of an electron in an inner shell with principal quantum number n is given by:

$$E_n = -\frac{{Z_n^{\rm eff}}^2}{n^2} R_{\rm H} \,, \tag{4.13}$$

where $Z_n^{\rm eff}$ is the effective nuclear charge, and $R_{\rm H} = 13.6\,{\rm eV}$. The difference between Z (the atomic number of the target) and $Z_n^{\rm eff}$ is caused by the screening effect of the other electrons. The energy of the optical transition from $n \to n'$ is thus given by:

$$h\nu = |E_{n'} - E_n| = \left| \frac{{Z_n^{\rm eff}}^2}{n^2} - \frac{{Z_{n'}^{\rm eff}}^2}{{n'}^2} \right| R_{\rm H} \,. \tag{4.14}$$

In practice, the wavelengths of the various series of emission lines are found to obey **Moseley's law**, where we make the approximation $Z_n^{\rm eff} = Z_{n'}^{\rm eff}$ and write both as $(Z - \sigma_n)$. For example, the K-shell lines are given by:[7]

$$\frac{hc}{\lambda} \approx (Z - \sigma_K)^2 R_H \left(\frac{1}{1^2} - \frac{1}{n^2} \right) \,, \tag{4.15}$$

where $n > 1$ and $\sigma_K \sim 3$. Similarly, the L-shell spectra obey:

$$\frac{hc}{\lambda} \approx (Z - \sigma_L)^2 R_H \left(\frac{1}{2^2} - \frac{1}{n^2} \right) \,, \tag{4.16}$$

[6] German: *brems* = braking (i.e. deceleration) + *strahlung* = radiation.

[7] There is no real scientific justification for the approximation $Z_n^{\rm eff} = Z_{n'}^{\rm eff}$ in Moseley's law. The law is an empirical one and reflects the fact that the transition wavelength is mainly dominated by the energy of the lower shell. Note also that close inspection of the line spectra reveals sub-structure due to the relatively small energy differences between the l states for a particular value of n, and further smaller splittings due to spin-orbit coupling.

Element	Z	Electronic configuration
Lithium	3	$1s^2 2s^1$
Sodium	11	[Ne] $3s^1$
Potassium	19	[Ar] $4s^1$
Rubidium	37	[Kr] $5s^1$
Cesium	55	[Xe] $6s^1$

Table 4.5: Alkali metals. The symbol [...] indicates that the inner shells are filled according to the electronic configuration of the noble gas element identified in the bracket.

where $n > 2$, and $\sigma_L \sim 10$. We can see that these are just the expected wavelengths predicted by the Bohr model, except that we have an effective charge of $(Z - \sigma_n)$ instead of Z. The phenomenological **screening parameter** σ_n that appears here accounts for the screening of the nucleus by the other electrons and varies from shell to shell.

X-ray absorption spectra show a complementary frequency dependence to the emission spectra. Figure 4.5(b) shows a typical X-ray absorption spectrum. A sharp increase in the absorption cross section[8] occurs whenever the photon energy crosses the threshold to eject an electron out of an inner shell to empty states above the highest occupied shell. This sharp increase in the absorption is called the **absorption edge**. The final state for the electron after the absorption transition could either be one of the excited states of the valence electrons or in the continuum above the ionization limit. The binding energy of the valence electrons is negligible on the scale of X-ray energies, and so we can effectively put $E_{n'} = 0$ in eqn 4.14 and hence obtain the energy of the absorption edge as:

$$h\nu^{\rm edge} = \frac{Z_n^{\rm eff\,2}}{n^2}\, R_{\rm H} \equiv \frac{(Z-\sigma_n)^2}{n^2}\, R_{\rm H}\,. \tag{4.17}$$

The absorption probability decreases as the electron gets promoted further into the continuum. Hence we see a peak in the absorption at $h\nu^{\rm edge}$ and a decrease thereafter. The K and L shell absorption edges are clearly visible at 88 keV and 15 keV respectively in Fig. 4.5(b) .

4.5 Effective potentials, screening, and alkali metals

The electrons in a multi-electron atom arrange themselves with the smallest number of electrons in unfilled shells outside inner filled shells. These outermost electrons are called the **valence electrons** of the atom. They are responsible for the chemical activity of the particular elements.

In order to work out the energy levels of the valence electrons, we need to solve the N-electron Schrödinger equation given in eqn 4.1. Within the central-field approximation, each valence electron satisfies a Schrödinger equation of the type given in eqn 4.6, which can be written in the form:

$$\left(-\frac{\hbar^2}{2m}\boldsymbol{\nabla}^2 + V_{\rm eff}^l(r)\right)\psi = E\,\psi\,. \tag{4.18}$$

The Coulomb repulsion from the core electrons is lumped into the effective potential $V_{\rm eff}^l(r)$. This is only an approximation to the real behaviour, but it can be reasonably good, depending on how well we work out $V_{\rm eff}^l(r)$. Note that the effective potential depends on l. This arises from the term in l that appears in eqn 4.10 and has important consequences, as we shall see below.

The overall dependence of $V_{\rm eff}(r)$ with r must look something like Fig. 4.6. At very large values of r, the outermost valence electron will be well outside any filled shells, and will thus only see an attractive potential equivalent to a charge of $+e$. On the other hand, if r is very small, the electron will see the full nuclear charge of $+Ze$. The potential at intermediate values of r must lie somewhere between these two limits: hence the generic form of $V_{\rm eff}(r)$ shown in Fig. 4.6. The task of calculating $V_{\rm eff}^l(r)$ keeps theoretical atomic physicists busy. Two common approximation techniques used to perform the calculations are called the **Hartree** and **Thomas-Fermi** methods.

As a specific example, we consider the **alkali metals** such as lithium, sodium and potassium, which come from group I of the periodic table. They have one valence electron outside filled inner shells, as

[8] Absorption coefficients are often expressed as "cross sections". The cross section is equal to the effective area of the beam that is blocked out by the absorption of an individual atom. If there are N atoms per unit volume, and the cross section is equal to $\sigma_{\rm abs}$, the absorption coefficient in $\rm m^{-1}$ is equal to $N\sigma_{\rm abs}$.

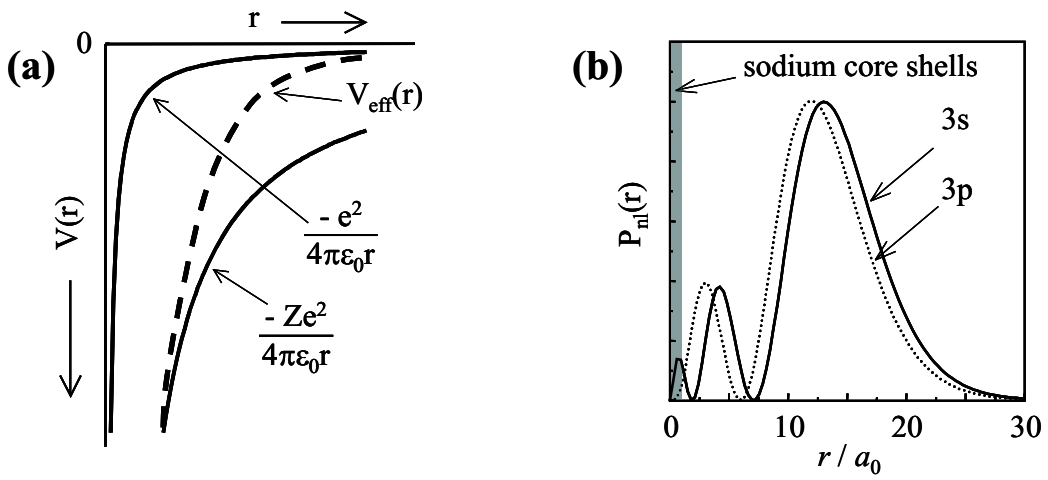

Figure 4.6: (a) Typical effective potential $V_{\rm eff}(r)$ for the valence electrons of an atom with atomic number Z. (b) Radial probability densities for hydrogenic 3s and 3p wave functions. a_0 is the Bohr radius (0.529 Å). The shaded region near $r = 0$ represents the inner core shells for the case of sodium with $Z = 11$.

l	$n = 3$	$n = 4$	$n = 5$	$n = 6$
0	1.373	1.357	1.352	1.349
1	0.883	0.867	0.862	0.859
2	0.010	0.011	0.013	0.011
3	–	0.000	-0.001	-0.008

Table 4.6: Values of the quantum defect $\delta(l)$ for sodium against n and l.

indicated in Table 4.5. They are therefore approximately one-electron systems, and can be understood by introducing a phenomenological number called the **quantum defect** to describe the energies. To see how this works, we consider the sodium atom.

The shell model picture of sodium is shown in Fig. 4.2. The optical spectra are determined by excitations of the outermost 3s electron. The energy of each (n, l) term of the valence electron is given by:

$$E_{nl} = -\frac{R_H}{[n - \delta(l)]^2}\,, \tag{4.19}$$

where $n \geq 3$ and $\delta(l)$ is the quantum defect. The quantum defect allows for the penetration of the inner shells by the valence electron.

The dependence of the quantum defect on l can be understood with reference to Fig. 4.6(b). This shows the radial probability densities $P_{nl}(r) = r^2|R(r)|^2$ for the 3s and 3p orbitals of a hydrogenic atom with $Z = 1$, which might be expected to be a reasonable approximation for the single valence electron of sodium. The shaded region near $r = 0$ represents the inner $n = 1$ and $n = 2$ shells with radii of $\sim 0.09a_0$ and $\sim 0.44a_0$ respectively. (See Section 4.3.) We see that both the 3s and 3p orbitals penetrate the inner shells, and that this penetration is much greater for the 3s electron. The electron will therefore see a larger effective nuclear charge for part of its orbit, and this will have the effect of reducing the energies. The energy reduction is largest for the 3s electron due to its larger core penetration.

The quantum defect $\delta(l)$ was introduced empirically to account for the optical spectra. In principle it should depend on both n and l, but it was found experimentally to depend mainly on l. This can be seen from the values of the quantum defect for sodium tabulated in Table 4.6. The corresponding energy spectrum is shown schematically in Fig. 4.7. Note that $\delta(l)$ is very small for $l \geq 2$.

We can use the quantum defect to calculate the wavelengths of the emission lines. The D lines correspond to the 3p $\rightarrow$ 3s transition. By using the values of δ given in Table 4.6, we find that the

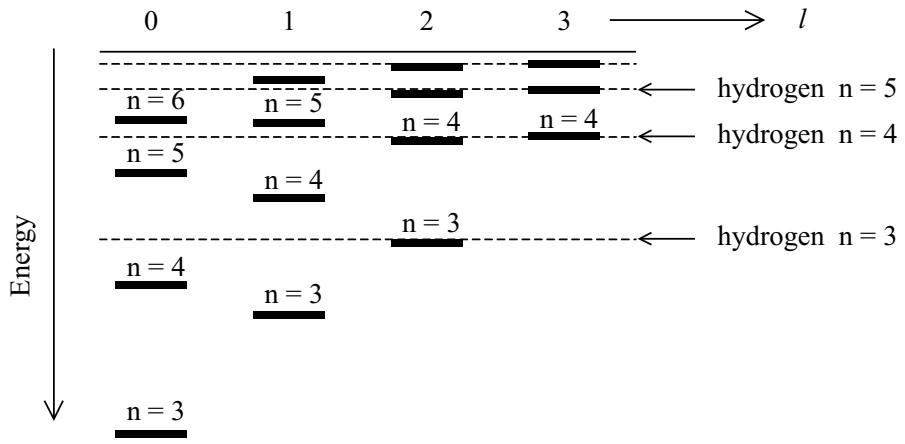

Figure 4.7: Schematic energy level diagram for sodium, showing the ordering of the energy levels.

wavelength is given by:

$$\begin{aligned} \frac{hc}{\lambda} &= R_H \left(\frac{1}{[3-\delta(3\mathrm{s})]^2} - \frac{1}{[3-\delta(3\mathrm{p})]^2} \right) \\ &= (1.10 \times 10^5\,\mathrm{cm}^{-1}) \times \left(\frac{1}{1.627^2} - \frac{1}{2.117^2} \right) . \end{aligned}$$

This gives the wave number $\overline{\nu} = 1.70 \times 10^4\,\mathrm{cm}^{-1}$, and so λ is equal to 590nm, as we would expect for the yellow D-lines of sodium.

Reading

Demtröder, W., *Atoms, Molecules and Photons*, §6.2–6.4, §7.5
Haken and Wolf, *The physics of atoms and quanta*, chapters 11, 18 & 19.
Phillips, A.C., *Introduction to Quantum Mechanics*, chapter 11.
Eisberg and Resnick, *Quantum Physics*, chapters 9 & 10.
Beisser, *Concepts of Modern Physics*, chapter 7.

Chapter 5

Angular momentum

We noted in Section 2.2 that the treatment of angular momentum is very important for understanding the properties of atoms. It is now time to explore these effects in detail, and to see how this leads to the classification of the quantized states of atoms by their angular momentum.

5.1 Conservation of angular momentum

In the Sections that follow, we are going to consider several different types of angular momentum, and the ways in which they are coupled together. Before going into the details, it is useful to stress one very important point related to conservation of angular momentum. In an isolated atom, there are many forces (and hence torques) acting inside the atom. These *internal* forces cannot change the *total* angular momentum of the atom, since conservation of angular momentum demands that the angular momentum of the atom as a whole must be conserved in the absence of any *external* torques. The total angular momentum of the atom is normally determined by its electrons. The total electronic angular momentum is written $\boldsymbol{J}$, and is specified by the quantum number J. The principle of conservation of angular momentum therefore requires that isolated atoms always have well-defined J states.[1] It is this J value that determines, for example, the magnetic dipole moment of the atom.

The principle of conservation of angular momentum does not apply, of course, when external perturbations are applied. The most obvious example is the perturbation caused by the emission or absorption of a photon. In this case the angular momentum of the atom must change because the photon itself carries angular momentum, and the angular momentum of the whole system (atom + photon) has to be conserved. The change in J is then governed by selection rules, as discussed, for example, in Section 5.8. Another obvious example is the effect of a strong external DC magnetic field. In this case it is possible for the magnetic field to produce states where the component of angular momentum along the direction of the field is well-defined, but not the total angular momentum. (See the discussion of the Paschen-Back effect in Section 7.1.3.)

5.2 Types of angular momentum

The electrons in atoms possess two different types of angular momentum, namely orbital and spin angular momentum. These are discussed separately below.

5.2.1 Orbital angular momentum

The orbital angular momentum of an electron was considered in Section 2.2. The electron orbits around the nucleus, and this gives it angular momentum $\boldsymbol{l}$. The angular momentum is specified by two quantum numbers: l and m. The latter is sometimes given an extra subscript (i.e. m_l) to distinguish it from the spin quantum number m_s considered below.

The magnitude of $\boldsymbol{l}$ is given by

$$|\boldsymbol{l}| = \sqrt{l(l+1)}\hbar\,, \tag{5.1}$$

[1] This statement about J has to be qualified somewhat when we add in the effects of the nucleus. The angular momentum of an atom is the resultant of the electronic angular momentum and the nuclear spin. The total angular momentum of an isolated atom has to be conserved, but the electrons can exchange angular momentum with the nucleus through **hyperfine** interactions. (See Section 6.7.2.) These interactions are very weak, and can usually be neglected except when explicitly considering nuclear effects.

and the component along the z axis by

$$l_z = m\hbar \,. \tag{5.2}$$

l can take positive integer values (including 0) and m can take values in integer steps from $-l$ to $+l$. The number of m states for each l state is therefore equal to $(2l+1)$. These m states are degenerate in isolated atoms, but can be split by external perturbations (e.g. magnetic or electric fields.)

In classical orbit problems, angular momentum is conserved when the force $\boldsymbol{F}$ is radial: i.e. $\boldsymbol{F} \equiv F\hat{\boldsymbol{r}}$, where $\hat{\boldsymbol{r}}$ is a unit vector parallel to $\boldsymbol{r}$. This follows from the equation of motion:

$$\frac{\mathrm{d}\boldsymbol{l}}{\mathrm{d}t} = \boldsymbol{\Gamma} = \boldsymbol{r} \times \boldsymbol{F} = \boldsymbol{r} \times F\hat{\boldsymbol{r}} = 0 \,, \tag{5.3}$$

where $\boldsymbol{\Gamma}$ is the torque. In the hydrogen atom, the Coulomb force on the electron acts towards the nucleus, and hence $\boldsymbol{l}$ is conserved. This is why the angular momentum ends up being quantized with well-defined constant values when we consider the quantum mechanics of the hydrogen atom. It is also the case that the individual electrons of many-electron atoms have well-defined l states. This follows because the central field approximation gives a very good description of the behaviour of many electron atoms (see Section 4.1), and the dominant resultant force on the electron is radial (i.e. central) in this limit.[2]

5.2.2 Spin angular momentum

A wealth of data derived from the optical, magnetic and chemical properties of atoms points to the fact that electrons possess an additional type of angular momentum called **spin**. The electron behaves as if it spins around its own internal axis, but this analogy should not be taken literally — the electron is, as far as we know, a point particle, and so cannot be spinning in any classical way. In fact, spin is a purely quantum effect with no classical explanation.

The discovery of spin goes back to the Stern-Gerlach experiment, in which a beam of atoms is deflected by a non-uniform magnetic field. (See Fig. 1.4). The force on a magnetic dipole in a non-uniform magnetic field is given by:[3]

$$F_z = \mu_z \frac{\mathrm{d}B}{\mathrm{d}z} \,, \tag{5.4}$$

where $\mathrm{d}B/\mathrm{d}z$ is the field gradient, which is assumed to point along the z direction, and μ_z is the z-component of the magnetic dipole of the atom. In Lecture Notes 6 we shall explore the origin of magnetic dipoles in detail. At this stage, all we need to know is that the magnetic dipole is directly proportional to the angular momentum of the atom. (See Section 6.1.)

The original Stern–Gerlach experiment was performed on silver atoms, which have a ground-state electronic configuration of [Kr] $4\mathrm{d}^{10}$ $5\mathrm{s}^1$. Filled shells have no net angular momentum, because there are as many positive m_l states occupied as negative ones. Furthermore, electrons in s-shells have $l = 0$ and therefore the orbital angular momentum of the atom is zero. This implies that the orbital magnetic dipole of the atom is also zero, and hence we expect no deflection. However, the experiment showed that the atoms were deflected either up or down, as indicated in Fig. 1.4.

In order to explain the up/down deflection of the atoms with no orbital angular momentum, we have to assume that each electron possesses an additional type of magnetic dipole moment. This magnetic dipole is attributed to the spin angular momentum. In analogy with orbital angular momentum, spin angular momentum is described by two quantum numbers s and m_s, where m_s can take the $(2s+1)$ values in integer steps from $-s$ to $+s$. The magnitude of the spin angular momentum is given by

$$|\boldsymbol{s}| = \sqrt{s(s+1)}\hbar \,, \tag{5.5}$$

and the component along the z axis is given by

$$s_z = m_s\hbar \,. \tag{5.6}$$

[2]The inclusion of non-central forces via the residual electrostatic interaction leads to some mixing of the orbital angular momentum states. This can explain why transitions that are apparently forbidden by selection rules can sometimes be observed, albeit with low transition probabilities.

[3]Note that we need a *non-uniform* magnetic field to deflect a magnetic dipole. A *uniform* magnetic field merely exerts a torque, not a force. We can understand this by analogy with electrostatics. Electric monopoles (i.e. free charges) can be moved by applying electric fields, but an electric dipole experiences no net force in a uniform electric field because the forces on the positive and negative charges cancel. If we wish to apply a force to an electric dipole, we therefore need to apply a non-uniform electric field, so that the forces on the two charges are different. Magnetic monopoles do not exist (as far as we know), and so all atomic magnets are dipoles. Hence we must apply a non-uniform magnetic field to exert a magnetic force on an atom.

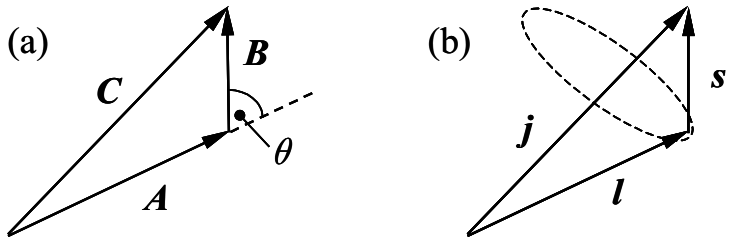

Figure 5.1: (a) Vector addition of two angular momentum vectors $\boldsymbol{A}$ and $\boldsymbol{B}$ to form the resultant $\boldsymbol{C}$. (b) Vector model of the atom. The spin-orbit interaction couples $\boldsymbol{l}$ and $\boldsymbol{s}$ together to form the resultant $\boldsymbol{j}$. The magnitudes of the vectors are given by: $|\boldsymbol{j}| = \sqrt{j(j+1)}\hbar$, $|\boldsymbol{l}| = \sqrt{l(l+1)}\hbar$, and $|\boldsymbol{s}| = \sqrt{s(s+1)}\hbar$.

The fact that atoms with a single s-shell valence electron (e.g. silver) are only deflected in two directions (i.e. up or down) implies that the spin quantum numbers of the electron must have the following values:

$$\begin{aligned} s &= 1/2\,, \\ m_s &= \pm 1/2\,. \end{aligned}$$

The Stern–Gerlach experiment is just one of many pieces of evidence that support the hypothesis for electron spin. Here is an incomplete list of other evidence for spin based on atomic physics:

- The periodic table of elements, which is the foundation of the whole subject of chemistry, cannot be explained unless we assume that the electrons possess spin.
- High resolution spectroscopy of atomic spectral lines shows that they frequently consist of closely-spaced multiplets. This fine structure is caused by spin–orbit coupling , which can only be explained by postulating that electrons possess spin. See Lecture Notes 6.
- If we ignore spin, we expect to observe the normal Zeeman effect when an atom is placed in an external magnetic field. However, most atoms display the *anomalous* Zeeman effect, which is a consequence of spin. See Lecture Notes 7.
- The ratio of the magnetic dipole moment to the angular momentum is called the gyromagnetic ratio. (See Section 6.1.) The gyromagnetic ratio can be measured directly by a number of methods. In 1915, Einstein and de Haas measured the gyromagnetic ratio of iron and came up with a value twice as large as expected. They rejected this result, assigning it to experimental errors. However, we now know that the magnetism in iron is caused by the spin rather the orbital angular momentum, and so the experimental value was correct. (The electron spin g-factor is 2: see Section 6.2.) This is a salutary lesson from the history that even great physicists like Einstein and de Haas can get their error analysis wrong!

5.3 Addition of angular momentum

Having discovered that electrons have different types of angular momentum, the question now arises as to how we add them together. Let us suppose that $\boldsymbol{C}$ is the resultant of two angular momentum vectors $\boldsymbol{A}$ and $\boldsymbol{B}$ as shown in Fig. 5.1(a), so that:

$$\boldsymbol{C} = \boldsymbol{A} + \boldsymbol{B}\,. \tag{5.7}$$

We assume for the sake of simplicity that $|\boldsymbol{A}| > |\boldsymbol{B}|$. (The argument is unaffected if $|\boldsymbol{A}| < |\boldsymbol{B}|$.) We define θ as the angle between the two vectors, as shown in figure 5.1(a).

In *classical* mechanics the angle θ can take any value from 0° to 180°. Therefore, $|\boldsymbol{C}|$ can take any value from $(|\boldsymbol{A}| + |\boldsymbol{B}|)$ to $(|\boldsymbol{A}| - |\boldsymbol{B}|)$. This is *not* the case in *quantum* mechanics, because the lengths of the angular momentum vectors must be quantized according to:

$$\begin{aligned} |\boldsymbol{A}| &= \sqrt{A(A+1)}\hbar \\ |\boldsymbol{B}| &= \sqrt{B(B+1)}\hbar \\ |\boldsymbol{C}| &= \sqrt{C(C+1)}\hbar\,, \end{aligned} \tag{5.8}$$

where A, B and C are the quantum numbers. This makes it apparent that θ can only take specific values in quantum mechanics. The rule for working out the allowed values of C from the known values of A and B is as follows:

$$C = A \oplus B = (A+B),\ (A+B-1),\ \cdots,\ |A-B|\,, \tag{5.9}$$

where the $\oplus$ symbol indicates that we are adding together angular momentum quantum numbers. Here are some examples of the rule given in eqn 5.9:

- $\boldsymbol{J} = \boldsymbol{L} + \boldsymbol{S}$, $L = 3$, $S = 1$:
  $J = 3 \oplus 1$, $3 + 1 = 4$, $|3 - 1| = 2$, therefore $J = 4, 3, 2$.
- $\boldsymbol{L} = \boldsymbol{l}_1 + \boldsymbol{l}_2$, $l_1 = 2$, $l_2 = 0$:
  $L = 2 \oplus 0$, $2 + 0 = 2$, $|2 - 0| = 2$, therefore $L = 2$.
- $\boldsymbol{S} = \boldsymbol{s}_1 + \boldsymbol{s}_2$, $s_1 = 1/2$, $s_2 = 1/2$:
  $S = 1/2 \oplus 1/2$, $1/2 + 1/2 = 1$, $|1/2 - 1/2| = 0$, therefore $S = 1, 0$.
- $\boldsymbol{J} = \boldsymbol{j}_1 + \boldsymbol{j}_2$, $j_1 = 5/2$, $j_2 = 3/2$:
  $J = 5/2 \oplus 3/2$, $5/2 + 3/2 = 4$, $|5/2 - 3/2| = 1$, therefore $J = 4, 3, 2, 1$.

5.4 Spin-orbit coupling

The orbital and spin angular momenta of electrons in atoms are not totally independent of each other, but interact through the **spin-orbit interaction**. Spin-orbit coupling and its effects are considered in detail in Lecture Notes 6, and at this stage we just need to know two basic things:

1. Spin-orbit coupling derives from the interaction between the magnetic dipole due to spin and the magnetic field that the electron experiences due to its orbital motion. We can thus write the spin-orbit interaction in the form (see eqn 6.32):

   $$\hat{H} = -\boldsymbol{\mu}_{\text{spin}} \cdot \boldsymbol{B}_{\text{orbital}} \propto \boldsymbol{l} \cdot \boldsymbol{s}\,, \tag{5.10}$$

   since $\boldsymbol{\mu}_{\text{spin}} \propto \boldsymbol{s}$ and $\boldsymbol{B}_{\text{orbital}} \propto \boldsymbol{l}$.

2. The spin-orbit interaction scales roughly as Z^2. (See eqn 6.42.) It is therefore weak in light atoms, and stronger in heavy atoms.

We introduce the spin-orbit interaction here because it is one of the mechanisms that is important in determining the angular momentum coupling schemes that apply in different atoms.

5.5 Angular momentum coupling in single electron atoms

If an atom has just a single electron, the addition of the orbital and spin angular momenta is relatively straightforward. The physical mechanism that couples the orbital and spin angular momenta together is the spin-orbit interaction, and the resultant total angular momentum vector $\boldsymbol{j}$ is defined by:

$$\boldsymbol{j} = \boldsymbol{l} + \boldsymbol{s}\,. \tag{5.11}$$

$\boldsymbol{j}$ is described by the quantum numbers j and m_j according to the usual rules for quantum mechanical angular momenta, namely:

$$|\boldsymbol{j}| = \sqrt{j(j+1)}\hbar\,, \tag{5.12}$$

and

$$j_z = m_j \hbar\,, \tag{5.13}$$

where m_j takes values of $j, (j-1), \cdots, -j$. The addition of $\boldsymbol{l}$ and $\boldsymbol{s}$ to form the resultant $\boldsymbol{j}$ is illustrated by Fig. 5.1(b).[4]

The allowed values of j are worked out by applying eqn 5.9, with the knowledge that the spin quantum number s is always equal to $1/2$. If the electron is in a state with orbital quantum number l, we then find $j = l \oplus s = (l \pm 1/2)$, except when $l = 0$, in which case we just have $j = 1/2$. In the second case, the angular momentum of the atom arises purely from the electron spin.

[4] Graphical representations of the type shown in Fig. 5.1 are called **vector models**. We shall encounter vector models again when we come to study the Zeeman effect in Lecture Notes 7.

5.6 Angular momentum coupling in multi-electron atoms

The Hamiltonian for an N-electron atom can be written in the form:

$$\hat{H} = \hat{H}_0 + \hat{H}_1 + \hat{H}_2 \,, \tag{5.14}$$

where:

$$\hat{H}_0 = \sum_{i=1}^{N} \left(-\frac{\hbar^2}{2m} \boldsymbol{\nabla}_i^2 - \frac{Ze^2}{4\pi\epsilon_0 r_i} + V_{\text{central}}(r_i) \right) , \tag{5.15}$$

$$\hat{H}_1 = \sum_{i>j}^{N} \frac{e^2}{4\pi\epsilon_0 |\boldsymbol{r}_i - \boldsymbol{r}_j|} - \sum_{i=1}^{N} V_{\text{central}}(r_i) \,, \tag{5.16}$$

$$\hat{H}_2 = \sum_{i=1}^{N} \xi(r_i) \boldsymbol{l}_i \cdot \boldsymbol{s}_i \,. \tag{5.17}$$

As shown in Section 4.1, $\hat{H}_0$ is the central-field Hamiltonian and $\hat{H}_1$ is the residual electrostatic potential. $\hat{H}_2$ is the spin-orbit interaction summed over the electrons of the atom.

In Chapter 4 we neglected both $\hat{H}_1$ and $\hat{H}_2$, and just concentrated on $\hat{H}_0$. This led to the conclusion that each electron occupies a state in a shell defined by the quantum numbers n and l. The reason why we neglected $\hat{H}_1$ is that the off-radial forces due to the electron-electron repulsion are smaller than the radial ones, while $\hat{H}_2$ was neglected because the spin-orbit effects are much smaller than the main terms in the Hamiltonian. It is now time to study what happens when these two terms are included. In doing so, there are two obvious limits to consider:[5]

- **LS coupling**: $\hat{H}_1 \gg \hat{H}_2$.
- **jj coupling**: $\hat{H}_2 \gg \hat{H}_1$.

Since the spin-orbit interaction scales approximately as Z^2, LS-coupling mainly occurs in atoms with small to medium Z, while jj-coupling occurs in some atoms with large Z. In the sections below, we focus on the LS-coupling limit. The less common case of jj-coupling is considered briefly in Section 5.10.

5.7 LS coupling

In the **LS-coupling** limit (alternatively called **Russell–Saunders coupling**), the residual electrostatic interaction is much stronger than the spin-orbit interaction. We therefore deal with the residual electrostatic interaction first and then apply the spin-orbit interaction as a perturbation. The LS coupling regime applies to most atoms of small and medium atomic number.

Let us first discuss some issues of notation. We shall need to distinguish between the quantum numbers that refer to the individual electrons within an atom and the state of the atom as a whole. The convention is:

- Lower case quantum numbers (j, l, s) refer to *individual electrons* within atoms.
- Upper case quantum numbers (J, L and S) refer to the angular momentum states of the *whole atom*.

For single electron atoms like hydrogen, there is no difference. However, in multi-electron atoms there is a real difference because we must distinguish between the angular momentum states of the individual electrons and the resultants which give the angular momentum states of the whole atom.

We can use this notation to determine the angular momentum states that the LS-coupling scheme produces. The residual electrostatic interaction has the effect of coupling the orbital and spin angular momenta of the individual electrons together, so that we find their resultants according to:

$$\boldsymbol{L} = \sum_i \boldsymbol{l}_i \,, \tag{5.18}$$

$$\boldsymbol{S} = \sum_i \boldsymbol{s}_i \,. \tag{5.19}$$

[5] In some atoms with medium-large Z (e.g. germanium $Z = 32$) we are in the awkward situation where neither limit applies. We then have **intermediate coupling**, and the behaviour is quite complicated to describe.

Filled shells of electrons have no net angular momentum, and so the summation only needs to be carried out over the valence electrons. In a many-electron atom, the rule given in eqn 5.9 usually allows several possible values of the quantum numbers L and S for a particular electronic configuration. Their energies will differ due to the residual electrostatic interaction. The atomic states defined by the values of L and S are called **terms**.

For each atomic term, we can find the total angular momentum of the whole atom from:

$$\boldsymbol{J} = \boldsymbol{L} + \boldsymbol{S}\,. \tag{5.20}$$

The values of J, the quantum number corresponding to $\boldsymbol{J}$, are found from L and S according to eqn 5.9. The states of different J for each LS-term have different energies due to the spin-orbit interaction. In analogy with eqn 5.10, the spin-orbit interaction of the whole atom is written:

$$\Delta E_{\rm so} \propto -\boldsymbol{\mu}_{\rm spin}^{\rm atom} \cdot \boldsymbol{B}_{\rm orbital}^{\rm atom} \propto \boldsymbol{L}\cdot\boldsymbol{S}\,, \tag{5.21}$$

where the 'atom' superscript indicates that we take the resultant values for the whole atom. The details of the spin-orbit interaction in the LS coupling limit are considered in Section 6.6. At this stage, all we need to know is that the spin-orbit interaction splits the LS terms into **levels** labelled by J.

It is convenient to introduce a shorthand notation to label the energy levels that occur in the LS coupling regime. Each level is labelled by the quantum numbers J, L and S and is represented in the form:

$$^{2S+1}\mathrm{L}_J\,.$$

The factors $(2S+1)$ and J appear as numbers, whereas L is a letter that follows the rule:

- S implies $L = 0$,
- P implies $L = 1$,
- D implies $L = 2$,
- F implies $L = 3$, etc.

Thus, for example, a $^2\mathrm{P}_{1/2}$ term is the energy level with quantum numbers $S = 1/2$, $L = 1$, and $J = 1/2$, while a $^3\mathrm{D}_3$ has $S = 1$, $L = 2$ and $J = 3$. The factor of $(2S+1)$ in the top left is called the **multiplicity**. It indicates the degeneracy of the level due to the spin: i.e. the number of M_S states available. If $S = 0$, the multiplicity is 1, and the terms are called **singlets**. If $S = 1/2$, the multiplicity is 2 and we have **doublet** terms. If $S = 1$ we have **triplet** terms, etc.

As an example, consider the (3s,3p) electronic configuration of magnesium, where one of the valence electrons is in an s-shell with $l = 0$ and the other is in a p-shell with $l = 1$. We first work out the LS terms:

- $L = l_1 \oplus l_2 = 0 \oplus 1 = 1$.
- $S = s_1 \oplus s_2 = 1/2 \oplus 1/2 = 1$ or 0.

We thus have two terms: a ^{3}P triplet and a ^{1}P singlet. The allowed levels are then worked out as follows:

- For the ^{3}P triplet, we have $J = L \oplus S = 1 \oplus 1 = 2$, 1, or 0. We thus have three levels: $^3\mathrm{P}_2$, $^3\mathrm{P}_1$, and $^3\mathrm{P}_0$.
- For the ^{1}P singlet, we have $J = L \oplus S = 1 \oplus 0 = 1$. We thus have a single $^1\mathrm{P}_1$ level.

These levels are illustrated in Fig. 5.2. The ordering of the energy states should not concern us at this stage. The main point to realize is the general way the states split as the new interactions are turned on, and the terminology used to designate the states.

5.8 Electric dipole selection rules in the LS coupling limit

When considering electric-dipole transitions between the states of many-electron atoms that have LS-coupling, a single electron makes a jump from one atomic shell to a new one. The rules that apply to this electron are the same as the ones discussed in Section 3.4. However, we also have to think about the angular momentum state of the whole atom as specified by the quantum numbers (L, S, J). The rules that emerge are as follows:

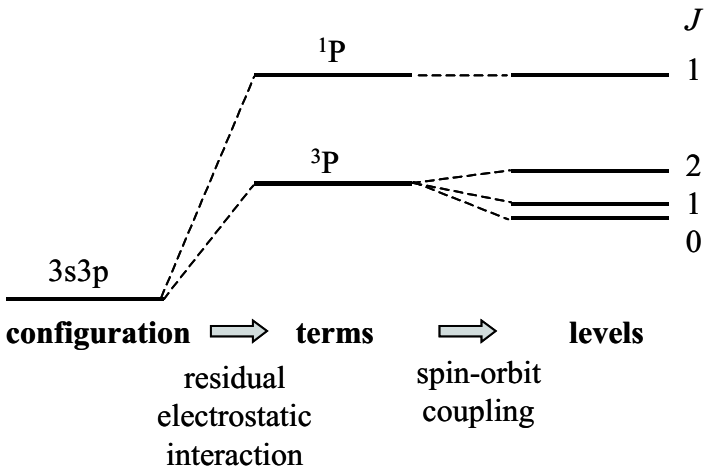

Figure 5.2: Splitting of the energy levels for the (3s,3p) configuration of magnesium in the LS coupling regime.

1. The parity of the wave function must change.
2. $\Delta l = \pm 1$ for the electron that jumps between shells.
3. $\Delta L = 0, \pm 1$, but $L = 0 \rightarrow 0$ is forbidden.
4. $\Delta J = 0, \pm 1$, but $J = 0 \rightarrow 0$ is forbidden.
5. $\Delta S = 0$.

Rule 1 follows from the odd parity of the dipole operator. Rule 2 applies the single-electron rule to the individual electron that makes the jump in the transition, and rule 3 applies this rule to the whole atom.[6] Rules 4 follows from the fact that the total angular momentum must be conserved in the transition, allowing us to write:

$$\boldsymbol{J}^{\text{initial}} = \boldsymbol{J}^{\text{final}} + \boldsymbol{J}^{\text{photon}} . \tag{5.22}$$

The photon carries one unit of angular momentum, and so we conclude from eqn 5.9 that $\Delta J = -1,\ 0,$ or $+1$. However, the $\Delta J = 0$ rule cannot be applied to $J = 0 \rightarrow 0$ transitions because it is not possible to satisfy eqn 5.22 in these circumstances. Finally, rule 5 is a consequence of the fact that the photon does not interact with the spin.[7]

5.9 Hund's rules

We have seen above that there are many terms in the energy spectrum of a multi-electron atom. Of these, one will have the lowest energy, and will form the **ground state**. All the others are excited states. Each atom has a *unique* ground state, which is determined by minimizing the energy of its valence electrons with the residual electrostatic and spin-orbit interactions included. In principle, this is a very complicated calculation. Fortunately, however, **Hund's rules** allow us to determine which level is the ground state for atoms that have LS-coupling without lengthy calculation. The rules are:

1. The term with the largest multiplicity (i.e. largest S) has the lowest energy.
2. For a given multiplicity, the term with the largest L has the lowest energy.
3. The level with $J = |L - S|$ has the lowest energy if the shell is less than half full. If the shell is more than half full, the level with $J = L + S$ has the lowest energy.

[6] $\Delta L = 0$ transitions are obviously forbidden in one-electron atoms, because $L = l$ and l must change. However, in atoms with more than one valence electron, it is possible to get transitions between different configurations that satisfy rule 2, but have the same value of L: e.g. $3p4p\,{}^3P_1 \rightarrow 3p4s\,{}^3P_2$.

[7] $\Delta S \neq 0$ transitions can be weakly allowed when the spin-orbit coupling is strong, because the spin is then mixed with the orbital motion.

The first of these rules basically tells us that the electrons try to align themselves with their spins parallel in order to minimize the exchange interaction. (See Chapter 8.) The other two follow from the minimizing the spin-orbit interaction.

Let us have a look at carbon as an example. Carbon has an atomic number $Z = 6$ with two valence electrons in the outermost 2p shell. Each valence electron therefore has $l = 1$ and $s = 1/2$. Consider first the (2p,np) excited state configuration with one electron in the 2p shell and the other in the np shell, where $n \geq 3$. We have from eqn 5.9 that $L = 1 \oplus 1 = 0$, 1 or 2, and $S = 1/2 \oplus 1/2 = 0$ or 1. We thus have three singlet terms (^{1}S, ^{1}P, ^{1}D), and three triplet terms (^{3}S, ^{3}P, ^{3}D). This gives rise to three singlet levels:

$$^1\mathrm{S}_0, \ ^1\mathrm{P}_1, \ ^1\mathrm{D}_2 \, ,$$

and seven triplet levels:

$$^3\mathrm{S}_1, \ ^3\mathrm{P}_0, \ ^3\mathrm{P}_1, \ ^3\mathrm{P}_2, \ ^3\mathrm{D}_1, \ ^3\mathrm{D}_2, \ ^3\mathrm{D}_3 \, .$$

We thus have a confusing array of *ten* levels in the energy spectrum for the (2p,np) configuration.

The situation in the ground state configuration (2p,2p) is simplified by the fact that the electrons are **equivalent**, i.e. in the *same* shell. The Pauli exclusion principle forbids the possibility that two or more electrons should have the same set of quantum numbers, and this means that $L + S$ must be equal to an even number. There is no easy explanation for this rule, but the simplest example of its application, namely to two electrons in the same s-shell, is considered in Section 8.3. For these two s-electrons, we have $L = 0 \oplus 0 = 0$ and $S = 1/2 \oplus 1/2 = 0$ or 1, giving rise to two terms: ^{1}S and ^{3}S. Both terms are allowed when the electrons are in different s-shells, but the $L + S$ rule tells us that only the singlet ^{1}S term is allowed if the electrons are in the same s-shell. The proof that the triplet term does not exist for the (1s,1s) ground-state configuration of helium is given in Section 8.3.

On applying the rule that $L + S$ must be even to the equivalent 2p electrons in the carbon ground state, we find that only the ^{1}S, ^{1}D, and ^{3}P terms are allowed, which means that only five of the ten levels listed above are possible:[8]

$$^1\mathrm{S}_0, \ ^1\mathrm{D}_2, \ ^3\mathrm{P}_0, \ ^3\mathrm{P}_1, \ ^3\mathrm{P}_2 \, .$$

We can now apply Hund's rules to find out which of these is the ground state. The first rule states that the triplet levels have the lower energy. Since these all have $L = 1$ we do not need to consider the second rule. The shell is less than half full, and so we have $J = |L - S| = 0$. The ground state is thus the ^{3}P$_0$ level. All the other levels are excited states.

It is important to notice that, if we had forgotten the rule that $L + S$ must be even, we would have incorrectly concluded from Hund's rules that the ground state is a ^{3}D$_1$ term, which does not exist for the (2p,2p) configuration. It is therefore safer to use a different version of Hund's rules, based on the allowed combinations of (m_s, m_l) sub-levels:

1. Maximize the spin and set $S = \sum m_s$.
2. Maximize the orbital angular momentum, subject to rule 1, and set $L = \sum m_l$.
3. $J = |L - S|$ if the shell is less than half full, otherwise $J = |L + S|$.

These rules should work in all cases, since they incorporate the Pauli exclusion principle properly.

As an example of how to use the second version of Hund's rules, we apply them again to the two 2p electrons of carbon. The two electrons can go into the six possible (m_s, m_l) sub-levels of the 2p shell.

1. To get the largest value of the spin, we must have both electron spins aligned with $m_s = +1/2$. This gives $S = 1/2 + 1/2 = 1$.
2. Having put both electrons into spin up states, we cannot now put both electrons into $m_l = +1$ states because of Pauli's exclusion principle. The best we can do is to put one into an $m_l = 1$ state and the other into an $m_l = 0$ state, as illustrated in Table 5.1. This gives $L = 1 + 0 = 1$.
3. The shell is less than half full, and so we have $J = |L - S| = 0$.

We thus deduce that the ground state is the ^{3}P$_0$ level, as before.

The ground state levels for the first 11 elements, as worked out from Hund's rules, are listed in Table 5.2. Experimental results confirm these predictions. Note that full shells always give ^{1}S$_0$ level with no net angular momentum: $S = L = J = 0$.

[8] The full derivation of the allowed states for the (np,np) configuration of a group IV atom is considered, for example, in Woodgate, *Elementary Atomic Structure*, 2nd Edition, Oxford University Press, 1980, Section 7.2.

	m_l		
m_s	–1	0	+1
+1/2		↑	↑
−1/2			

Table 5.1: Distribution of the two valence electrons of the carbon ground state within the m_s and m_l states of the 2p shell.

Z	Element	Configuration	Ground state
1	H	$1s^1$	$^2S_{1/2}$
2	He	$1s^2$	$^1S_0$
3	Li	$1s^2\ 2s^1$	$^2S_{1/2}$
4	Be	$1s^2\ 2s^2$	$^1S_0$
5	B	$1s^2\ 2s^2\ 2p^1$	$^2P_{1/2}$
6	C	$1s^2\ 2s^2\ 2p^2$	$^3P_0$
7	N	$1s^2\ 2s^2\ 2p^3$	$^4S_{3/2}$
8	O	$1s^2\ 2s^2\ 2p^4$	$^3P_2$
9	F	$1s^2\ 2s^2\ 2p^5$	$^2P_{3/2}$
10	Ne	$1s^2\ 2s^2\ 2p^6$	$^1S_0$
11	Na	$1s^2\ 2s^2\ 2p^6\ 3s^1$	$^2S_{1/2}$

Table 5.2: Electronic configurations and ground state terms of the first 11 elements in the periodic table.

It is important to be aware that Hund's rules *cannot* be used to find the energy ordering of excited states with reliability. For example, consider the (2p,3p) excited state configuration of carbon, which has the ten possible levels listed previously. Hund's rules predict that the $^3D_1$ level has the lowest energy, but the lowest state is actually the $^1P_1$ level.

5.10 jj coupling

The spin-orbit interaction gets larger as Z increases. (See, for example, eqn 6.42.) This means that in some atoms with large Z (eg tin with $Z = 50$) we can have a situation in which the spin-orbit interaction is much stronger than the residual electrostatic interaction. In this regime, **jj coupling** coupling occurs. The spin-orbit interaction couples the orbital and spin angular momenta of the individual electrons together first, and we then find the resultant $\boldsymbol{J}$ for the whole atom by adding together the individual $\boldsymbol{j}$s:

$$\begin{aligned} \boldsymbol{j}_i &= \boldsymbol{l}_i + \boldsymbol{s}_i \\ \boldsymbol{J} &= \sum_{i=1}^{N} \boldsymbol{j}_i \end{aligned} \tag{5.23}$$

These J states are then split by the weaker residual electrostatic potential, which acts as a perturbation.

Reading

Demtröder, W., *Atoms, Molecules and Photons*, §5.5–6, 6.2–5.
Haken and Wolf, *The physics of atoms and quanta*, chapters 12, 17, 19.
Eisberg and Resnick, *Quantum Physics*, chapters 8, 10.
Foot, *Atomic physics*, §2.3.1, chapter 5.
Beisser, *Concepts of Modern Physics*, §7.7 – 8.

Chapter 6

Fine structure

In the previous five sets of notes we have been mainly studying the **gross structure** of atoms. When we consider the gross structure, we include only the largest interaction terms in the Hamiltonian, namely, the electron kinetic energy, the electron-nuclear attraction, and the electron-electron repulsion.

It is now time to start considering the smaller interactions in the atom that arise from magnetic effects. In this chapter we shall consider only those effects caused by *internal* magnetic fields, leaving the discussion of the effects produced by *external* fields to the next set of notes. The internal fields within atoms cause **fine structure** in atomic spectra. We shall start by considering the fine structure of hydrogen and then move on to many-electron atoms. At the end of these notes we shall also look briefly at **hyperfine structure**, which is a similar, but smaller, effect due to the magnetic interactions between the electrons and the nucleus.

6.1 Orbital magnetic dipoles

The quantum numbers n and l were first introduced in the old quantum theory of Bohr and Sommerfeld. The **principal quantum number** n was introduced in the Bohr model as a fundamental postulate concerning the quantization of the angular momentum (see eqn 1.5), while the **orbital quantum number** l was introduced a few years later by Sommerfeld as a patch-up to account for the possibility that the atomic orbits might be elliptical rather than circular. In Lecture Notes 2, we saw how these two quantum numbers naturally re-appear in the full quantum mechanical treatment of the hydrogen atom. Then, in Section 4.1, we saw how they carry across to many-electron atoms.

Two key results that drop out of the quantum mechanical treatment of atoms are:

- The magnitude L of the orbital angular momentum of an electron is given by (see eqn 2.32):

$$L = \sqrt{l(l+1)}\hbar\,, \tag{6.1}$$

  where l can take integer values up to $(n-1)$.

- The component of the angular momentum along a particular axis (usually taken as the z axis) is quantized in units of $\hbar$ and its value is given by (see eqn 2.33):

$$L_z = m_l\hbar\,, \tag{6.2}$$

  where the magnetic quantum number m_l can take integer values from $-l$ to $+l$.

These two relationships give rise to the vector model of angular momentum illustrated in Fig. 2.1.

The orbital motion of the electron causes it to have a magnetic moment. Let us first consider an electron in a circular Bohr orbit, as illustrated in Fig. 6.1(a). The electron orbit is equivalent to a current loop, and we know from electromagnetism that current loops behave like magnets. The electron in the Bohr orbit is equivalent to a little magnet with a magnetic dipole moment μ given by:

$$\mu = i \times \text{Area} = -(e/T) \times (\pi r^2)\,, \tag{6.3}$$

where T is the period of the orbit. Now $T = 2\pi r/v$, and so we obtain

$$\mu = -\frac{ev}{2\pi r}\pi r^2 = -\frac{e}{2m_{\rm e}}m_{\rm e}vr = -\frac{e}{2m_{\rm e}}L, \tag{6.4}$$

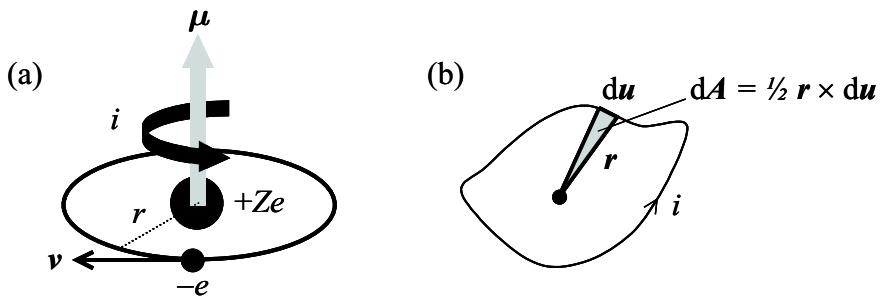

Figure 6.1: (a) The orbital motion of the electron around the nucleus in a circular Bohr orbit is equivalent to a current loop, which generates a magnetic dipole moment. (b) Magnetic dipole moment of an electron in a non-circular orbit.

where we have substituted L for the orbital angular momentum $m_e vr$.

This relationship can easily be generalized to the case of electrons in non-circular orbits. Consider an electron at position vector $\boldsymbol{r}$ in a non-circular orbit with an origin O. The magnetic dipole moment is given by:

$$\boldsymbol{\mu} = \oint i \, \mathrm{d}\boldsymbol{A} \,, \tag{6.5}$$

where i is the current in the loop and $\mathrm{d}\boldsymbol{A}$ is the incremental area swept out by the electron as it performs its orbit. The incremental area $\mathrm{d}\boldsymbol{A}$ is related to the path element $\mathrm{d}\boldsymbol{u}$ by:

$$\mathrm{d}\boldsymbol{A} = \frac{1}{2} \boldsymbol{r} \times \mathrm{d}\boldsymbol{u} \,, \tag{6.6}$$

and so eqn 6.5 becomes:

$$\boldsymbol{\mu} = \frac{1}{2} \oint i \, \boldsymbol{r} \times \mathrm{d}\boldsymbol{u} \,. \tag{6.7}$$

We can write the current as $i = \mathrm{d}q/\mathrm{d}t$, where q is the charge, which implies:

$$\begin{aligned} \boldsymbol{\mu} &= \frac{1}{2} \oint \frac{\mathrm{d}q}{\mathrm{d}t} \boldsymbol{r} \times \mathrm{d}\boldsymbol{u} \,, \\ &= \frac{1}{2} \oint \mathrm{d}q \, \boldsymbol{r} \times \frac{\mathrm{d}\boldsymbol{u}}{\mathrm{d}t} \,, \\ &= \frac{1}{2} \oint \mathrm{d}q \, \boldsymbol{r} \times \boldsymbol{v} \,, \\ &= \frac{1}{2m_e} \oint \mathrm{d}q \, \boldsymbol{r} \times \boldsymbol{p} \,, \end{aligned} \tag{6.8}$$

where $\boldsymbol{v}$ is the velocity, and $\boldsymbol{p}$ is the momentum. The angular momentum is defined as usual by

$$\boldsymbol{L} = \boldsymbol{r} \times \boldsymbol{p} \tag{6.9}$$

and so we finally obtain:

$$\boldsymbol{\mu} = \frac{1}{2m_e} \oint \boldsymbol{L} \mathrm{d}q = \frac{1}{2m_e} \boldsymbol{L} \oint \mathrm{d}q = \frac{1}{2m_e} \boldsymbol{L}(-e) \,, \tag{6.10}$$

as in eqn 6.4. Note that the result works because the angular momentum $\boldsymbol{L}$ is a constant of the motion in the central field approximation (see Section 5.2.1), and so it can be taken out of the integral.

Equation 6.4 shows us that the orbital angular momentum is directly related to the magnetic dipole moment. The quantity $e/2m_e$ that appears is called the **gyromagnetic ratio**. It specifies the proportionality constant between the angular momentum of an electron and its magnetic moment. It is apparent from eqns 6.1 and 6.4 that the magnitude of atomic magnetic dipoles is given by:

$$|\boldsymbol{\mu}| = \frac{e}{2m_e} \hbar \sqrt{l(l+1)} = \mu_B \sqrt{l(l+1)} \,, \tag{6.11}$$

where μ_B is the **Bohr magneton** defined by:

$$\mu_B = \frac{e\hbar}{2m_e} = 9.27 \times 10^{-24} \, \mathrm{JT}^{-1}. \tag{6.12}$$

This shows that the size of atomic dipoles is of order $\mu_{\rm B}$. In many cases we are interested in the z component of the magnetic dipole, which is given from eqns 6.2 and 6.4 as:

$$\mu_z = -\frac{e}{2m_{\rm e}} L_z = -\mu_{\rm B} m_l \,, \tag{6.13}$$

where m_l is the orbital magnetic quantum number.

6.2 Spin magnetism

We have seen in Section 5.2.2 that electrons also have spin angular momentum. The deflections measured in the Stern-Gerlach experiment (see Fig. 1.4) enabled the magnitude of the magnetic moment due to the spin angular momentum to be determined. The component along the z axis was found to obey:

$$\mu_z = -g_{\rm s}\mu_{\rm B} m_s \,, \tag{6.14}$$

where $g_{\rm s}$ is the **g-value** of the electron, and $m_s = \pm 1/2$ is the magnetic quantum number due to spin. This is identical in form to eqn 6.13 apart from the factor of $g_{\rm s}$. The experimental value of $g_{\rm s}$ was found to be close to 2. The Dirac equation predicts that $g_{\rm s}$ should be exactly equal to 2, and more recent calculations based on quantum electrodynamics (QED) give a value of 2.0023192, which agrees very accurately with the most precise experimental data.

6.3 Spin-orbit coupling

The fact that electrons in atoms have both orbital and spin angular momentum leads to a new interaction term in the Hamiltonian called **spin-orbit coupling**. Sophisticated theories of spin-orbit coupling (e.g. those based on the Dirac equation) indicate that it is actually a relativistic effect. At this stage it is more useful to consider spin-orbit coupling as the interaction between the magnetic field due to the orbital motion of the electron and the magnetic moment due to its spin. This more intuitive approach is the one we adopt here. We start by giving a simple order of magnitude estimate based on the semi-classical Bohr model, and then take a more general approach that works for the fully quantum mechanical picture.

6.3.1 Spin-orbit coupling in the Bohr model

The easiest way to understand the spin-orbit coupling is to consider the single electron of a hydrogen atom in a Bohr-like circular orbit around the nucleus, and then shift the origin to the electron, as indicated in Fig. 6.2. In this frame, the electron is stationary and the nucleus is moving in a circular orbit of radius r_n. The orbit of the nucleus is equivalent to a current loop, which produces a magnetic field at the origin. Now the magnetic field produced by a circular loop of radius r carrying a current i is given by:

$$B_z = \frac{\mu_0 i}{2r} \,, \tag{6.15}$$

where z is taken to be the direction perpendicular to the loop. As in Section 6.1, the current i is given by the charge Ze divided by the orbital period $T = 2\pi r/v$. On substituting for the velocity and radius in the Bohr model from eqns 1.15 and 1.16, we find:

$$B_z = \frac{\mu_0 Z e v_n}{4\pi r_n^2} = \left(\frac{Z^4}{n^5}\right) \frac{\mu_0 \alpha c e}{4\pi a_0^2} \,, \tag{6.16}$$

where $\alpha = e^2/2\epsilon_0 hc \approx 1/137$ is the **fine structure constant** defined in eqn 1.18. For hydrogen with $Z = n = 1$, this gives $B_z \approx 12\,\text{Tesla}$, which is a large field.

The electron at the origin experiences this orbital field and we thus have a magnetic interaction energy of the form:

$$\Delta E_{\rm so} = -\boldsymbol{\mu}_{\rm spin} \cdot \boldsymbol{B}_{\rm orbital} \,, \tag{6.17}$$

which, from eqn 6.14, becomes:

$$\Delta E_{\rm so} = g_{\rm s}\mu_{\rm B} m_s B_z = \pm \mu_{\rm B} B_z \,, \tag{6.18}$$

where we have used $g_{\rm s} = 2$ and $m_s = \pm 1/2$ in the last equality. By substituting from eqn. 6.16 and making use of eqn 6.12, we find:

$$|\Delta E_{\rm so}| = \left(\frac{Z^4}{n^5}\right) \frac{\mu_0 \alpha c e^2 \hbar}{8\pi m_{\rm e} a_0^2} \equiv \alpha^2 \frac{Z^2}{n^3} |E_n| \,, \tag{6.19}$$

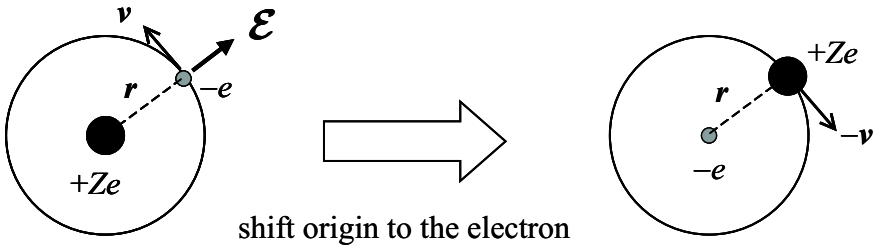

Figure 6.2: An electron moving with velocity $\boldsymbol{v}$ through the electric field $\boldsymbol{\mathcal{E}}$ of the nucleus experiences a magnetic field equal to $(\boldsymbol{\mathcal{E}}\times\boldsymbol{v})/c^2$. The magnetic field can be understood by shifting the origin to the electron and calculating the magnetic field due to the orbital motion of the nucleus around the electron. The velocity of the nucleus in this frame is equal to $-\boldsymbol{v}$.

where E_n is the quantized energy given by eqn 1.10. For the $n = 1$ orbit of hydrogen, this gives:

$$|\Delta E_{\rm so}| = \alpha^2 R_H = 13.6\,{\rm eV}/137^2 = 0.7\,{\rm meV} \equiv 6\,{\rm cm}^{-1}\,.$$

This shows that the spin-orbit interaction is about 10^4 times smaller than the gross structure energy in hydrogen. Note that the relative size of the spin-orbit interaction grows as Z^2, so that spin-orbit effects are expected to become more important in heavier atoms, which is indeed the case. Note also that eqn 6.19 can be re-written using eqn 1.16 as

$$|\Delta E_{\rm so}| = \left(\frac{v_n}{c}\right)^2 \frac{|E_n|}{n}\,, \tag{6.20}$$

which shows that the spin-orbit interaction energy is of the same magnitude as the relativistic corrections that would be expected for the Bohr model. This is hardly surprising, given that Dirac tells us that we should really think of spin-orbit coupling as a relativistic effect.

6.3.2 Spin-orbit coupling beyond the Bohr model

In this sub-section we repeat the calculation above but without making use of the semi-classical results from the Bohr model. The electrons experience a magnetic field as they move through the electric field of the nucleus. If the electron velocity is $\boldsymbol{v}$, it will see the nucleus orbiting around it with a velocity of $-\boldsymbol{v}$, as shown in Fig. 6.2. The magnetic field generated at the electron can be calculated by the Biot-Savart law as shown by Fig. 6.3. This gives the magnetic field at the origin of a loop carrying a current i as:

$$\boldsymbol{B} = \frac{\mu_0}{4\pi}\oint_{\rm loop} i\,\frac{{\rm d}\boldsymbol{u}\times\boldsymbol{r}}{r^3}\,, \tag{6.21}$$

where ${\rm d}\boldsymbol{u}$ is an orbital path element. For simplicity we consider the case of a circular orbit with constant r. In this case we have:

$$\oint i\,{\rm d}\boldsymbol{u} = \oint \frac{{\rm d}q}{{\rm d}t}\,{\rm d}\boldsymbol{u} = Ze\frac{{\rm d}\boldsymbol{u}}{{\rm d}t} = Ze(-\boldsymbol{v})\,.$$

We thus obtain:

$$\boldsymbol{B} = -\frac{\mu_0}{4\pi}\frac{Ze}{r^3}\boldsymbol{v}\times\boldsymbol{r} = \frac{\mu_0}{4\pi}\frac{Ze}{r^3}\boldsymbol{r}\times\boldsymbol{v}\,. \tag{6.22}$$

For a Coulomb field the electric field $\boldsymbol{\mathcal{E}}$ is given by:

$$\boldsymbol{\mathcal{E}} = \frac{Ze}{4\pi\epsilon_0 r^2}\hat{\boldsymbol{r}} = \frac{Ze}{4\pi\epsilon_0 r^3}\boldsymbol{r}\,, \tag{6.23}$$

where the hat symbol on $\hat{\boldsymbol{r}}$ in the first equality indicates that it is a unit vector. On combining equations 6.22 and 6.23 we obtain:

$$\boldsymbol{B} = \mu_0\epsilon_0\,\boldsymbol{\mathcal{E}}\times\boldsymbol{v}\,. \tag{6.24}$$

We know from Maxwell's equations that $\mu_0\epsilon_0 = 1/c^2$, and so we can re-write this as:

$$\boldsymbol{B} = \frac{1}{c^2}\,\boldsymbol{\mathcal{E}}\times\boldsymbol{v}\,. \tag{6.25}$$

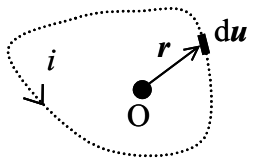

Figure 6.3: The magnetic field at the origin O due to a loop carrying a current i is calculated by the Biot-Savart law given in Eq. 6.21. The field points out of the paper.

The same formula can also be derived for the more general case of non-circular orbits and non-Coulombic electric fields such as those found in multi-electron atoms.

The spin-orbit interaction energy is given by:

$$\Delta E_{\rm so} = -\boldsymbol{\mu}_{\rm spin}\cdot\boldsymbol{B}_{\rm orbital}\,, \tag{6.26}$$

where $\boldsymbol{\mu}_{\rm spin}$ is the magnetic moment due to spin, which is given by:

$$\boldsymbol{\mu}_{\rm spin} = -g_{\rm s}\frac{|e|}{2m_{\rm e}}\boldsymbol{s} = -g_{\rm s}\frac{\mu_{\rm B}}{\hbar}\boldsymbol{s}\,. \tag{6.27}$$

On substituting Eqs. 6.25 and 6.27 into Eq. 6.26, we obtain:

$$\Delta E_{\rm so} = \frac{g_{\rm s}\mu_{\rm B}}{\hbar c^2}\boldsymbol{s}\cdot(\boldsymbol{\mathcal{E}}\times\boldsymbol{v})\,. \tag{6.28}$$

If we have a **central field** (ie the potential V is a function of r only), we can write:[1]

$$\boldsymbol{\mathcal{E}} = \frac{1}{e}\frac{\boldsymbol{r}}{r}\frac{{\rm d}V}{{\rm d}r}\,. \tag{6.29}$$

On making use of this, the spin-orbit energy becomes:

$$\Delta E_{\rm so} = \frac{g_{\rm s}\mu_{\rm B}}{\hbar c^2 e m_{\rm e}}\left(\frac{1}{r}\frac{{\rm d}V}{{\rm d}r}\right)\boldsymbol{s}\cdot(\boldsymbol{r}\times\boldsymbol{p})\,, \tag{6.30}$$

where we have substituted $\boldsymbol{v} = \boldsymbol{p}/m_{\rm e}$. On recalling that the angular momentum $\boldsymbol{l}$ is defined as $\boldsymbol{r}\times\boldsymbol{p}$, we find:

$$\Delta E_{\rm so} = \frac{g_{\rm s}\mu_{\rm B}}{\hbar c^2 e m_{\rm e}}\left(\frac{1}{r}\frac{{\rm d}V}{{\rm d}r}\right)\boldsymbol{s}\cdot\boldsymbol{l}\,. \tag{6.31}$$

This calculation of $\Delta E_{\rm so}$ does not take proper account of relativistic effects. In particular, we moved the origin from the nucleus to the electron, which is not really allowed because the electron is accelerating all the time and is therefore not an inertial frame. The translation to a rotating frame gives rise to an extra effect called the **Thomas precession** which reduces the energy by a factor of 2. (See Eisberg and Resnick, Appendix O.) On taking the Thomas precession into account, and recalling that $\mu_{\rm B} = e\hbar/2m_{\rm e}$, we obtain the final result:

$$\Delta E_{\rm so} = \frac{g_{\rm s}}{2}\frac{1}{2c^2m_{\rm e}^2}\left(\frac{1}{r}\frac{{\rm d}V}{{\rm d}r}\right)\boldsymbol{l}\cdot\boldsymbol{s}\,. \tag{6.32}$$

This is the same as the result derived from the Dirac equation, except that $g_{\rm s}$ is exactly equal to 2 in Dirac's theory. Equation 6.32 shows that the spin and orbital angular momenta are coupled together. If we have a simple Coulomb field and take $g_{\rm s} = 2$, we find

$$\Delta E_{\rm so} = \frac{Ze^2}{8\pi\epsilon_0 c^2 m_{\rm e}^2}\left(\frac{1}{r^3}\right)\boldsymbol{l}\cdot\boldsymbol{s}\,. \tag{6.33}$$

We can use this formula for hydrogenic atoms, while we can use the more general form given in Eq. 6.32 for more complicated multi-electron atoms where the potential will differ from the Coulombic $1/r$ dependence due to the repulsion between the electrons.

[1] It is easy to verify that this works for a Coulomb field where $V = -Ze^2/4\pi\epsilon_0 r$ and $\boldsymbol{\mathcal{E}}$ is given by eqn 6.23.

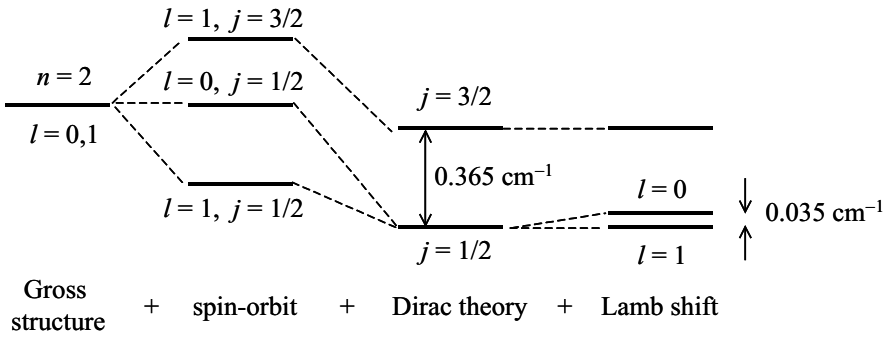

Figure 6.4: Fine structure in the $n = 2$ level of hydrogen.

6.4 Evaluation of the spin-orbit energy for hydrogen

The magnitude of the spin-orbit energy can be calculated from eqn 6.32 as:

$$\Delta E_{\rm so} = \frac{1}{2c^2 m_{\rm e}^2} \left\langle \frac{1}{r}\frac{{\rm d}V}{{\rm d}r} \right\rangle \langle \boldsymbol{l}\cdot\boldsymbol{s}\rangle \,, \tag{6.34}$$

where we have taken $g_{\rm s} = 2$, and the $\langle\cdots\rangle$ notation indicates that we take expectation values:

$$\left\langle \frac{1}{r}\frac{{\rm d}V}{{\rm d}r} \right\rangle = \iiint \psi^*_{nlm} \left(\frac{1}{r}\frac{{\rm d}V}{{\rm d}r}\right) \psi_{nlm}\, r^2 \sin\theta \,{\rm d}r{\rm d}\theta{\rm d}\phi \,. \tag{6.35}$$

The function $({\rm d}V/{\rm d}r)/r$ depends only on r, and so we are left to calculate an integral over r only:

$$\left\langle \frac{1}{r}\frac{{\rm d}V}{{\rm d}r} \right\rangle = \int_0^\infty |R_{nl}(r)|^2 \left(\frac{1}{r}\frac{{\rm d}V}{{\rm d}r}\right) r^2 {\rm d}r \,, \tag{6.36}$$

where $R_{nl}(r)$ is the radial wave function. This integral can be evaluated exactly for the case of the Coulomb field in hydrogen where $({\rm d}V/{\rm d}r)/r \propto 1/r^3$, and the radial wave functions are known exactly. (See Table 2.2.) We then have, for $l \geq 1$:

$$\left\langle \frac{1}{r}\frac{{\rm d}V}{{\rm d}r} \right\rangle \propto \left\langle \frac{1}{r^3} \right\rangle = \frac{Z^3}{a_0^3 n^3 l(l+\frac{1}{2})(l+1)} \,. \tag{6.37}$$

This shows that we can re-write eqn 6.34 in the form:

$$\Delta E_{\rm so} = C_{nl} \,\langle \boldsymbol{l}\cdot\boldsymbol{s}\rangle \,, \tag{6.38}$$

where C_{nl} is a constant that depends only on n and l.

We can evaluate $\langle \boldsymbol{l}\cdot\boldsymbol{s}\rangle$ by realizing from eqn 5.11 that we must have:

$$\boldsymbol{j}^2 = (\boldsymbol{l}+\boldsymbol{s})^2 = \boldsymbol{l}^2 + \boldsymbol{s}^2 + 2\boldsymbol{l}\cdot\boldsymbol{s} \,. \tag{6.39}$$

This implies that:

$$\langle \boldsymbol{l}\cdot\boldsymbol{s}\rangle = \left\langle \frac{1}{2}(\boldsymbol{j}^2 - \boldsymbol{l}^2 - \boldsymbol{s}^2) \right\rangle = \frac{\hbar^2}{2}[j(j+1) - l(l+1) - s(s+1)] \,. \tag{6.40}$$

We therefore find:

$$\Delta E_{\rm so} = C'_{nl}\,[j(j+1) - l(l+1) - s(s+1)] \,, \tag{6.41}$$

where $C'_{nl} = C_{nl}\hbar^2/2$. On using eqn 6.37 we obtain the final result for states with $l \geq 1$:

$$\Delta E_{\rm so} = -\frac{\alpha^2 Z^2}{2n^2} E_n \frac{n}{l(l+\frac{1}{2})(l+1)} [j(j+1) - l(l+1) - s(s+1)] \,, \tag{6.42}$$

where $\alpha \approx 1/137$ is the **fine structure constant**, and $E_n = -R_{\rm H}Z^2/n^2$ is equal to the gross energy. For states with $l = 0$ it is apparent from eqn 6.34 that $\Delta E_{\rm so} = 0$.

The fact that j takes values of $l+1/2$ and $l-1/2$ for $l \geq 1$ means that the spin-orbit interaction splits the two j states with the same value of l. We thus expect the electronic states of hydrogen with $l \geq 1$ to split into doublets. However, the actual fine structure of hydrogen is more complicated for two reasons:

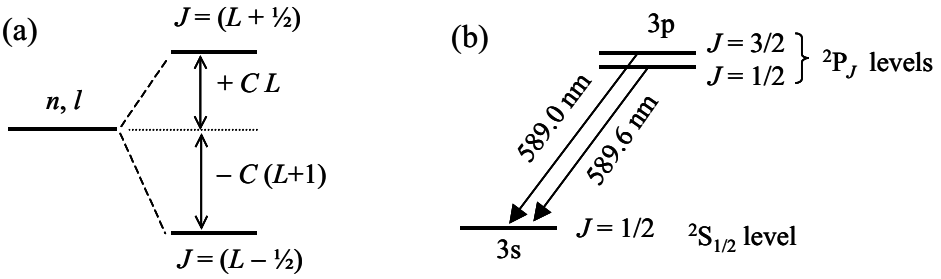

Figure 6.5: Spin-orbit interactions in alkali atoms. (a) The spin-orbit interaction splits the nl states into a doublet if $l \neq 0$. (b) Fine structure in the yellow sodium D lines.

1. States with the same n but different l are degenerate.

2. The spin-orbit interaction is small.

The first point is a general property of pure one-electron systems, and the second follows from the scaling of $\Delta E_{\rm so}/E_n$ with Z^2. A consequence of point 2 is that other relativistic effects that have been neglected up until now are of a similar magnitude to the spin-orbit coupling. In atoms with higher values of Z, the spin-orbit coupling is the dominant relativistic correction, and we can neglect the other effects.

The fine structure of the $n = 2$ level in hydrogen is illustrated in figure 6.4. The fully relativistic Dirac theory predicts that states with the same j are degenerate. The degeneracy of the two $j = 1/2$ states is ultimately lifted by a quantum electrodynamic (QED) effect called the Lamb shift. The complications of the fine structure of hydrogen due to other relativistic and QED effects means that hydrogen is not the paradigm for understanding spin-orbit effects. The alkali metals considered below are in fact simpler to understand.

6.5 Spin-orbit coupling in alkali atoms

Alkali atoms have a single valence electron outside close shells. Closed shells have no angular momentum, and so the angular momentum state $|L, S, J\rangle$ of the atom is determined entirely by the valence electron. By analogy with the results for hydrogen given in eqns 6.38 and eqn 6.41, we can write the spin-orbit interaction term as:

$$\Delta E_{SO} \propto \langle \boldsymbol{L} \cdot \boldsymbol{S} \rangle \propto \left[J(J+1) - L(L+1) - S(S+1) \right]. \tag{6.43}$$

It follows immediately that the spin-orbit energy is zero when the valence electron is in an s-shell, since $\boldsymbol{L} \cdot \boldsymbol{S} = 0$ when $L = 0$. (Alternatively: $J = S$ if $L = 0$, so $J(J+1) - L(L+1) - S(S+1) = 0$.)

Now consider the case when the valence electron is in a shell with $l \neq 0$. We now have $L = l$ and $S = 1/2$, so that $\boldsymbol{L} \cdot \boldsymbol{S} \neq 0$. J has two possible values, namely $J = L \oplus S = L \oplus 1/2 = L \pm 1/2$. On writing eqn 6.43 in the form:

$$\Delta E_{SO} = C \left[J(J+1) - L(L+1) - S(S+1) \right], \tag{6.44}$$

the spin-orbit energy of the $J = (L + 1/2)$ state is given by:

$$\Delta E_{\rm so} = C \left[(L + \frac{1}{2})(L + \frac{3}{2}) - L(L+1) - \frac{1}{2} \cdot \frac{3}{2} \right] = +CL\,,$$

while for the $J = (L - 1/2)$ level we have:

$$\Delta E_{\rm so} = C \left[(L - \frac{1}{2})(L + \frac{1}{2}) - L(L+1) - \frac{1}{2} \cdot \frac{3}{2} \right] = -C(L+1)\,.$$

Hence the term defined by the quantum numbers n and l is split by the spin-orbit coupling into two new states, as illustrated in figure 6.5(a). This gives rise to the appearance of doublets in the atomic spectra. The magnitude of the splitting is smaller than the gross energy by a factor $\sim \alpha^2 = 1/137^2$. (See Eq. 6.42.) This is why these effects are called "fine structure", and α is called the "fine structure constant".

As an example, let us consider sodium, which has 11 electrons, with one valence electron outside filled 1s, 2s and 2p shells. It can therefore be treated as a one electron system, provided we remember that

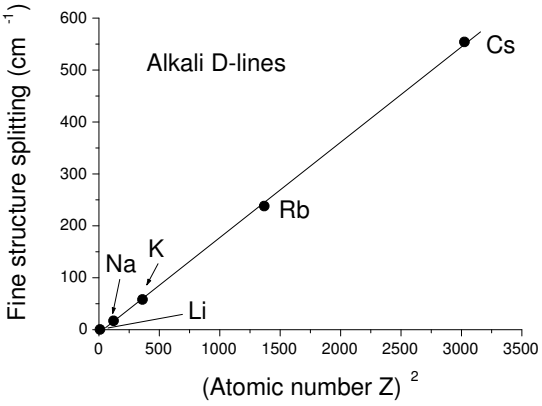

Figure 6.6: Spin-orbit splitting of the first excited state of the alkali atoms versus Z^2, as determined by the fine structure splitting of the D-lines. (See Table 6.1.)

this is only an approximation. One immediate consequence is that the differing l states arising from the same value of n are not degenerate as they are in hydrogen. (See section 4.5.) The bright yellow D lines of sodium correspond to the 3p $\rightarrow$ 3s transition.

It is well known that the D-lines actually consist of a doublet, as shown in Fig. 6.5(b). The doublet arises from the spin-orbit coupling. The ground state is a $^2S_{1/2}$ level with zero spin-orbit splitting. The excited state is split into the two levels derived from the different J values for $L = 1$ and $S = 1/2$, namely the $^2P_{3/2}$ and $^2P_{1/2}$ levels. The two transitions in the doublet are therefore:

$$^2P_{3/2} \rightarrow {}^2S_{1/2}$$

and

$$^2P_{1/2} \rightarrow {}^2S_{1/2}\,.$$

The energy difference of $17\,\mathrm{cm}^{-1}$ between them arises from the spin-orbit splitting of the two J states of the ^{2}P term.

Similar arguments can be applied to the other alkali elements. The spin–orbit energy splittings of their first excited states are tabulated in Table 6.1. Note that the splitting increases with Z, and that the splitting energy is roughly proportional to Z^2, as shown in Fig. 6.6. This is an example of the fact that spin–orbit interactions generally increase with the atomic number, so that the spin–orbit coupling is stronger in heavier elements.

Element	Z	Ground state	1st excited state	Transition	ΔE (cm^{-1})
Lithium	3	[He] 2s	2p	2p →2s	0.33
Sodium	11	[Ne] 3s	3p	3p →3s	17
Potassium	19	[Ar] 4s	4p	4p →4s	58
Rubidium	37	[Kr] 5s	5p	5p →5s	238
Cesium	55	[Xe] 6s	6p	6p →6s	554

Table 6.1: Spin-orbit splitting ΔE of the D lines of the alkali elements. The energy splitting is equal to the difference of the energies of the $J = 3/2$ and $J = 1/2$ levels of the first excited state.

6.6 Spin-orbit coupling in many-electron atoms

We have seen in Chapter 5 that atoms with more than one valence electron can have different types of angular momentum coupling. We restrict our attention here to atoms with LS-coupling, which is the most common type, as explained in Section 5.7. In LS-coupling, the residual electrostatic interaction

couples the orbital and spin angular momenta together according to eqns 5.18 and 5.19. The resultants are then coupled together to give the total angular momentum $\boldsymbol{J}$ according to

$$\boldsymbol{J} = \boldsymbol{L} + \boldsymbol{S}\,. \tag{6.45}$$

The rules for coupling of angular momenta produce several J states for each LS-term, with J running from $L+S$ down to $|L-S|$ in integer steps.[2] These J states experience different spin-orbit interactions, and so are shifted in energy from each other. Hence the spin-orbit coupling splits the J states of a particular LS-term into fine structure multiplets.

The splitting of the J states can be evaluated as follows. The spin-orbit interaction takes the form:

$$\Delta E_{\rm so} = -\boldsymbol{\mu}_{\rm spin} \cdot \boldsymbol{B}_{\rm orbital} \propto \langle \boldsymbol{L} \cdot \boldsymbol{S} \rangle\,, \tag{6.46}$$

which implies (cf. eqns 6.38 – 6.41):

$$\Delta E_{SO} = C_{LS}\,[J(J+1) - L(L+1) - S(S+1)]\,. \tag{6.47}$$

It follows from eqn 6.47 that levels with the same L and S but different J are separated by an energy which is proportional to J. This is called the **interval rule**. Figure 5.2 shows an example of the interval rule for the ^{3}P term of the (3s,3p) configuration of magnesium.

6.7 Nuclear effects in atoms

For most of the time in atomic physics we just take the nucleus to be a heavy charged particle sitting at the centre of the atom. However, careful analysis of the spectral lines can reveal small effects that give us direct information about the nucleus. The main effects that can be observed generally fall into two categories, namely **isotope shifts** and **hyperfine structure**.

6.7.1 Isotope shifts

There are two main processes that give rise to isotope shifts in atoms, namely mass effects and field effects.

Mass effects The mass m that enters the Schrödinger equation is the *reduced* mass, not the bare electron mass $m_{\rm e}$ (cf. eqn 1.9). Changes in the nuclear mass therefore make small changes to m and hence to the atomic energies.

Field effects Electrons in s shells have a finite probability of penetrating the nucleus, and are therefore sensitive to its charge distribution.

Both effects cause small shifts in the wavelengths of the spectral lines from different isotopes of the same element. The heavy isotope of hydrogen, namely deuterium, was discovered in this way through its mass effect.

6.7.2 Hyperfine structure

In high–resolution spectroscopy, it is necessary to consider effects relating to the magnetic interaction between the electron angular momentum ($\boldsymbol{J}$) and the nuclear spin ($\boldsymbol{I}$). The angular momentum of the electrons creates a magnetic field at the nucleus which is proportional to $\boldsymbol{J}$. The spin of the nucleus gives it a magnetic dipole moment which is proportional to $\boldsymbol{I}$, and we therefore have an interaction energy term of the form:

$$\Delta E_{\rm hyperfine} = -\boldsymbol{\mu}_{\rm nucleus} \cdot \boldsymbol{B}_{\rm electron} \propto \langle \boldsymbol{I} \cdot \boldsymbol{J} \rangle\,. \tag{6.48}$$

This gives rise to **hyperfine** splittings in the atomic terms. The magnitude of the splittings is very small because the nuclear dipole is about 2000 times smaller than that of the electron. This follows from the small gyromagnetic ratio of the nucleus, which is inversely proportional to its mass. (See eqn 6.4.) The splittings are therefore about three orders of magnitude smaller than the fine structure splittings: hence the name "hyperfine".

Hyperfine states are labelled by the total angular momentum $\boldsymbol{F}$ of the whole atom (i.e. nucleus plus electrons), where

$$\boldsymbol{F} = \boldsymbol{I} + \boldsymbol{J}. \tag{6.49}$$

[2]There is only one J state, and hence no fine structure splitting, when one or both of L or S are zero.

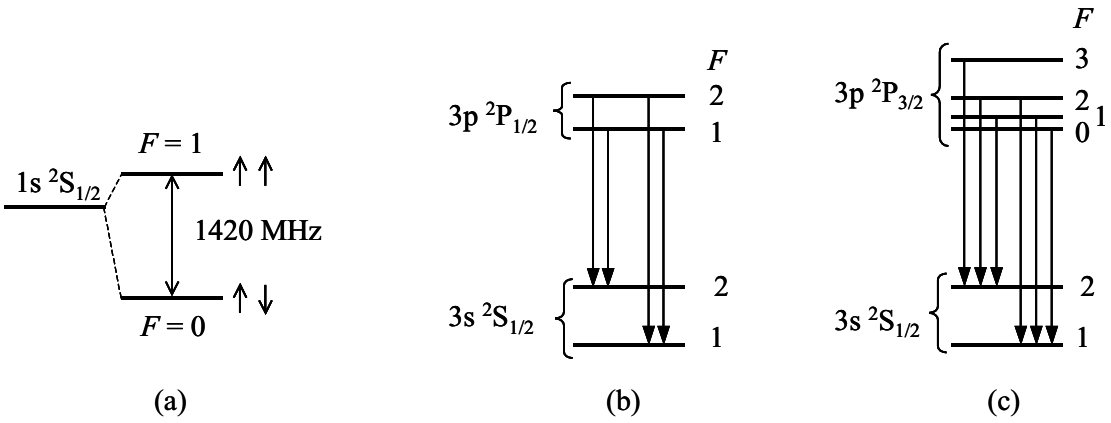

Figure 6.7: (a) Hyperfine structure of the 1s ground state of hydrogen. The arrows indicate the relative directions of the electron and nuclear spin. (b) Hyperfine transitions for the sodium D_1 line. (c) Hyperfine transitions for the sodium D_2 line. Note that the hyperfine splittings are not drawn to scale. The splittings of the sodium levels are as follows: $^2S_{1/2}$, 1772 MHz; $^2P_{1/2}$, 190 MHz; $^2P_{3/2}$ $(3 \to 2)$, 59 MHz; $^2P_{3/2}$ $(2 \to 1)$, 34 MHz; $^2P_{3/2}$ $(1 \to 0)$, 16 MHz.

In analogy with the $|LSJ\rangle$ states of fine structure, the electric dipole selection rule for transitions between hyperfine states is:

$$\Delta F = 0, \pm 1\,, \tag{6.50}$$

with the exception that $F = 0 \to 0$ transitions are forbidden. Let us consider two examples to see how this works.

The hydrogen 21 cm line

Consider the ground state of hydrogen. The nucleus consists of just a single proton, and we therefore have $I = 1/2$. The hydrogen ground state is the 1s $^2S_{1/2}$ term, which has $J = 1/2$. The hyperfine quantum number F is then found from $F = I \oplus J = 1/2 \oplus 1/2 = 1$ or 0. These two hyperfine states correspond to the cases in which the spins of the electron and the nucleus are aligned parallel ($F = 1$) or antiparallel ($F = 0$). The two F states are split by the hyperfine interaction by 0.0475 cm^{-1} (5.9×10^{-6} eV). (See Fig. 6.7(a).) Transitions between these levels occur at 1420 MHz ($\lambda = 21$ cm), and are very important in radio astronomy. Radio frequency transitions such as these are also routinely exploited in **nuclear magnetic resonance** (NMR) spectroscopy.

Hyperfine structure of the sodium D lines

The sodium D lines originate from 3p $\to$ 3s transitions. As discussed in Section 6.5, there are two lines with energies split by the spin-orbit coupling, as indicated in Fig. 6.5(b).

Consider first the lower energy D_1 line, which is the $^2P_{1/2} \to ^2S_{1/2}$ transition. The nucleus of sodium has $I = 3/2$, and so we have $F = 3/2 \oplus 1/2 = 2$ or 1 for both the upper and lower levels of the transition, as shown in Fig. 6.7(b). Note that the hyperfine splittings are not drawn to scale in Fig. 6.7(b): the splitting of the $^2S_{1/2}$ level is 1772 MHz, which is much larger than that of the $^2P_{1/2}$, namely 190 MHz. This is a consequence of the fact that s-electrons have higher probability densities at the nucleus, and hence experience stronger hyperfine interactions. All four transitions are allowed by the selection rules, and so we observe four lines. Since the splitting of the upper and lower levels are so different, we obtain two doublets with relative frequencies of (0, 190) MHz and (1772, 1962) MHz. These splittings should be compared to the much larger ($\sim 5 \times 10^{11}$ Hz) splitting between the two J states caused by the spin-orbit interaction. Since the hyperfine splittings are much smaller, they are not routinely observed in optical spectroscopy, and specialized techniques using narrow band lasers are typically employed nowadays.

Now consider the higher energy D_2 line, which is the $^2P_{3/2} \to ^2S_{1/2}$ transition. In the upper level we have $J = 3/2$, and hence $F = I \oplus J = 3/2 \oplus 3/2 = 3$, 2, 1, or 0. There are therefore four hyperfine states for the $^2P_{3/2}$ level, as shown in Fig. 6.7(c). The hyperfine splittings of the $^2P_{3/2}$ level are again much smaller than that of the $^2S_{1/2}$ level, on account of the low probability density of p-electrons near the nucleus. Six transitions are allowed by the selection rules, with the $F = 3 \to 1$ and $F = 0 \to 2$

transitions being forbidden by the $|\Delta F| \leq 1$ selection rule. We thus have six hyperfine lines, which split into two triplets at relative frequencies of (0, 34, 59) MHz and (1756, 1772, 1806) MHz.

Reading

Demtröder, W., *Atoms, Molecules and Photons*, §5.4–8.
Haken and Wolf, *The physics of atoms and quanta*, chapters 12, 20.
Eisberg and Resnick, *Quantum Physics*, chapters 8, 10.
Foot, *Atomic physics*, §2.3, 4.5–6, chapter 6.
Beisser, *Concepts of Modern Physics*, §7.8.

Chapter 7

External fields: the Zeeman and Stark effects

In the previous sets of notes we have been considering the effects of the internal electric and magnetic fields within atoms. We now wish to consider the effects of external fields. We shall start by looking at magnetic fields and then move on to consider electric fields.

7.1 Magnetic fields

The first person to study the effects of magnetic fields on the optical spectra of atoms was Zeeman in 1896. He observed that the transition lines split when the field is applied. Further work showed that the interaction between the atoms and the field can be classified into two regimes:

- Weak fields: the **Zeeman effect**, either **normal** or **anomalous**;
- Strong fields: the **Paschen-Back effect**.

The "normal" Zeeman effect is so-called because it agrees with the classical theory developed by Lorentz. The "anomalous" Zeeman effect is caused by electron spin, and is therefore a completely quantum result. The criterion for deciding whether a particular field is "weak" or "strong" will be discussed in Section 7.1.3. In practice, we usually work in the weak-field (i.e. Zeeman) limit.

7.1.1 The normal Zeeman effect

The normal Zeeman effect is observed in atoms with no spin. The total spin of an N-electron atom is given by:

$$\boldsymbol{S} = \sum_{i=1}^{N} \boldsymbol{s}_i \,. \tag{7.1}$$

Filled shells have no net spin, and so we only need to consider the valence electrons here. Since all the individual electrons have spin 1/2, it will not be possible to obtain $S = 0$ from atoms with an odd number of valence electrons. However, if there is an even number of valence electrons, we can obtain $S = 0$ states. For example, if we have two valence electrons, then the total spin quantum number $S = 1/2 \oplus 1/2$ can be either 0 or 1. In fact, the ground states of divalent atoms from group II of the periodic table (electronic configuration $n\mathrm{s}^2$) always have $S = 0$ because the two electrons align with their spins antiparallel.

The magnetic moment of an atom with no spin will originate entirely from its orbital motion:

$$\boldsymbol{\mu} = -\frac{\mu_\mathrm{B}}{\hbar}\boldsymbol{L} \,, \tag{7.2}$$

where $\mu_\mathrm{B}/\hbar = e/2m_\mathrm{e}$ is the **gyromagnetic ratio**. (See eqn 6.4.) The interaction energy between a magnetic dipole $\boldsymbol{\mu}$ and a uniform magnetic field $\boldsymbol{B}$ is given by:

$$\Delta E = -\boldsymbol{\mu} \cdot \boldsymbol{B} \,. \tag{7.3}$$

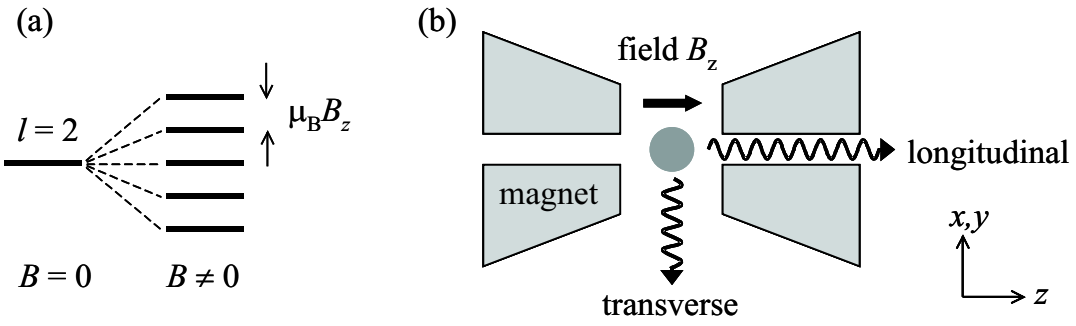

Figure 7.1: The normal Zeeman effect. (a) Splitting of the degenerate m_l states of an atomic level with $l = 2$ by a magnetic field. (b) Definition of longitudinal (Faraday) and transverse (Voigt) observations. The direction of the field defines the z axis.

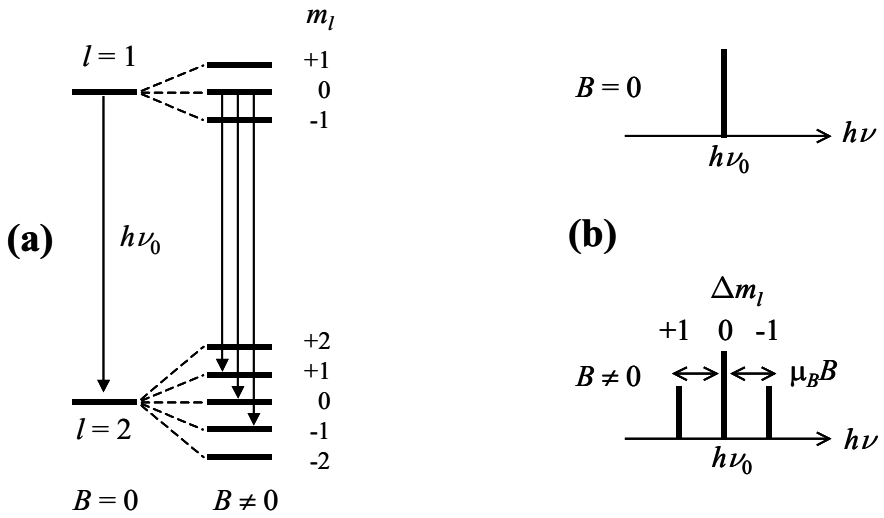

Figure 7.2: The normal Zeeman effect for a p $\rightarrow$ d transition. (a) The field splits the degenerate m_l levels equally. Optical transitions can occur if $\Delta m_l = 0, \pm 1$. (Only the transitions originating from the $m_l = 0$ level of the $l = 1$ state are identified here for the sake of clarity.) (b) The spectral line splits into a triplet when observed transversely to the field. The $\Delta m_l = 0$ transition is unshifted, but the $\Delta m_l = \pm 1$ transitions occur at $(h\nu_0 \mp \mu_B B_z)$.

We set up the axes of our spherically-symmetric atom so that the z axis coincides with the direction of the field. In this case we have:

$$\boldsymbol{B} = \begin{pmatrix} 0 \\ 0 \\ B_z \end{pmatrix} ,$$

and the interaction energy of the atom is therefore:

$$\Delta E = -\mu_z B_z = \mu_B B_z m_l \,, \tag{7.4}$$

where m_l is the orbital magnetic quantum number. Equation 7.4 shows us that the application of an external $\boldsymbol{B}$-field splits the degenerate m_l states evenly. This is why m_l is called the **magnetic quantum number**. The splitting of the m_l states of an $l = 2$ electron is illustrated in Fig. 7.1(a).

The effect of the magnetic field on the spectral lines can be worked out from the splitting of the levels. Consider the transitions between two Zeeman-split atomic levels as shown in Fig. 7.2. The selection rules listed in Table 3.1 of Chapter 3 indicate that we can have transitions with $\Delta m_l = 0$ or ± 1. The gives rise to three transitions whose frequencies are given by:

$$\begin{aligned} h\nu &= h\nu_0 + \mu_B B_z \qquad \Delta m_l = -1 \,, \\ h\nu &= h\nu_0 \qquad\qquad\quad \Delta m_l = 0 \,, \\ h\nu &= h\nu_0 - \mu_B B_z \qquad \Delta m_l = +1 \,. \end{aligned} \tag{7.5}$$

Δm_l	Energy	Polarization	
		Longitudinal observation	Transverse observation
+1	$h\nu_0 - \mu_B B$	σ^+	$\boldsymbol{\mathcal{E}} \perp \boldsymbol{B}$
0	$h\nu_0$	not observed	$\boldsymbol{\mathcal{E}} \parallel \boldsymbol{B}$
–1	$h\nu_0 + \mu_B B$	σ^-	$\boldsymbol{\mathcal{E}} \perp \boldsymbol{B}$

Table 7.1: The normal Zeeman effect. The last two columns refer to the polarizations observed in longitudinal (Faraday) and transverse (Voigt) observation conditions. The direction of the circular ($\sigma^{\pm}$) polarization in longitudinal observation is defined relative to $\boldsymbol{B}$. In transverse observation, all lines are linearly polarized.

This is the same result as that derived by classical theory.

The polarization of the Zeeman lines is determined by the selection rules, and the conditions of observation. If we are looking along the field (**longitudinal** observation), the photons must be propagating in the z direction. (See Fig. 7.1(b).) Light waves are transverse, and so only the x and y polarizations are possible. The z-polarized $\Delta m_l = 0$ line is therefore absent, and we just observe the σ^+ and σ^- circularly polarized $\Delta m_l = \pm 1$ transitions. When observing at right angles to the field (**transverse** observation), all three lines are present. The $\Delta m_l = 0$ transition is linearly polarized parallel to the field, while the $\Delta m_l = \pm 1$ transitions are linearly polarized at right angles to the field. These results are summarized in Table 7.1.[1]

7.1.2 The anomalous Zeeman effect

The anomalous Zeeman effect is observed in atoms with non-zero spin. This will include all atoms with an odd number of electrons. In the LS-coupling regime, the spin-orbit interaction couples the spin and orbital angular momenta together to give the resultant total angular momentum $\boldsymbol{J}$ according to:

$$\boldsymbol{J} = \boldsymbol{L} + \boldsymbol{S}\,. \tag{7.6}$$

The orbiting electrons in the atom are equivalent to a classical magnetic gyroscope. The torque applied by the field causes the atomic magnetic dipole to precess around $\boldsymbol{B}$, an effect called **Larmor precession**. The external magnetic field therefore causes $\boldsymbol{J}$ to precess slowly about $\boldsymbol{B}$. Meanwhile, $\boldsymbol{L}$ and $\boldsymbol{S}$ precess more rapidly about $\boldsymbol{J}$ due to the spin-orbit interaction. This situation is illustrated in Fig. 7.3(a). The speed of the precession about $\boldsymbol{B}$ is proportional to the field strength. If we turn up the field, the Larmor precession frequency will eventually be faster than the spin-orbit precession of $\boldsymbol{L}$ and $\boldsymbol{S}$ around $\boldsymbol{J}$. This is the point where the behaviour ceases to be Zeeman-like, and we are in the strong field regime of the Paschen-Back effect.

The interaction energy of the atom is equal to the sum of the interactions of the spin and orbital magnetic moments with the field:

$$\Delta E = -\mu_z B_z = -(\mu_z^{\rm spin} + \mu_z^{\rm orbital}) B_z = \langle g_{\rm s} \boldsymbol{S}_z + \boldsymbol{L}_z \rangle \frac{\mu_{\rm B}}{\hbar} B_z\,, \tag{7.7}$$

where $g_{\rm s} = 2$, and the symbol $\langle \cdots \rangle$ implies, as usual, that we take expectation values. The normal Zeeman effect is obtained by setting $\boldsymbol{S}_z = 0$ and $\boldsymbol{L}_z = m_l \hbar$ in this formula. In the case of the precessing atomic magnet shown in Fig. 7.3(a), neither $\boldsymbol{S}_z$ nor $\boldsymbol{L}_z$ are constant. Only $\boldsymbol{J}_z = M_J \hbar$ is well-defined. We must therefore first project $\boldsymbol{L}$ and $\boldsymbol{S}$ onto $\boldsymbol{J}$, and then re-project this component onto the z axis. The effective dipole moment of the atom is therefore given by:

$$\boldsymbol{\mu} = -\left\langle |\boldsymbol{L}| \cos\theta_1 \frac{\boldsymbol{J}}{|\boldsymbol{J}|} + 2|\boldsymbol{S}| \cos\theta_2 \frac{\boldsymbol{J}}{|\boldsymbol{J}|} \right\rangle \frac{\mu_{\rm B}}{\hbar}\,, \tag{7.8}$$

[1] In solid-state physics, the longitudinal and transverse observation conditions are frequently called the **Faraday** and **Voigt** geometries, respectively.

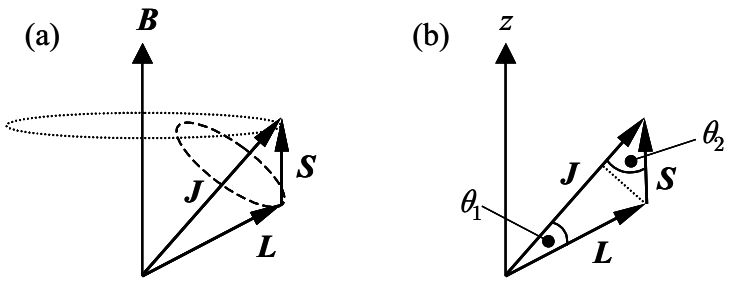

Figure 7.3: (a) Slow precession of $\boldsymbol{J}$ around $\boldsymbol{B}$ in the anomalous Zeeman effect. The spin-orbit interaction causes $\boldsymbol{L}$ and $\boldsymbol{S}$ to precess much more rapidly around $\boldsymbol{J}$. (b) Definition of the projection angles θ_1 and θ_2 used in the calculation of the Landé g factor.

where the factor of 2 in the second term comes from the fact that $g_s = 2$. The angles θ_1 and θ_2 that appear here are defined in Fig. 7.3(b), and can be calculated from the scalar products of the respective vectors:

$$\begin{aligned} \boldsymbol{L}\cdot\boldsymbol{J} &= |\boldsymbol{L}|\,|\boldsymbol{J}|\cos\theta_1\,, \\ \boldsymbol{S}\cdot\boldsymbol{J} &= |\boldsymbol{S}|\,|\boldsymbol{J}|\cos\theta_2\,, \end{aligned} \tag{7.9}$$

which implies that:

$$\boldsymbol{\mu} = -\left\langle \frac{\boldsymbol{L}\cdot\boldsymbol{J}}{|\boldsymbol{J}|^2} + 2\frac{\boldsymbol{S}\cdot\boldsymbol{J}}{|\boldsymbol{J}|^2}\right\rangle \frac{\mu_{\rm B}}{\hbar}\,\boldsymbol{J}\,. \tag{7.10}$$

Now equation 7.6 implies that $\boldsymbol{S} = \boldsymbol{J} - \boldsymbol{L}$, and hence that:

$$\boldsymbol{S}\cdot\boldsymbol{S} = (\boldsymbol{J}-\boldsymbol{L})\cdot(\boldsymbol{J}-\boldsymbol{L}) = \boldsymbol{J}\cdot\boldsymbol{J} + \boldsymbol{L}\cdot\boldsymbol{L} - 2\boldsymbol{L}\cdot\boldsymbol{J}\,.$$

We therefore find that:

$$\boldsymbol{L}\cdot\boldsymbol{J} = (\boldsymbol{J}\cdot\boldsymbol{J} + \boldsymbol{L}\cdot\boldsymbol{L} - \boldsymbol{S}\cdot\boldsymbol{S})/2\,,$$

so that:

$$\begin{aligned} \left\langle \frac{\boldsymbol{L}\cdot\boldsymbol{J}}{|\boldsymbol{J}|^2}\right\rangle &= \frac{[J(J+1)+L(L+1)-S(S+1)]\hbar^2/2}{J(J+1)\hbar^2}\,, \\ &= \frac{[J(J+1)+L(L+1)-S(S+1)]}{2J(J+1)}\,. \end{aligned} \tag{7.11}$$

Similarly:

$$\boldsymbol{S}\cdot\boldsymbol{J} = (\boldsymbol{J}\cdot\boldsymbol{J} + \boldsymbol{S}\cdot\boldsymbol{S} - \boldsymbol{L}\cdot\boldsymbol{L})/2\,,$$

and so:

$$\begin{aligned} \left\langle \frac{\boldsymbol{S}\cdot\boldsymbol{J}}{|\boldsymbol{J}|^2}\right\rangle &= \frac{[J(J+1)+S(S+1)-L(L+1)]\hbar^2/2}{J(J+1)\hbar^2}\,, \\ &= \frac{[J(J+1)+S(S+1)-L(L+1)]}{2J(J+1)}\,. \end{aligned} \tag{7.12}$$

We therefore conclude that:

$$\boldsymbol{\mu} = -\left(\frac{[J(J+1)+L(L+1)-S(S+1)]}{2J(J+1)} + 2\frac{[J(J+1)+S(S+1)-L(L+1)]}{2J(J+1)}\right)\frac{\mu_{\rm B}}{\hbar}\,\boldsymbol{J}\,. \tag{7.13}$$

This can be written in the form:

$$\boldsymbol{\mu} = -g_J\frac{\mu_{\rm B}}{\hbar}\boldsymbol{J}\,, \tag{7.14}$$

where g_J is the **Landé g-factor** given by:

$$g_J = 1 + \frac{J(J+1)+S(S+1)-L(L+1)}{2J(J+1)}\,. \tag{7.15}$$

This implies that

$$\mu_z = -g_J\mu_{\rm B}M_J\,, \tag{7.16}$$

Level	J	L	S	g_J
$^2P_{3/2}$	3/2	1	1/2	4/3
$^2P_{1/2}$	1/2	1	1/2	2/3
$^2S_{1/2}$	1/2	0	1/2	2

Table 7.2: Landé g-factors evaluated from eqn 7.15 for the levels involved in the sodium D lines.

and hence that the interaction energy with the field is:

$$\Delta E = -\mu_z B_z = g_J \mu_\mathrm{B} B_z M_J \,. \tag{7.17}$$

This is the final result for the energy shift of an atomic state in the anomalous Zeeman effect. Note that we just obtain $g_J = 1$ if $S = 0$, as we would expect for an atom with only orbital angular momentum. Similarly, if $L = 0$ so that the atom only has spin angular momentum, we find $g_J = 2$. Classical theories always predict $g_J = 1$. The departure of g_J from unity is caused by the spin part of the magnetic moment, and is a purely quantum effect.

The spectra can be understood by applying the following selection rules on J and M_J:

$$\Delta J = 0, \pm 1 \,;$$

$$\Delta M_J = 0, \pm 1 \,.$$

These rules have to be applied in addition to the $\Delta l = \pm 1$ and $\Delta S = 0$ rules. (See discussion in § 5.8.)[2] $\Delta J = 0$ transitions are forbidden when $J = 0$ for both states, and $\Delta M_J = 0$ transitions are forbidden in a $\Delta J = 0$ transition. The transition energy shift is then given by:

$$\begin{aligned} h\Delta\nu &= (h\nu - h\nu_0) \,, \\ &= \left(g_J^{\text{upper}} M_J^{\text{upper}} - g_J^{\text{lower}} M_J^{\text{lower}}\right) \mu_\mathrm{B} B_z \,, \end{aligned} \tag{7.18}$$

where $h\nu_0$ is the transition energy at $B_z = 0$ and the superscripts refer to the upper and lower states respectively.

The polarizations of the transitions follow the same patterns as for the normal Zeeman effect:

- With *longitudinal* observation the $\Delta M_J = 0$ transitions are absent and the $\Delta M_J = \pm 1$ transitions are $\sigma^\pm$ circularly polarized.
- With *transverse* observation the $\Delta M_J = 0$ transitions are linearly polarized along the z axis (i.e. parallel to $\boldsymbol{B}$) and the $\Delta M_J = \pm 1$ transitions are linearly polarized in the x-y plane (i.e. perpendicular to $\boldsymbol{B}$).

Example: The sodium D lines

The sodium D lines correspond to the 3p → 3s transition. At $\boldsymbol{B} = 0$, the spin-orbit interaction splits the upper 3p ^{2}P term into the $^2P_{3/2}$ and $^2P_{1/2}$ levels separated by $17\,\mathrm{cm}^{-1}$. The lower $^2S_{1/2}$ level has no spin-orbit interaction. The Landé g-factors of the levels worked out from eqn 7.15 are given in Table 7.2.

The splitting of the lines in the field is shown schematically in Fig. 7.4. The $^2P_{3/2}$ level splits into four M_J states, while the two $J = 1/2$ levels each split into two states. The splittings are different for each level because of the different Landé factors. On applying the $\Delta M_J = 0, \pm 1$ selection rule, we find four allowed transitions for the D_1 line and six for the D_2. These transitions are listed in Table 7.3.

The results tabulated in Table 7.3 can be compared to those predicted by the normal Zeeman effect. In the normal Zeeman effect we observe three lines with an energy spacing equal to $\mu_\mathrm{B} B$. In the anomalous effect, there are more than three lines, and the spacing is different to the classical value: in fact, the lines are not evenly spaced. Furthermore, none of the lines occur at the same frequency as the unperturbed line at $B = 0$.

[2] There are no selection rules on M_L and M_S here because L_z and S_z are not constants of the motion when L and S are coupled by the spin-orbit interaction.

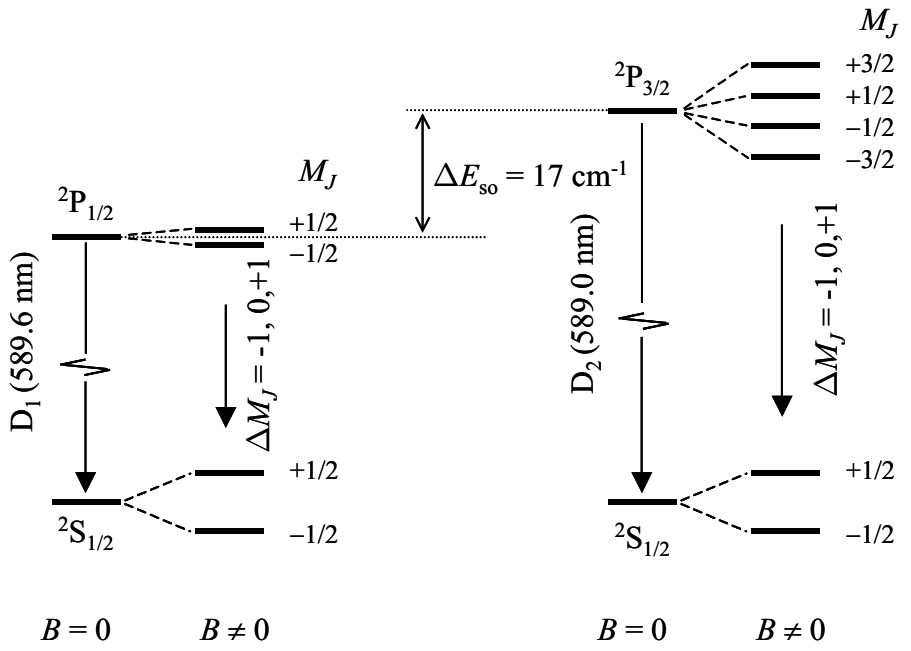

Figure 7.4: Splitting of the sodium D-lines by a weak magnetic field. Note that the Zeeman splittings are smaller than the spin-orbit splitting, as must be the case in the "weak" field limit.

7.1.3 The Paschen-Back effect

The Paschen-Back effect is observed at very strong magnetic fields. The criterion for observing the Paschen-Back effect is that the interaction with the external magnetic field should be much stronger than the spin-orbit interaction:

$$\mu_B B_z \gg \Delta E_{so} \,. \tag{7.19}$$

If we satisfy this criterion, then the precession speed around the external field will be much faster than the spin-orbit precession. This means that the interaction with the external field is now the largest perturbation, and so it should be treated first, before the perturbation of the spin-orbit interaction.

Another way to think of the strong-field limit is that it occurs when the external field is much stronger than the internal field of the atom arising from the orbital motion. We saw in Section 6.3 that the internal fields in most atoms are large. For example, the Bohr model predicts an internal field of 12 T for the $n = 1$ shell of hydrogen. (See eqn 6.16.) This is a very strong field, that can only be obtained in the laboratory by using powerful superconducting magnets. This internal field strength is typical of many atoms, and so it will frequently be the case the field required to observe the Paschen-Back effect is so large that we never go beyond the Zeeman regime in the laboratory.[3] For example, in sodium, the field strength equivalent to the spin-orbit interaction for the D-lines is given by:

$$B_z = \frac{\Delta E_{so}}{\mu_B} = \frac{17\,\mathrm{cm}^{-1}}{9.27 \times 10^{-24}\,\mathrm{JT}^{-1}} = 36\,\mathrm{T}\,,$$

which is not achievable in normal laboratory conditions. On the other hand, since the spin-orbit interaction decreases with the atomic number Z, the splitting for the equivalent transition in lithium (i.e. the 2p $\rightarrow$ 2s transition) is only $0.3\,\mathrm{cm}^{-1}$. This means that we can reach the strong field regime for fields $\gg 0.6$ T. This is readily achievable, and allows the Paschen-Back effect to be observed.

In the Paschen-Back effect, the spin-orbit interaction is assumed to be negligibly small, and $\boldsymbol{L}$ and $\boldsymbol{S}$ are therefore no longer coupled together. Each precesses separately around $\boldsymbol{B}$, as sketched in Fig. 7.5. The precession rates for $\boldsymbol{L}$ and $\boldsymbol{S}$ are different because of the different g-values. Hence the magnitude of the resultant $\boldsymbol{J}$ varies with time: the quantum number J is no longer a constant of the motion.

The interaction energy is now calculated by adding the separate contributions of the spin and orbital energies:

$$\Delta E = -\mu_z B_z = -(\mu_z^{\mathrm{orbital}} + \mu_z^{\mathrm{spin}}) B_z = (M_L + g_s M_S)\mu_B B_z \,. \tag{7.20}$$

[3]There are extremely large magnetic fields present in the Sun due to the circulating plasma currents. This means that the Paschen-Back effect can be observed for elements like sodium in solar spectra.

M_J^{upper}	M_J^{lower}	ΔM_J	Transition energy shift	
			D_1 line	D_2 line
$+\frac{3}{2}$	$+\frac{1}{2}$	-1		$+1$
$+\frac{1}{2}$	$+\frac{1}{2}$	0	$-\frac{2}{3}$	$-\frac{1}{3}$
$+\frac{1}{2}$	$-\frac{1}{2}$	-1	$+\frac{4}{3}$	$+\frac{5}{3}$
$-\frac{1}{2}$	$+\frac{1}{2}$	$+1$	$-\frac{4}{3}$	$-\frac{5}{3}$
$-\frac{1}{2}$	$-\frac{1}{2}$	0	$+\frac{2}{3}$	$+\frac{1}{3}$
$-\frac{3}{2}$	$-\frac{1}{2}$	$+1$		-1

Table 7.3: Anomalous Zeeman effect for the sodium D lines. The transition energy shifts are worked out from eqn 7.18 and are quoted in units of $\mu_{\rm B}B_z$.

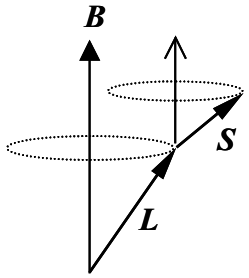

Figure 7.5: Precession of $\boldsymbol{L}$ and $\boldsymbol{S}$ around $\boldsymbol{B}$ in the Paschen-Back effect.

The shift of the spectral lines is given by:

$$\Delta(h\nu) = (\Delta M_L + g_{\rm s}\Delta M_S)\mu_{\rm B}B_z\,. \tag{7.21}$$

We have noted before that optical transitions do not affect the spin, and so we must have $\Delta M_S = 0$. The frequency shift is thus given by:

$$\Delta(h\nu) = \mu_{\rm B}B_z\,\Delta M_L\,, \tag{7.22}$$

where $\Delta M_L = 0$ or ± 1. In other words, we revert to the normal Zeeman effect.

Putting it all together

The change of the spectra as we increase B from zero is illustrated for the p $\rightarrow$ s transitions of an alkali atom in Fig. 7.6. At $B = 0$ the lines are split by the spin-orbit interaction. At weak fields we observe the anomalous Zeeman effect, while at strong fields we change to the Paschen-back effect.

7.1.4 Magnetic field effects for hyperfine levels

Everything we have said so far has ignored the *hyperfine* structure of the atom. The whole process can be repeated to calculate the Zeeman and Paschen-Back energy shifts for the hyperfine levels. In this case, the energy splittings at $B = 0$ are much smaller, due to the much smaller gyromagnetic ratio of the nucleus compared to the electron. (See Section 6.7.2.) This implies that the change from the weak-field to the strong-field limit occurs at much smaller field strengths than for the states split by fine-structure interactions. We shall not consider the hyperfine states further in this course.

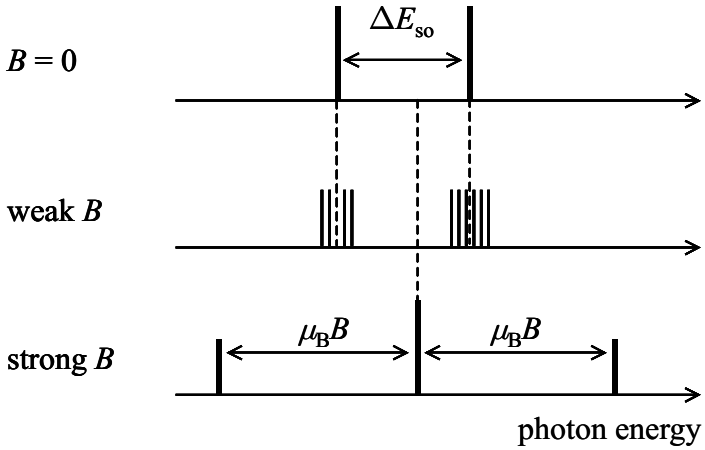

Figure 7.6: Schematic progression of the optical spectra for the p → s transitions of an alkali atom with increasing field.

7.2 The concept of 'good' quantum numbers

It is customary to refer to quantum numbers that relate to constants of the motion as 'good' quantum numbers. In this discussion of the effects of magnetic fields, we have used six different quantum numbers to describe the angular momentum state of the atom: J, M_J, L, M_L, S, M_S. However, we cannot know all of these at the same time. In fact, we can only know four: (L, S, J, M_J) in the weak-field limit, or (L, S, M_L, M_S) in the strong-field limit. In the weak-field limit, L_z and S_z are not constant which implies that J and M_J are 'good' quantum numbers but M_L and M_L are not. Similarly, in the strong-field limit, the coupling between $\boldsymbol{L}$ and $\boldsymbol{S}$ is broken and so $\boldsymbol{J}$ and J_z are not constants of the motion: M_L and M_S are good quantum numbers, but J and M_J are not.

A similar type of argument applies to the two angular momentum coupling schemes discussed in Section 5.6, namely LS-coupling and jj-coupling. As an example, consider the total angular momentum state of a two electron atom. In the LS-coupling scheme, we specify (L, S, J, M_J), whereas in the jj-coupling scheme we have (j_1, j_2, J, M_J). In both cases, we have four 'good' quantum numbers, which tell us the precisely measurable quantities. The other quantum numbers are unknown because the physical quantities they represent are not constant. In LS-coupling we cannot know the j values of the individual electrons because the residual electrostatic potential overpowers the spin-orbit effect, whereas in the jj-coupling scheme we cannot know L and S. Note, however, that J and M_J are good quantum numbers in both coupling limits. This means that we can always describe the Zeeman energy of the atom by eqn 7.17, although in the case of jj-coupling, the formula for the g_J factor given in eqn 7.15 will not be valid because L and S are not good quantum numbers.

7.3 Electric fields

The shifting and splitting of spectral lines in an *electric* field is called the **Stark effect**. This effect was first observed in 1913. In most atoms we observe the **quadratic Stark effect** and we therefore consider this effect first. We then move on to consider the **linear Stark effect**, which is observed for the excited states of hydrogen, and in other atoms at very strong fields. The Stark shift of an atom is harder to observe than the Zeeman shift, which explains why magnetic effects are more widely studied in atomic physics. However, large Stark effects are readily observable in solid state physics, and we therefore conclude by briefly considering the **quantum-confined Stark effect**.

7.3.1 The quadratic Stark effect

Most atoms show a small *red shift* (i.e. a shift to lower energy) which is proportional to the *square* of the electric field. This phenomenon is therefore called the *quadratic* Stark effect. The energy of an atom in an electric field $\boldsymbol{\mathcal{E}}$ is given by

$$E = -\boldsymbol{p} \cdot \boldsymbol{\mathcal{E}}\,, \tag{7.23}$$

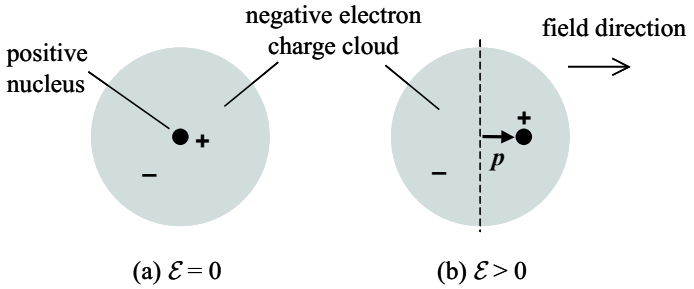

Figure 7.7: Effect of an electric field $\mathcal{E}$ on the electron cloud of an atom. (a) When $\mathcal{E} = 0$, the negatively-charged electron cloud is arranged symmetrically about the nucleus, and there is no electric dipole. (b) When the electric field is applied, the electron cloud is displaced, and a net dipole parallel to the field is induced.

where $\boldsymbol{p}$ is the electric dipole of the atom. We can understand the quadratic Stark effect intuitively with reference to Fig. 7.7. The negatively-charged electron clouds of an atom are spherically symmetric about the positively-charged nucleus in the absence of applied fields. A charged sphere acts like a point charge at its centre, and it is thus apparent that atoms do not normally possess a dipole moment, as shown in Fig. 7.7(a). When a field is applied, the electron cloud and the nucleus experience opposite forces, which results in a net displacement of the electron cloud with respect to the nucleus, as shown in Fig. 7.7(b). This creates a dipole $\boldsymbol{p}$ which is parallel to $\mathcal{E}$ and whose magnitude is proportional to $|\boldsymbol{\mathcal{E}}|$. This can be expressed mathematically by writing:

$$\boldsymbol{p} = \alpha \boldsymbol{\mathcal{E}} \,, \tag{7.24}$$

where α is the **polarizability** of the atom. The energy shift of the atom is found by calculating the energy change on increasing the field strength from zero:

$$\Delta E = -\int_0^{\mathcal{E}} \boldsymbol{p} \cdot \mathrm{d}\boldsymbol{\mathcal{E}}' = -\int_0^{\mathcal{E}} \alpha \mathcal{E}' \mathrm{d}\mathcal{E}' = -\frac{1}{2}\alpha \mathcal{E}^2 \,, \tag{7.25}$$

which predicts a quadratic red shift, as required. The magnitude of the red shift is generally rather small. This is because the electron clouds are tightly bound to the nucleus, and it therefore requires very strong electric fields to induce a significant dipole.

We can understand the quadratic Stark effect in more detail by applying perturbation theory.[4] The perturbation caused by the field is of the form:

$$\begin{aligned} H' &= -\sum_i (-e\boldsymbol{r}_i) \cdot \boldsymbol{\mathcal{E}} \,, \\ &= e\mathcal{E} \sum_i z_i \,, \end{aligned} \tag{7.26}$$

where the field is assumed to point in the $+z$ direction. In principle, the sum is over all the electrons, but in practice, we need only consider the valence electrons, because the electrons in closed shells are very strongly bound to the nucleus and are therefore very hard to perturb. In writing eqn 7.26, we take, as always, $\boldsymbol{r}_i$ to be the relative displacement of the electron with respect to the nucleus.

For simplicity, we shall just consider the case of alkali atoms which possess only one valence electron. In this case, the perturbation to the valence electron caused by the field reduces to:

$$H' = e\mathcal{E}z \,. \tag{7.27}$$

The *first-order* energy shift is given by:

$$\Delta E = \langle \psi | H' | \psi \rangle = e\mathcal{E} \langle \psi | z | \psi \rangle \,, \tag{7.28}$$

where

$$\langle \psi | z | \psi \rangle = \iiint_{\text{all space}} \psi^* z \, \psi \, \mathrm{d}^3\boldsymbol{r} \,. \tag{7.29}$$

[4]Many of you will not have done perturbation theory yet, as it is normally first encountered in detail in course PHY309, which is taken in the second semester. You will therefore have to take the results presented here on trust.

Now unperturbed atomic states have definite parities. (See discussion in Section 3.4.) The product $\psi^*\psi = |\psi^2|$ is therefore an even function, while z is an odd function. It is therefore apparent that

$$\langle\psi|z|\psi\rangle = \iiint_{\text{all space}} (\text{even function}) \times (\text{odd function})\, \mathrm{d}^3\boldsymbol{r} = 0\,.$$

The first-order energy shift is therefore zero, which explain why the energy shift is quadratic in the field, rather than linear.

The quadratic energy shift can be calculated by *second-order* perturbation theory. In general, the energy shift of the ith state predicted by second-order perturbation theory is given by:

$$\Delta E_i = \sum_{j\neq i} \frac{|\langle\psi_i|H'|\psi_j\rangle|^2}{E_i - E_j}\,, \tag{7.30}$$

where the summation runs over all the other states of the system, and E_i and E_j are the unperturbed energies of the states. The condition of validity is that the magnitude of the perturbation, namely $|\langle\psi_i|H'|\psi_j\rangle|$, should be small compared to the unperturbed energy splittings. For the Stark shift of the valence electron of an alkali atom, this becomes:

$$\Delta E_i = e^2\mathcal{E}^2 \sum_{j\neq i} \frac{|\langle\psi_i|z|\psi_j\rangle|^2}{E_i - E_j}\,. \tag{7.31}$$

We see immediately that the shift is expected to quadratic in the field, which is indeed the case for most atoms.

As a specific example, we consider sodium, which has a single valence electron in the 3s shell. We first consider the ground state $3\mathrm{s}\,{}^2\mathrm{S}_{1/2}$ term. The summation in eqn 7.31 runs over all the excited states of sodium, namely the 3p, 3d, 4s, 4p, ... states. Now in order that the matrix element $\langle\psi_i|z|\psi_j\rangle$ should be non-zero, it is apparent that the states i and j must *opposite* parities. In this case, we would have:

$$\langle\psi_i|z|\psi_j\rangle = \iiint_{\text{all space}} (\text{even/odd parity}) \times (\text{odd parity}) \times (\text{odd/even parity})\, \mathrm{d}^3\boldsymbol{r} \neq 0\,,$$

since the integrand is an even function. On the other hand, if the states have the same parities, we have:

$$\langle\psi_i|z|\psi_j\rangle = \iiint_{\text{all space}} (\text{even/odd parity}) \times (\text{odd parity}) \times (\text{even/odd parity})\, \mathrm{d}^3\boldsymbol{r} = 0\,,$$

since the integrand is an odd function. Since the parity varies as $(-1)^l$, the s and d states do not contribute to the Stark shift of the 3s state, and the summation in eqn 7.31 is only over the p and f excited states. Owing to the energy difference factor in the denominator, the largest perturbation to the 3s state will arise from the first excited state, namely the 3p state. Since this lies above the 3s state, the energy difference in the denominator is negative, and the energy shift is therefore negative. Indeed, it is apparent that the quadratic Stark shift of the ground state of an atom will always be negative, since the denominator will be negative for all the available states of the system. This implies that the Stark effect will always correspond to a *red shift* for the ground state level.

There is no easy way to calculate the size of the energy shift, but we can give a rough order of magnitude estimate. If we neglect the contributions of the even parity excited states above the 3p state, the energy shift will be given by:

$$\Delta E_{3\mathrm{s}} \approx -e^2\mathcal{E}^2 \frac{|\langle\psi_{3\mathrm{s}}|z|\psi_{3\mathrm{p}}\rangle|^2}{E_{3\mathrm{p}} - E_{3\mathrm{s}}}\,.$$

The expectation value of z over the atom must be smaller than a, where a is the atomic radius of sodium, namely 0.18 nm. Hence with $E_{3\mathrm{p}} - E_{3\mathrm{s}} = 2.1\,\mathrm{eV}$, we then have:

$$\Delta E_{3\mathrm{s}} \lesssim -\frac{e^2a^2}{E_{3\mathrm{p}} - E_{3\mathrm{s}}}\mathcal{E}^2,$$

which implies from eqn 7.25 that $\alpha_{3\mathrm{s}} \lesssim 3.2\times10^{-20}\,\mathrm{eV\,m^2\,V^{-2}}$. This predicts a shift of $\lesssim -1\times10^{-5}\,\mathrm{eV}$ ($-0.08\,\mathrm{cm^{-1}}$) in a field of $2.5\times10^7\,\mathrm{V/m}$, which compares reasonably well with the experimental value of $-0.6\times10^{-5}\,\mathrm{eV}$ ($-0.05\,\mathrm{cm^{-1}}$).

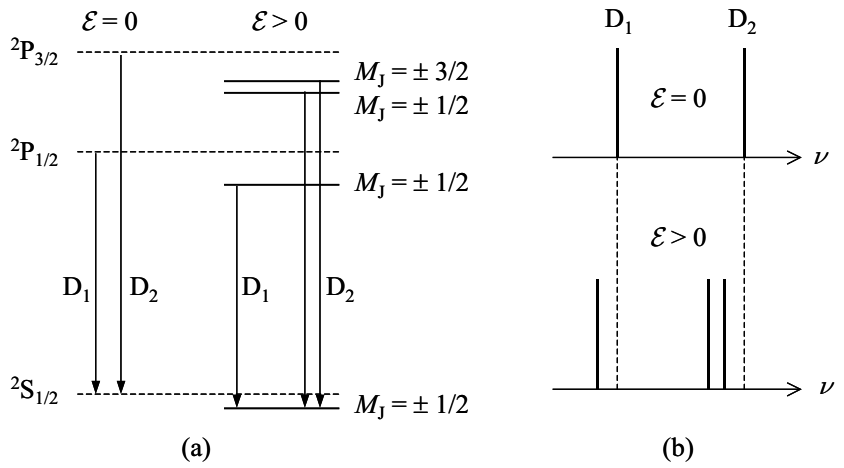

Figure 7.8: (a) Shift of the $^2S_{1/2}$, $^2P_{1/2}$, and $^2P_{3/2}$ terms of an alkali atom in an electric field. Note that the red shifts of the upper levels are larger than that of the lower level. (b) Red shift of the D_1 ($^2P_{1/2} \rightarrow {}^2S_{1/2}$) and the D_2 ($^2P_{3/2} \rightarrow {}^2S_{1/2}$) lines in the field.

The order of magnitude calculation given above can also provide a useful estimation of the field strength at which the second-order perturbation approximation breaks down. As mentioned above, this will occur when the magnitude of the perturbation become comparable to the unperturbed energy splitting, that is when:

$$e\mathcal{E}|\langle\psi_{3s}|z|\psi_{3p}\rangle| \sim (E_{3p} - E_{3s})\,.$$

On setting $|\langle\psi_{3s}|z|\psi_{3p}\rangle| = a$ as before, we find $\mathcal{E} \sim 10^{10}\,\mathrm{V/m}$, which is an extremely large field. The second-order perturbation approach will therefore be a good approximation in most practical situations.

Now consider the Stark shift of the 3p state. The 3p state has odd parity, and so the non-zero contributions in eqn 7.31 will now arise from the even parity ns and nd states:

$$\Delta E_{3p} = e^2\mathcal{E}^2\left(\frac{|\langle\psi_{3p}|z|\psi_{3s}\rangle|^2}{E_{3p} - E_{3s}} + \frac{|\langle\psi_{3p}|z|\psi_{3d}\rangle|^2}{E_{3p} - E_{3d}} + \frac{|\langle\psi_{3p}|z|\psi_{4s}\rangle|^2}{E_{3p} - E_{4s}} + \cdots\right).$$

The first term gives a positive shift, while all subsequent terms are negative. Therefore, it is not immediately obvious that the Stark shift of excited states like the 3p state will be negative. However, since the energy difference of the excited states tends to get smaller as we go up the ladder of levels, it will generally be the case that the negative terms dominate, and we have a red shift as for the ground state. Moreover, the red shift is generally expected to be larger than that of the ground state for the same reason (i.e. the smaller denominator). In the case of the 3p state of sodium, the largest contribution comes from the 3d state which lies 1.51 eV above the 3p state, even though the 4s state is closer (relative energy +1.09 eV). This is because of the smaller value of the matrix element for the s states.

Explicit evaluation of the matrix elements indicates that the Stark shift at a given field strength depends on M_J^2. This means that electric fields do not completely break the degeneracy of the M_J sub-levels of a particular $|J\rangle$ term. This contrasts with the Zeeman effect, where the energy shift is proportional to M_J, and the degeneracy if fully lifted. The Stark shift of the sodium D lines is shown schematically in Fig. 7.8. All states are shifted to lower energy, with those of the same M_J values being shifted equally for a given level, as indicated in Fig. 7.8(a). The shifts of the upper 3p levels are larger than that of the lower 3s $^2S_{1/2}$ term, and both spectral lines therefore show a net shift to lower energy, as indicated in Fig. 7.8(b). Owing to the degeneracy of the sub-levels with the same $|M_J|$, the D_1 ($^2P_{1/2} \rightarrow {}^2S_{1/2}$) line does not split, while the D_2 ($^2P_{3/2} \rightarrow {}^2S_{1/2}$) line splits into a doublet.

An interesting consequence of the perturbation caused by the electric field is that the unperturbed atomic states get mixed with other states of the opposite parity. For example, the 3s state has even parity at $\mathcal{E} = 0$, but acquires a small admixture of the odd parity 3p state as the field is increased. This means that parity forbidden transitions (eg s→s, p→p, d→s, etc.) become weakly allowed as the field is increased. Since we are dealing with a second-order perturbation, the intensity of these forbidden transitions increases in proportion to $\mathcal{E}^2$.

7.3.2 The linear Stark effect

Stark's original experiment of 1913 was performed on the Balmer lines of hydrogen.[5] In contrast to what has been discussed in the previous subsection, the shift was quite large, and varied linearly with the field. The reason for this is that the l states of hydrogen are degenerate. This means that we have states of opposite parities with the same energy, so that the second-order energy shift given by eqn 7.31 diverges. We therefore have to take a new approach to calculate the Stark shift by employing *degenerate* perturbation theory.

Consider first the 1s ground state of hydrogen. This level is unique, and hence the second-order perturbation approach is valid. A small quadratic red-shift therefore occurs, as discussed in the previous sub-section.

Now consider the $n = 2$ shell, which has four levels, namely the $m = 0$ level from the 2s term, and the $m = -1$, 0, and $+1$ levels of the 2p term. In the absence of an applied field, these four levels are degenerate. If the atom is in the $n = 2$ shell, it is equally likely to be in any of the four degenerate levels. We must therefore write its wave function as:

$$\psi_{n=2} = \sum_{i=1}^{4} c_i \psi_i \,, \tag{7.32}$$

where the subscript i identifies the quantum numbers $\{n, l, m\}$, that is:

$$\psi_1 \equiv \psi_{2,0,0} \,; \qquad \psi_2 \equiv \psi_{2,1,-1} \,; \qquad \psi_3 \equiv \psi_{2,1,0} \,; \qquad \psi_4 \equiv \psi_{2,1,+1} \,.$$

The first-order energy shift from eqn 7.28 becomes:

$$\Delta E = e\mathcal{E} \sum_{i,j} c_i c_j \langle \psi_i | z | \psi_j \rangle \,. \tag{7.33}$$

Unlike the case of the ground state, we can see from parity arguments that some of the matrix elements are non-zero. For example, ψ_1 has even parity, but ψ_3 has odd parity. We therefore have:

$$\begin{aligned} \langle \psi_1 | z | \psi_3 \rangle &= \iiint_{\text{all space}} \psi_1^* \, z \, \psi_3 \, \mathrm{d}^3\boldsymbol{r} \,, \\ &= \iiint_{\text{all space}} (\text{even parity}) \times (\text{odd parity}) \times (\text{odd parity}) \, \mathrm{d}^3\boldsymbol{r} \,, \\ &\neq 0 \,. \end{aligned}$$

This implies that we can observe a *linear* shift of the levels with the field. It turns out that $\langle \psi_1 | z | \psi_3 \rangle$ is the only non-zero matrix element. This is because the perturbation $H' = e\mathcal{E}z$ commutes with $\hat{L}_z$, and so the only non-zero matrix elements are those between states with the same m value but opposite parity, that is, between the two $m = 0$ levels derived from the 2s and 2p states.

It can easily be evaluated from the hydrogenic wave functions of the $n = 2$ levels given in Tables 2.1 and 2.2 that:

$$\langle \psi_1 | z | \psi_3 \rangle = -3a_0 \,,$$

where a_0 is the Bohr radius of hydrogen. We then find by degenerate perturbation theory that the field splits the $n = 2$ shell into a triplet, with energies of $-3ea_0\mathcal{E}$, 0, and $+3ea_0\mathcal{E}$ with respect to the unperturbed level. Note that this shift is linear in the field and has a much larger magnitude than that calculated for the quadratic Stark effect. For example, at $\mathcal{E} = 2.5 \times 10^7$ V/m, we find shifts of $\pm 4 \times 10^{-3}$ eV ($32\,\mathrm{cm}^{-1}$), which are more than two orders of magnitude larger than the shifts of the levels in sodium at the same field strength. This, of course, explains why the linear Stark effect in hydrogen was the first electric-field induced phenomenon to be discovered.

It was mentioned in Section 7.3.1 that the second-order perturbation analysis is expected to break down at large field strengths when the field-induced perturbation becomes comparable to the splittings of the unperturbed levels. We made an estimate of this for the 3s level of sodium and concluded that extremely large fields were required for the strong-field limit to be reached. However, the fields required for the breakdown of the second-order approach for the excited states can be significantly smaller, because some atoms can have different parity excited states which are relatively close to each other. We would then expect the behaviour to change as the field is increased. At low fields we would observe the quadratic

[5] The Balmer series of hydrogen corresponds to those lines that terminate on the $n = 2$ level. These lines occur in the visible spectral region.

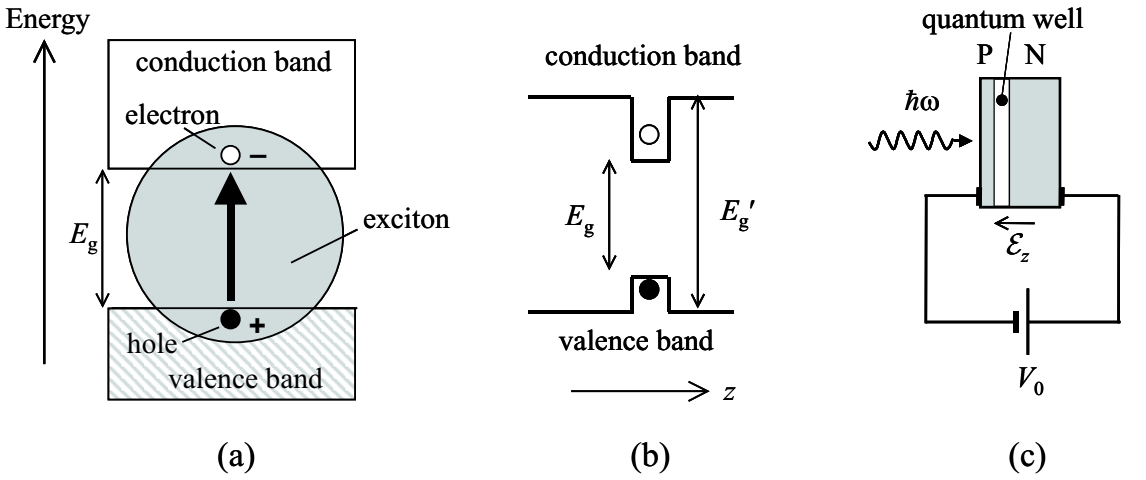

Figure 7.9: The quantum confined Stark effect. (a) Excitons are created by optical transitions from the valence to the conduction band of a semiconductor. (b) A quantum well is formed when a thin layer of a semiconductor with a band gap E_g is sandwiched between layers of another semiconductor with a larger band gap E_g'. (c) Electric fields are applied to an exciton in a quantum well by embedding the quantum well within a P-N junction and applying reverse bias.

Stark effect, but when the field is sufficiently large that the perturbation is comparable to the energy splitting, we would effectively have degenerate levels with different parities. This would then result in a *linear* shift determined by degenerate perturbation theory. This change from the quadratic Stark effect at low fields to the linear Stark effect at high fields was first studied for the (1s, 4l) excited state configuration of helium by Foster in 1927.

7.3.3 The quantum-confined Stark effect

An optical transition between the valence and conduction bands of a semiconductor leaves a positively-charged hole in the valence band, and a negatively-charged electron in the conduction band, as shown in Fig. 7.9(a). The electron and hole can bind together to form a hydrogen-like atom called an **exciton**. The binding energy of the exciton is rather small, due to the high relative dielectric constant ϵ_r of the semiconductor, and also because of the low reduced effective mass of the exciton. Typical values might be $\epsilon_r \sim 10$ and $m \sim 0.1 m_e$, which implies from eqn 1.10 that the 1s binding energy would be $\sim 0.01\,\text{eV}$.[6]

From the discussion given in Section 7.3.1, we would expect the 1s exciton state to show a quadratic Stark shift as an electric field is applied. However, in bulk semiconductors the excitons are very unstable to applied electric fields due to their low binding energy, which implies that the electrostatic force between the electron and hole is relatively small. The electrons and holes are pushed in opposite directions, and the exciton then easily gets ripped apart by the field. This effect is called **field ionization**. It can also be observed in atomic physics, but only at extremely high field strengths.

The situation in a *quantum-confined* structure such as a semiconductor **quantum well** or **quantum dot** is rather different. Consider the case of the quantum well shown in Fig. 7.9(b). The quantum well is formed by sandwiching a thin semiconductor with a band gap of E_g between layers of another semiconductor with a larger band gap E_g'. This then gives rise to spatial discontinuities in the conduction and valence band energies as shown in the figure. The excitons that are formed by optical transitions across the smaller band gap are then trapped in the finite potential well created by the band discontinuities.

A strong electric field can be applied to the quantum well by embedding it within a P-N junction, and then applying reverse bias, as shown in Fig. 7.9(c). P-N junctions conduct when forward bias is applied, but not under reverse bias. In the latter case, the applied voltage is dropped across the narrow junction region, thereby generating an electric field that is controlled by the reverse bias. The excitons that are created by optical transitions are now stable to the field, because the barriers of the quantum well prevent them from being ripped apart. The electrons are pushed to one side of the quantum well, and the holes to the other, which creates a dipole of magnitude $\sim ed$, where d is the width of the quantum well. With $d \sim 10\,\text{nm}$, much larger dipoles can be created than in atomic physics, resulting in correspondingly larger

[6]Note that the factor of ϵ_0^2 in the denominator of eqn 1.10 has to be replaced by $(\epsilon_r \epsilon_0)^2$ in a dielectric medium.

Stark shifts. This effect is called the **quantum-confined Stark effect**, and is widely used for making electro-optical modulators. The quantum-confined Stark effect will be studied in more detail in course PHY475.

Reading

Demtröder, W., *Atoms, Molecules and Photons*, sections 5.2, 5.6, 7.2 and 11.9.
H. Haken and H.C. Wolf, *The physics of atoms and quanta*, chapters 13 and 15.
Eisberg and Resnick, *Quantum Physics*, section 10.6.
Beisser, *Concepts of Modern Physics*, section 6.10.
Foot, *Atomic Physics*, sections 1.8 and 5.5

Chapter 8

Helium and exchange symmetry

In this chapter we will look at atoms with two valence electrons. This includes helium, and the group II elements: beryllium, magnesium, calcium, etc. As we will see, this leads to the idea of the exchange energy. We shall use helium as the main example, as it is a true two electron system and illustrates the physical points most clearly.

8.1 Exchange symmetry

Consider a multi-electron atom with N electrons, as illustrated in figure 8.1(a). The wave function of the atom will be a function of the co-ordinates of the individual electrons:

$$\Psi \equiv \Psi(\boldsymbol{r}_1, \boldsymbol{r}_2, \cdots, \boldsymbol{r}_K, \boldsymbol{r}_L, \cdots \boldsymbol{r}_N)$$

However, the electrons are **indistinguishable** particles. It is not physically possible to stick labels on the individual electrons and then keep tabs on them as the move around their orbits. This means that the many-electron wave function must have **exchange symmetry**:

$$|\Psi(\boldsymbol{r}_1, \boldsymbol{r}_2, \cdots, \boldsymbol{r}_K, \boldsymbol{r}_L, \cdots \boldsymbol{r}_N)|^2 = |\Psi(\boldsymbol{r}_1, \boldsymbol{r}_2, \cdots, \boldsymbol{r}_L, \boldsymbol{r}_K, \cdots \boldsymbol{r}_N)|^2 \,. \tag{8.1}$$

This says that nothing happens if we switch the labels of any pair of electrons. Equation 8.1 will be satisfied if

$$\Psi(\boldsymbol{r}_1, \boldsymbol{r}_2, \cdots, \boldsymbol{r}_K, \boldsymbol{r}_L, \cdots \boldsymbol{r}_N) = \pm\, \Psi(\boldsymbol{r}_1, \boldsymbol{r}_2, \cdots, \boldsymbol{r}_L, \boldsymbol{r}_K, \cdots \boldsymbol{r}_N) \,. \tag{8.2}$$

The + sign in equation 8.2 applies if the particles are **bosons**. These are said to be **symmetric** with respect to particle exchange. The − sign applies to **fermions**, which are **anti-symmetric** with respect to particle exchange.

Electrons have spin 1/2 and are therefore fermions. Hence the wave function of a multi-electron atom must be *anti-symmetric* with respect to particle exchange. This is a very fundamental property, and is the physical basis of the Pauli exclusion principle, as we shall see below.

The discussion of exchange symmetry gets quite complicated when there are lots of electrons, and so we shall just concentrate on helium here.

8.2 Helium wave functions

Figure 8.1(b) shows a schematic diagram of a helium atom. It consists of one nucleus with $Z = 2$ and two electrons. The position co-ordinates of the electrons are written $\boldsymbol{r}_1$ and $\boldsymbol{r}_2$ respectively.

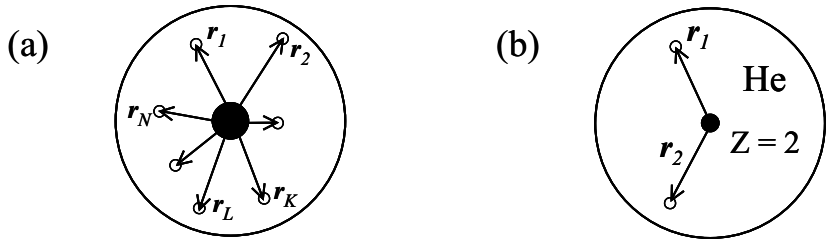

Figure 8.1: (a) A multi-electron atom with N electrons. (b) The helium atom.

ψ_{spatial}	ψ_{spin}
symmetric	anti-symmetric ($S = 0$)
anti-symmetric	symmetric ($S = 1$

Table 8.1: Allowed combinations of the exchange symmetries of the spatial and spin wave functions of fermionic particles.

The quantum state in the helium atom will be specified both by the spatial co-ordinates and by the spin of the two electrons. The two-electron wave function is therefore written as a product of a spatial wave function and a spin wave function:

$$\Psi = \psi_{\text{spatial}}(\boldsymbol{r}_1, \boldsymbol{r}_2)\, \psi_{\text{spin}}\,. \tag{8.3}$$

As we have seen above, the fact that electrons are indistinguishable fermions requires that the two-electron wave function Ψ must be anti-symmetric with respect to exchange of electrons 1 and 2. Table 8.1 lists the two possible combinations of wave function symmetries that can produce an antisymmetric total wave function.

Let us first consider the spatial wave function. The state of the atom will be specified by the configuration of the two electrons. In the ground state both electrons are in the 1s shell, and so we have a configuration of $1s^2$. In the excited states, one or both of the electrons will be in a higher shell. The configuration is thus given by the n, l values of the two electrons, and we write the configuration as $(n_1 l_1,\ n_2 l_2)$. This means that the spatial part of the helium wave function must contain terms of the type $u_A(\boldsymbol{r}_1)\, u_B(\boldsymbol{r}_2)$, where $u_{nl}(\boldsymbol{r})$ is the wave function for an electron with quantum numbers n and l, and the subscripts A and B stand for the quantum numbers n, l of the two electrons.

The discussion above does not take account of the fact that the electrons are indistinguishable: we cannot distinguish between the state with electron 1 in state A and electron 2 in state B, and *vice versa*. $u_B(\boldsymbol{r}_1)\, u_A(\boldsymbol{r}_2)$ is therefore an equally valid wave function for the particular electronic configuration. The wave function for the configuration A, B must therefore take the form:

$$\psi_{AB}(\boldsymbol{r}_1, \boldsymbol{r}_2) = \frac{1}{\sqrt{2}}\Big(u_A(\boldsymbol{r}_1)\, u_B(\boldsymbol{r}_2) \pm u_B(\boldsymbol{r}_1)\, u_A(\boldsymbol{r}_2)\Big)\,. \tag{8.4}$$

The $1/\sqrt{2}$ factor ensures that $\psi_{AB}(\boldsymbol{r}_1, \boldsymbol{r}_2)$ is correctly normalized. It is easy to verify that the wave function with the + sign is symmetric with respect to particle exchange, while the wave function with the − sign is antisymmetric. From Table 8.1, we see that these must be paired off with anti-symmetric and symmetric spin wave functions respectively.

Let us now consider the spin wave function. We have two spin 1/2 electrons, and so the total spin quantum number S is given by $S = 1/2 \oplus 1/2 = 1$ or 0. $S = 0$ states are called **singlets** because they only have one possible M_S value, namely 0, while $S = 1$ states are called **triplets** because they have three possible M_S values, namely +1, 0, and −1.

There are four possible ways of combining the spins of the two electrons so that the total wave function has exchange symmetry. These are listed in Table 8.2. The component of $\boldsymbol{S}$ along the z-axis is obtained by adding together the s_z values of the individual electrons. This gives the S_z value of the whole helium atom, and hence the spin quantum number M_S.

Inspection of Table 8.2 shows us that we have three symmetric spin states with M_S values of +1, 0 and −1 and one antisymmetric spin wave function with $M_S = 0$. The $M_S = +1$ and $M_S = -1$ wave functions are derived unambiguously from the triplet state. On the other hand, the two $M_S = 0$ wave functions could come from either the singlet or triplet states. However, the spin states must have well-defined exchange symmetries, and the $M_S = \pm 1$ wave functions are clearly symmetric. This implies that the symmetric $M_S = 0$ wave function comes from the triplet state, and hence that the anti-symmetric wave function corresponds to the singlet state. We thus conclude that triplet states have symmetric spin wave functions, while singlets have anti-symmetric spin wave functions. We then see from Table 8.1 that singlets and triplets must be paired off with symmetric and antisymmetric spatial wave functions respectively.

The final conclusions about the wave functions are summarized in Table 8.3. The essential point is that the singlets and triplets have *different spatial* wave functions. This has a strong effect on the energy

Spin wave function	symmetry	M_S
$\uparrow_1 \uparrow_2$	+	+1
$\frac{1}{\sqrt{2}}(\uparrow_1 \downarrow_2 + \downarrow_1 \uparrow_2)$	+	0
$\frac{1}{\sqrt{2}}(\uparrow_1 \downarrow_2 - \downarrow_1 \uparrow_2)$	−	0
$\downarrow_1 \downarrow_2$	+	−1

Table 8.2: Spin wave functions for a two-electron system. The arrows indicate whether the spin of the individual electrons is up or down (ie $+\frac{1}{2}$ or $-\frac{1}{2}$). The + sign in the symmetry column applies if the wave function is symmetric with respect to particle exchange, while the − sign indicates that the wave function is anti-symmetric. The S_z value is indicated by the quantum number for M_S, which is obtained by adding the m_s values of the two electrons together.

S	M_S	ψ_{spin}	ψ_{spatial}
0	0	$\frac{1}{\sqrt{2}}(\uparrow_1 \downarrow_2 - \downarrow_1 \uparrow_2)$	$\frac{1}{\sqrt{2}}\Big(u_A(\boldsymbol{r}_1)\,u_B(\boldsymbol{r}_2) + u_B(\boldsymbol{r}_1)\,u_A(\boldsymbol{r}_2)\Big)$
1	+1	$\uparrow_1 \uparrow_2$	$\frac{1}{\sqrt{2}}\Big(u_A(\boldsymbol{r}_1)\,u_B(\boldsymbol{r}_2) - u_B(\boldsymbol{r}_1)\,u_A(\boldsymbol{r}_2)\Big)$
	0	$\frac{1}{\sqrt{2}}(\uparrow_1 \downarrow_2 + \downarrow_1 \uparrow_2)$	
	−1	$\downarrow_1 \downarrow_2$	

Table 8.3: Spin and spatial wave functions for a two-electron atom with electronic configuration designated by the labels A and B.

of the atom as we shall see below. This is a surprising result when you consider that the spin and spatial co-ordinates are basically independent of each other.

8.3 The Pauli exclusion principle

Let us suppose that we try to put the two electrons in the same atomic shell. The ground state of helium is an example of such a configuration, with both electrons in the 1s shell. The spatial wave functions will be given by eqn 8.4 with $A = B$. The antisymmetric combination with the − sign in the middle is zero in this case. From Table 8.3 we see that this implies that there are no triplet $S = 1$ states if both electrons are in the same shell.

The fact that the triplet state does not exist for the helium ground state is a demonstration of the rule that $L + S$ must be even if the electrons are in the same shell. In the case of the $1s^2$ configuration, we have $L = 0$, and therefore $S = 1$ is not allowed. This rule was introduced without any justification in Section 5.9. The general justification of the rule is beyond the scope of this course, but the example of the helium ground state at least demonstrates that the rule is true for the simplest case.

The absence of the triplet state for $1s^2$ configuration is equivalent to the **Pauli exclusion principle**. We are trying to put two electrons in the same state as defined by the n, l, m_l quantum numbers. This is only possible if the two electrons have different m_s values. In other words, their spins must be aligned anti-parallel. The $S = 1$ state contains terms with both spins pointing in the same direction, and is therefore not allowed. The analysis of the symmetry of the wave function discussed here thus shows us that the Pauli exclusion principle is a consequence of the fact that electrons are indistinguishable fermions.

8.3.1 Slater determinants

We note in passing that the anti-symmetric wave function given in eqn. 8.4 can be written as a determinant:

$$\psi_{\rm spatial} = \frac{1}{\sqrt{2}} \begin{vmatrix} u_A(\boldsymbol{r}_1) & u_A(\boldsymbol{r}_2) \\ u_B(\boldsymbol{r}_1) & u_B(\boldsymbol{r}_2) \end{vmatrix} . \tag{8.5}$$

This can be generalized to give the correct anti-symmetric wave function when we have more than two electrons:

$$\Psi = \frac{1}{\sqrt{N!}} \begin{vmatrix} u_\alpha(1) & u_\alpha(2) & \cdots & u_\alpha(N) \\ u_\beta(1) & u_\beta(2) & \cdots & u_\beta(N) \\ \vdots & \vdots & \ddots & \vdots \\ u_\nu(1) & u_\nu(2) & \cdots & u_\nu(N) \end{vmatrix} , \tag{8.6}$$

where $\{\alpha, \beta, \cdots, \nu\}$ each represent a set of quantum numbers $\{n, l, m_l, m_s\}$ for the individual electrons, and $\{1, 2, \cdots, N\}$ are the electron labels. Determinants of this type are called **Slater determinants**. Note that the determinant is zero if any two rows are equal, which tells us that each electron in the atom must have a unique set of quantum numbers, as required by the Pauli exclusion principle.

We shall not make further use of Slater determinants in this course. They are mentioned here for completeness.

8.4 The exchange energy

The Hamiltonian for the helium atom before we consider fine-structure effects is given by:

$$\hat{H} = \left(-\frac{\hbar^2}{2m}\nabla_1^2 - \frac{2e^2}{4\pi\epsilon_0 r_1} \right) + \left(-\frac{\hbar^2}{2m}\nabla_2^2 - \frac{2e^2}{4\pi\epsilon_0 r_2} \right) + \frac{e^2}{4\pi\epsilon_0 r_{12}} , \tag{8.7}$$

where $r_{12} = |\boldsymbol{r}_1 - \boldsymbol{r}_2|$. The first two terms enclosed in brackets account for the kinetic energy of the two electrons and their attraction towards the nucleus, which has a charge of $+2e$. The final term is the Coulomb repulsion between the two electrons. It is this Coulomb repulsion which makes the equations difficult to deal with.

In § 4.1 and following we described how to deal with a many-electron Hamiltonian by splitting it into a central field and a residual electrostatic interaction. In the case of helium, we just have one Coulomb repulsion term and it is easier to go back to first principles. We can then use the correctly symmeterized wave functions to calculate the energies for specific electronic configurations of the helium atom.

The energy of the electronic configuration $(n_1 l_1,\ n_2 l_2)$ is found by computing the expectation value of the Hamiltonian:

$$\langle E \rangle = \int\int \psi^*_{\rm spatial}\, \hat{H}\, \psi_{\rm spatial}\, {\rm d}^3\boldsymbol{r}_1 {\rm d}^3\boldsymbol{r}_2 . \tag{8.8}$$

The spin wave functions do not appear here because the Hamiltonian does not affect the spin directly, and so the spin wave functions just integrate out to unity.

We start by re-writing the Hamiltonian given in eqn 8.7 in the following form:

$$\hat{H} = \hat{H}_1 + \hat{H}_2 + \hat{H}_{12} , \tag{8.9}$$

where

$$\hat{H}_i = -\frac{\hbar^2}{2m}\nabla_i^2 - \frac{2e^2}{4\pi\varepsilon_0 r_i} , \tag{8.10}$$

$$\hat{H}_{12} = \frac{e^2}{4\pi\varepsilon_0 \left|\boldsymbol{r}_1 - \boldsymbol{r}_2\right|} . \tag{8.11}$$

The energy can be split into three parts:

$$E = E_1 + E_2 + E_{12} , \tag{8.12}$$

where:

$$E_i = \int\int \psi^*_{\rm spatial} \hat{H}_i \psi_{\rm spatial} {\rm d}^3\boldsymbol{r}_1 {\rm d}^3\boldsymbol{r}_2 , \tag{8.13}$$

and

$$E_{12} = \int\int \psi^*_{\rm spatial} \hat{H}_{12} \psi_{\rm spatial} {\rm d}^3\boldsymbol{r}_1 {\rm d}^3\boldsymbol{r}_2 . \tag{8.14}$$

The first two terms in eqn 8.12 represent the energies of the two electrons in the absence of the electron-electron repulsion. These are just equal to the hydrogenic energies of each electron:

$$E_1 + E_2 = -\frac{4R_H}{n_1^2} - \frac{4R_H}{n_2^2}\,, \tag{8.15}$$

where the factor of $4 \equiv Z^2$ accounts for the nuclear charge. The third term is the electron-electron Coulomb repulsion energy:

$$E_{12} = \int\int \psi^*_{\rm spatial}\,\frac{e^2}{4\pi\epsilon_0 r_{12}}\,\psi_{\rm spatial}\,{\rm d}^3\boldsymbol{r}_1{\rm d}^3\boldsymbol{r}_2\,. \tag{8.16}$$

The detailed evaluation of this integral for the correctly symmeterized wave functions given in eqn 8.4 is discussed in § 8.7. The end result is:

$$E_{12} = D_{AB} \pm J_{AB}, \tag{8.17}$$

where the + sign is for singlets and the − sign is for triplets. D_{AB} is the **direct** Coulomb energy given by:

$$D_{AB} = \frac{e^2}{4\pi\epsilon_0}\int\int u^*_A(\boldsymbol{r}_1)\,u^*_B(\boldsymbol{r}_2)\,\frac{1}{r_{12}}\,u_A(\boldsymbol{r}_1)\,u_B(\boldsymbol{r}_2)\,{\rm d}^3\boldsymbol{r}_1\,{\rm d}^3\boldsymbol{r}_2\,, \tag{8.18}$$

and J_{AB} is the **exchange** Coulomb energy given by

$$J_{AB} = \frac{e^2}{4\pi\epsilon_0}\int\int u^*_A(\boldsymbol{r}_1)\,u^*_B(\boldsymbol{r}_2)\,\frac{1}{r_{12}}\,u_B(\boldsymbol{r}_1)\,u_A(\boldsymbol{r}_2)\,{\rm d}^3\boldsymbol{r}_1\,{\rm d}^3\boldsymbol{r}_2\,. \tag{8.19}$$

Note that in the exchange integral, we are integrating the expectation value of $1/r_{12}$ with each electron in a different shell. This is why it is called the "exchange" energy. The total energy of the configuration $(n_1l_1,\ n_2l_2)$ is thus given by:

$$E(n_1l_1,\ n_2l_2) = -\frac{4R_H}{n_1^2} - \frac{4R_H}{n_2^2} + D_{AB} \pm J_{AB}\,, \tag{8.20}$$

where the + sign applies to singlet ($S = 0$) states and the − sign to triplets ($S = 1$). We thus see that the energies of the singlet and triplet states differ by $2J_{AB}$. This splitting of the spin states is a direct consequence of the exchange symmetry.

Note that:

- The exchange splitting is *not* a small energy. It is part of the gross structure of the atom. This contrasts with the other spin-dependent effect that we have considered, namely the spin-orbit interaction, which is a small relativistic correction and only contributes to the "fine" structure of the atom. The value of $2J_{AB}$ for the first excited state of helium, namely the 1s2s configuration, is 0.80 eV.

- We can give a simple physical reason why the symmetry of the spatial wave function (and hence the spin) affects the energy so much. If we put $\boldsymbol{r}_1 = \boldsymbol{r}_2$ into eqn 8.4, we see that we get $\psi_{\rm spatial} = 0$ for the anti-symmetric state. This means that the two electrons have a low probability of coming close together in the triplet state, and hence reduces their Coulomb repulsion energy. On the other hand, $\psi_{\rm spatial}(\boldsymbol{r}_1 = \boldsymbol{r}_2) \neq 0$ for singlet states with symmetric spatial wave functions. They therefore have a larger Coulomb repulsion energy.

- The exchange energy is sometimes written in the form

$$\Delta E_{\rm exchange} \propto -J\,\boldsymbol{s}_1 \cdot \boldsymbol{s}_2\,. \tag{8.21}$$

  This emphasizes the point that the change of energy is related to the relative alignment of the electron spins. If both spins are aligned, as they are in the triplet states, the energy goes down. If the spins are anti-parallel, the energy goes up.

- The notation given in eqn 8.21 is extensively used when explaining the phenomenon of **ferromagnetism** in the subject of magnetism. The energy that induces the spins to align parallel to each other is caused by the spin-dependent change of the Coulomb repulsion energy of the electrons. The magnetic energy of the electrons due to the dipole-dipole interaction is completely negligible on this scale.

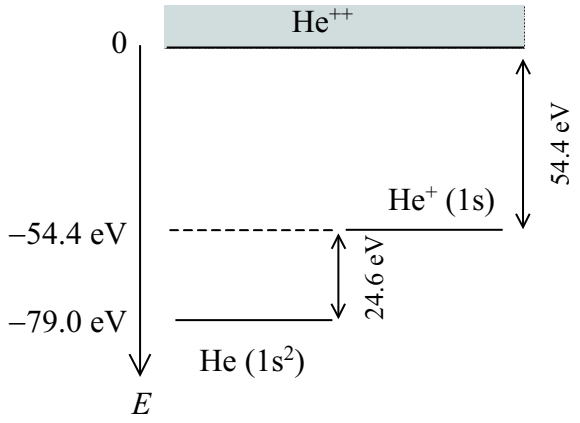

Figure 8.2: The ionization energies of helium atom.

8.5 The helium term diagram

The term diagram for helium can be worked out if we can evaluate the direct and exchange Coulomb energies. The total energy for each configuration is given by eqn 8.20.

The ground state

In the ground state both electrons are in the 1s shell, and so we have a configuration of $1s^2$. We have seen above that we can only have $S = 0$ for this configuration. The energy is thus given by:

$$\begin{aligned} E(1s^2) &= -\frac{4R_H}{1^2} - \frac{4R_H}{1^2} + \left(D_{1s^2} + J_{1s^2}\right) \\ &= -54.4\,\text{eV} - 54.4\,\text{eV} + 29.8\,\text{eV} \\ &= -79.0\,\text{eV}\ . \end{aligned} \tag{8.22}$$

The computation of the direct and exchange energies is non-trivial (to say the least) and keeps theoretical atomic physicists busy. The value of 29.8 eV given here can be deduced experimentally from the first ionization potential (see below).

Ionization potentials

The excited states are made by promoting one of the electrons to higher shells. When the second electron has been promoted into the energy continuum at $n_2 = \infty$, we are left with a singly ionized helium atom: He^+. This is now a hydrogenic system. We have one electron in the 1s shell orbiting around a nucleus with charge $+2e$, and the energy is just $-Z^2R_H = -54.4\,\text{eV}$. We thus deduce that the first ionization potential of helium is $-54.4 - (-79.0) = 24.6\,\text{eV}$. The second ionization potential (ie the energy required to liberate the second electron) is then equal to 54.4 eV. This point is illustrated in Fig. 8.2.

Optical spectra

The first few excited states of helium are listed in Table 8.4. We do not need to consider "two electron jump" excited states such as the 2s2s configuration here. This is because the Bohr model tells us that we need an energy of about $2 \times \frac{3}{4}R_H$ to promote two electrons to the $n = 2$ shell. This is larger than the first ionization energy.

For each excited state we have two spin states corresponding to S equal to 0 or 1. The triplet $S = 1$ terms are at lower energy than the singlets due to the exchange energy. (See eqn 8.17.) The $\Delta S = 0$ selection rule tells us that we cannot get optical transitions between the singlets and triplet terms. The transitions involving singlet states have a normal Zeeman effect since $S = 0$, but the triplet transitions have an anomalous Zeeman effect since $S \neq 0$.

The energy term diagram for the first few excited states are shown in Fig. 8.3. The energy of the (1s, nl) state approaches the hydrogenic energy $-R_H/n^2$ when n is large. This is because the excited electron is well outside the 1s shell, which just partly screens the nuclear potential. The outer electron just sees $Z_{\text{eff}} = 1$, and we have a hydrogenic potential.

Ground state	1s 1s ($\equiv$ 1s^2)
First excited state	1s 2s
Second excited state	1s 2p
Third excited state	1s 3s
Fourth excited state	1s 3p
$\vdots$	
Ionization limit	1s ∞l

Table 8.4: Electron configurations for the states of the helium atom.

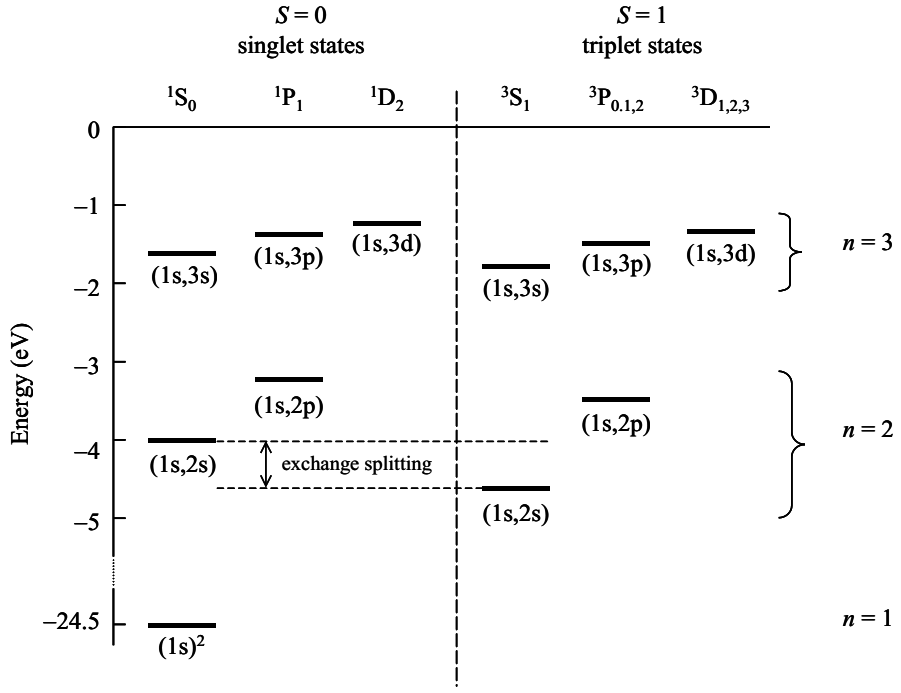

Figure 8.3: Approximate energy term diagram for helium. The diagram is split into singlet and triplet states because only $\Delta S = 0$ transitions are allowed by the selection rules. The energy difference between the singlet and triplet terms for the same configuration is caused by the exchange energy, as identified for the 1s2s configuration.

Excited states states such as the 1s 2s configuration are said to be **metastable**. They cannot relax easily to the ground state. The relaxation would involve a 2s $\rightarrow$ 1s transition, which is forbidden by the $\Delta l = \pm 1$ selection rule. Furthermore, the relaxation of the triplet 1s 2s configuration is further forbidden by the $\Delta S = 0$ selection rule. These states therefore have very long lifetimes.

8.6 Optical spectra of group II elements

The principles that we have been discussing here with respect to helium apply equally well to other two-electron atoms. In particular, they apply to the elements in group IIA of the periodic table (e.g. Be, Mg, Ca.) These atoms have two valence electrons in an s-shell outside a filled shell. The term diagram for group IIA elements would appear generically similar to Fig. 8.3, and the optical spectra would follow similar rules, with singlet and triplet transitions split by the exchange energy. The singlet and triplet transitions have normal and anomalous Zeeman effects, respectively.

8.7 Appendix: Detailed evaluation of the exchange integrals

Our task is to evaluate the gross energy for a specific electronic configuration of helium. We restrict ourselves to configurations of the type (1s,nl), since these are the ones that give rise to the excited states that are observed in the optical spectra. From eqn 8.4 we see that spatial part of the wave function is given by:

$$\Psi(\boldsymbol{r}_1,\boldsymbol{r}_2) = \frac{1}{\sqrt{2}}\Big(u_{1s}(\boldsymbol{r}_1)u_{nl}(\boldsymbol{r}_2) \pm u_{nl}(\boldsymbol{r}_1)u_{1s}(\boldsymbol{r}_2)\Big)$$

where we take the + sign for singlets with $S = 0$ and the − sign for triplets with $S = 1$.

Our task is to evaluate the three terms in eqn 8.12. We first tackle E_1:

$$\begin{aligned} E_1 &= \int\int \Psi^*\,\hat{H}_1\,\Psi\,\mathrm{d}^3\boldsymbol{r}_1\mathrm{d}^3\boldsymbol{r}_2 \\ &= \frac{1}{2}\int\int\Big(u^*_{1s}(\boldsymbol{r}_1)\,u^*_{nl}(\boldsymbol{r}_2) \pm u^*_{nl}(\boldsymbol{r}_1)\,u^*_{1s}(\boldsymbol{r}_2)\Big) \\ &\qquad \hat{H}_1\Big(u^*_{1s}(\boldsymbol{r}_1)\,u^*_{nl}(\boldsymbol{r}_2) \pm u^*_{nl}(\boldsymbol{r}_1)\,u^*_{1s}(\boldsymbol{r}_2)\Big)\,\mathrm{d}^3\boldsymbol{r}_1\,\mathrm{d}^3\boldsymbol{r}_2\,, \end{aligned}$$

where the + sign applies for singlet states and the − sign for triplets. This splits into four integrals:

$$\begin{aligned} E_1 &= \frac{1}{2}\int\int u^*_{1s}(\boldsymbol{r}_1)u^*_{nl}(\boldsymbol{r}_2)\hat{H}_1u_{1s}(\boldsymbol{r}_1)u_{nl}(\boldsymbol{r}_2)\mathrm{d}^3\boldsymbol{r}_1\mathrm{d}^3\boldsymbol{r}_2 \\ &\quad +\frac{1}{2}\int\int u^*_{nl}(\boldsymbol{r}_1)u^*_{1s}(\boldsymbol{r}_2)\hat{H}_1u_{nl}(\boldsymbol{r}_1)u_{1s}(\boldsymbol{r}_2)\mathrm{d}^3\boldsymbol{r}_1\mathrm{d}^3\boldsymbol{r}_2 \\ &\quad \pm\frac{1}{2}\int\int u^*_{1s}(\boldsymbol{r}_1)u^*_{nl}(\boldsymbol{r}_2)\hat{H}_1u_{nl}(\boldsymbol{r}_1)u_{1s}(\boldsymbol{r}_2)\;\mathrm{d}^3\boldsymbol{r}_1\mathrm{d}^3\boldsymbol{r}_2 \\ &\quad \pm\frac{1}{2}\int\int u^*_{nl}(\boldsymbol{r}_1)u^*_{1s}(\boldsymbol{r}_2)\hat{H}_1u_{1s}(\boldsymbol{r}_1)u_{nl}(\boldsymbol{r}_2)\mathrm{d}^3\boldsymbol{r}_1\mathrm{d}^3\boldsymbol{r}_2\,. \end{aligned}$$

We now use the fact that $u_{nl}(\boldsymbol{r}_1)$ is an eigenstate of $\hat{H}_1$:

$$\hat{H}_1\,u_{nl}(\boldsymbol{r}_1) = E_{nl}\,u_{nl}(\boldsymbol{r}_1)\,,$$

and that $\hat{H}_1$ has no effect on $\boldsymbol{r}_2$, to obtain:

$$\begin{aligned} E_1 &= \frac{1}{2}E_{1s}\int u^*_{1s}(\boldsymbol{r}_1)u_{1s}(\boldsymbol{r}_1)\mathrm{d}^3\boldsymbol{r}_1\int u^*_{nl}(\boldsymbol{r}_2)u_{nl}(\boldsymbol{r}_2)\mathrm{d}^3\boldsymbol{r}_2 \\ &\quad +\frac{1}{2}E_{nl}\int u^*_{nl}(\boldsymbol{r}_1)u_{nl}(\boldsymbol{r}_1)\mathrm{d}^3\boldsymbol{r}_1\int u^*_{1s}(\boldsymbol{r}_2)u_{1s}(\boldsymbol{r}_2)\mathrm{d}^3\boldsymbol{r}_2 \\ &\quad \pm\frac{1}{2}E_{nl}\int u^*_{1s}(\boldsymbol{r}_1)u_{nl}(\boldsymbol{r}_1)\;\mathrm{d}^3\boldsymbol{r}_1\int u^*_{nl}(\boldsymbol{r}_2)u_{1s}(\boldsymbol{r}_2)\mathrm{d}^3\boldsymbol{r}_2 \\ &\quad \pm\frac{1}{2}E_{1s}\int u^*_{nl}(\boldsymbol{r}_1)u_{1s}(\boldsymbol{r}_1)\mathrm{d}^3\boldsymbol{r}_1\int u^*_{1s}(\boldsymbol{r}_2)u_{nl}(\boldsymbol{r}_2)\mathrm{d}^3\boldsymbol{r}_2 \\ &= \frac{1}{2}E_{1s} + \frac{1}{2}E_{nl} + 0 + 0\,. \end{aligned}$$

The integrals in the first two terms are unity because the u_{nl} wave functions are normalized, while the last two terms are zero by orthogonality.

The evaluation of E_2 follows a similar procedure:

$$\begin{aligned} E_2 &= \int\int \Psi^*\hat{H}_2\Psi\mathrm{d}^3\boldsymbol{r}_1\mathrm{d}^3\boldsymbol{r}_2\,, \\ &= +\frac{1}{2}\int\int u^*_{1s}(\boldsymbol{r}_1)u^*_{nl}(\boldsymbol{r}_2)\hat{H}_2u_{1s}(\boldsymbol{r}_1)u_{nl}(\boldsymbol{r}_2)\mathrm{d}^3\boldsymbol{r}_1\mathrm{d}^3\boldsymbol{r}_2 \\ &\quad +\frac{1}{2}\int\int u^*_{nl}(\boldsymbol{r}_1)u^*_{1s}(\boldsymbol{r}_2)\hat{H}_2u_{nl}(\boldsymbol{r}_1)u_{1s}(\boldsymbol{r}_2)\mathrm{d}^3\boldsymbol{r}_1\mathrm{d}^3\boldsymbol{r}_2 \\ &\quad \pm\frac{1}{2}\int\int u^*_{1s}(\boldsymbol{r}_1)u^*_{nl}(\boldsymbol{r}_2)\hat{H}_2u_{nl}(\boldsymbol{r}_1)u_{1s}(\boldsymbol{r}_2)\mathrm{d}^3\boldsymbol{r}_1\mathrm{d}^3\boldsymbol{r}_2 \\ &\quad \pm\frac{1}{2}\int\int u^*_{nl}(\boldsymbol{r}_1)u^*_{1s}(\boldsymbol{r}_2)\hat{H}_2u_{nl}(\boldsymbol{r}_1)u_{1s}(\boldsymbol{r}_2)\mathrm{d}^3\boldsymbol{r}_1\mathrm{d}^3\boldsymbol{r}_2 \\ &= +\frac{1}{2}E_{nl} + \frac{1}{2}E_{1s} + 0 + 0\,. \end{aligned}$$

Finally, we have to evaluate the Coulomb repulsion term:

$$\begin{aligned} E_{12} &= \int\int \Psi^* \frac{e^2}{4\pi\epsilon_0 r_{12}} \Psi \, \mathrm{d}^3\boldsymbol{r}_1 \mathrm{d}^3\boldsymbol{r}_2 \\ &= \frac{1}{2}\int\int \Big(u^*_{1s}(\boldsymbol{r}_1)\, u^*_{nl}(\boldsymbol{r}_2) \pm u^*_{nl}(\boldsymbol{r}_1)\, u^*_{1s}(\boldsymbol{r}_2)\Big) \frac{e^2}{4\pi\epsilon_0 r_{12}} \\ &\qquad \Big(u^*_{1s}(\boldsymbol{r}_1)\, u^*_{nl}(\boldsymbol{r}_2) \pm u^*_{nl}(\boldsymbol{r}_1)\, u^*_{1s}(\boldsymbol{r}_2)\Big) \, \mathrm{d}^3\boldsymbol{r}_1 \, \mathrm{d}^3\boldsymbol{r}_2 \,, \end{aligned}$$

where again the + sign applies for singlet states and the − sign for triplets. The four terms are:

$$\begin{aligned} E_{12} &= +\frac{1}{2}\frac{e^2}{4\pi\epsilon_0}\int\int u^*_{1s}(\boldsymbol{r}_1)u^*_{nl}(\boldsymbol{r}_2)\frac{1}{r_{12}}u_{1s}(\boldsymbol{r}_1)u_{nl}(\boldsymbol{r}_2)\mathrm{d}^3\boldsymbol{r}_1\mathrm{d}^3\boldsymbol{r}_2 \\ &\quad +\frac{1}{2}\frac{e^2}{4\pi\epsilon_0}\int\int u^*_{nl}(\boldsymbol{r}_1)u^*_{1s}(\boldsymbol{r}_2)\frac{1}{r_{12}}u_{nl}(\boldsymbol{r}_1)u_{1s}(\boldsymbol{r}_2)\mathrm{d}^3\boldsymbol{r}_1\mathrm{d}^3\boldsymbol{r}_2 \\ &\quad \pm\frac{1}{2}\frac{e^2}{4\pi\epsilon_0}\int\int u^*_{1s}(\boldsymbol{r}_1)u^*_{nl}(\boldsymbol{r}_2)\frac{1}{r_{12}}u_{nl}(\boldsymbol{r}_1)u_{1s}(\boldsymbol{r}_2)\mathrm{d}^3\boldsymbol{r}_1\mathrm{d}^3\boldsymbol{r}_2 \\ &\quad \pm\frac{1}{2}\frac{e^2}{4\pi\epsilon_0}\int\int u^*_{nl}(\boldsymbol{r}_1)u^*_{1s}(\boldsymbol{r}_2)\frac{1}{r_{12}}u_{1s}(\boldsymbol{r}_1)u_{nl}(\boldsymbol{r}_2)\mathrm{d}^3\boldsymbol{r}_1\mathrm{d}^3\boldsymbol{r}_2 \\ &= +\frac{D}{2}+\frac{D}{2}\pm\frac{J}{2}\pm\frac{J}{2}\,, \end{aligned}$$

where D and J are given by eqns 8.18 and 8.19 respectively.

The total energy is thus given by

$$\begin{aligned} E &= E_{1s} + E_{nl} + D \pm J \\ &= -4R_\mathrm{H} - 4R_\mathrm{H}/n^2 + D \pm J\,, \end{aligned}$$

where the + sign applies to singlets and the − sign to triplets. (cf eqn 8.20 with $n_1 = 1$ and $n_2 = n$.)

Reading

Demtröder, W., *Atoms, Molecules and Photons*, section 6.1.
Haken and Wolf, *The physics of atoms and quanta*, chapters 17 and 19.
Foot, *Atomic physics*, Chapter 3.
Eisberg and Resnick, *Quantum Physics*, chapter 9.
Beisser, *Concepts of Modern Physics*, chapter 7.